Examining Mechanism of Toxicity of Copper Oxide Nanoparticles to Saccharomyces Cerevisiae and Caenorhabditis Elegans

Michael Joseph Mashock
Marquette University

EXAMINING MECHANISM OF TOXICITY OF COPPER OXIDE NANOPARTICLES TO *SACCHAROMYCES CEREVISIAE* AND *CAENORHABDITIS ELEGANS*

by

Michael J. Mashock, B.S.

A Dissertation submitted to the Faculty of the Graduate School,
Marquette University,
In Partial Fulfillment of the Requirements for
The Degree of Doctor of Philosophy

Milwaukee, Wisconsin

May 2016

ABSTRACT
EXAMINING MECHANISM OF TOXICITY OF COPPER OXIDE NANOPARTICLES TO *SACCHAROMYCES CEREVISIAE* AND *CAENORHABDITIS ELEGANS*

Michael J. Mashock, B.S.

Marquette University, 2016

Copper oxide nanoparticles (CuO NPs) are an up and coming technology increasingly being used in industrial and consumer applications and thus may pose risk to humans and the environment. In the present study, the toxic effects of CuO NPs were studied with two model organisms *Saccharomyces cerevisiae* and *Caenorhabditis elegans*.

The role of released Cu ions during dissolution of CuO NPs in growth media were studied with freshly suspended, aged NPs, and the released Cu^{2+} fraction. Exposures to the different Cu treatments showed significant inhibition of *S. cerevisiae* cellular metabolic activity. Inhibition from the NPs was inversely proportional to size and was not fully explained by the released Cu ions. *S. cerevisiae* cultures grown under respiring conditions demonstrated greater metabolic sensitivity when exposed to CuO NPs compared to cultures undergoing fermentation. The cellular response to both CuO NPs and released Cu ions on gene expression was analyzed via microarray analysis after an acute exposure. It was observed that both copper exposures resulted in an increase in carbohydrate storage, a decrease in protein production, protein misfolding, increased membrane permeability, and cell cycle arrest. Cells exposed to NPs up-regulated genes related to oxidative phosphorylation but also may be inducing cell cycle arrest by a different mechanism than that observed with released Cu ions.

The effect of CuO NPs on *C. elegans* was examined by using several toxicological endpoints. The CuO NPs displayed a more inhibitory effect, compared to copper sulfate, on nematode reproduction, feeding, and development. We investigated the effects of copper oxide nanoparticles and copper sulfate on neuronal health, a known tissue vulnerable to heavy metal toxicity. In transgenic *C. elegans* with neurons expressing a green fluorescent protein reporter, neuronal degeneration was observed in up to 10% of the population after copper oxide nanoparticle exposure. Additionally, nematode mutant strains containing gene knockouts in the divalent-metal transporters *smf-1* and *smf-2* showed increased tolerance to copper exposure. These results lend credence to the hypothesis that some toxicological effects to eukaryotic organisms from copper oxide nanoparticle exposure may be due to properties specific to the nanoparticles and not solely from the released copper ions.

ACKNOWLEDGEMENTS

Michael J. Mashock, B.S.

To those who have helped to make me the man I have become. More specifically dedicated to my dear good friend Dr. Anthony Kappell who truly helped me through the hard times by sharing my frustrations. This body of work is additionally dedicated to my grandmother, Sophie Spolar, as well as to my other half, Mark.

TABLE OF CONTENTS

LIST OF TABLES

LIST OF FIGURES

ABBREVIATIONS:

Ag	Silver
AOV	Analysis of variance
ATP	Adenine triphosphate
CeO_2	Cesium oxide
CFU	Colony forming units
COPAS	Complex object parametric analyzer and sorter
Cu	Copper
CuO	Copper oxide
$CuSO_4$	Copper sulfate
DNA	Deoxyribonucleic acid
EDS	Energy-dispersive x-ray spectroscopy
EDTA	Ethylenediaminetetraacetic acid
ESR	Environmental stress response
Fe	Iron
H_2O_2	Hydrogen peroxide
HMDS	Hexamethyldisilazane
HNO_3	Nitric acid
HSD	Honest significance difference
HSP	Heat shock protein
ICPMS	Inductively coupled plasma mass spectrometry
KEGG	Kyoto encyclopedia of genes and genomes
LogFC	Log_2 fold change
MeO	Metal oxide
NGM	Nematode growth medium

NTA	Nanoparticle tracking analysis
NPs	Nanoparticles
O_2^-	Superoxide radical
$OH^·$	Hydroxyl radical
ORF	Open reading frame
OsO_4	Osmium tetroxide
PBS	Phosphate buffered solution
PD	Parkinson's disease
PI	Propidium iodide
RNA	Ribonucleic acid
ROS	Reactive oxygen species
SEM	Scanning electron microscopy
SNPs	Single nucleotide polymorphisms
TEM	Transmission electron microscopy
TiO_2	Titanium dioxide
UV	Ultraviolet
Zn	Zinc
ZnO	Zinc oxide

CHAPTER 1

INTRODUCTION

1.1 Relevance of copper oxide nanoparticle research

The novel properties of nanoparticles (NPs), characterized by their small size and unique physical and chemical properties, have led to a drastic increase in the incorporation of NPs into commercial products. Nanotechnology is expected to become a $1.5 trillion market by 2016 [1]. In this context, nanotechnology is already being discussed as a key technology for the 21st century [2]. Metal oxide (MeO) NPs, such as those made from copper oxide (CuO), zinc oxide (ZnO), and titanium dioxide (TiO_2), are a type of nanomaterial commonly employed in consumer products including sunscreen, food preservatives, clothing, electronics, transistors, polymers, medicines, and pesticides. CuO NPs are one of the top four most produced MeO NPs and have uses in gas sensors, batteries, solar cells, catalytic processes (fuels), and even wound dressings [3]. The increased use of NPs will predictably lead to accidental introduction into the environment via consumer use or manufacturing. Therefore, the potential of nanoparticles to affect human health and the environment is of significant concern [4].

1.2 Complexity of studying copper oxide nanoparticle toxicity

Studying the toxicity of NPs is complex as nanoparticles have physicochemical traits that are different from their bulk chemicals including chemical composition, size distribution, shape, crystal structure, surface area, and surface charge. The NPs chemical and physical properties can vary between production methods but can even vary between separate batches produced by the same manufacturer. As such, the relationships between NPs toxicity and their physicochemical properties are important to

understand [5] but are currently understudied [6]. Smaller NPs tend to induce greater toxicity compared to larger NPs and thus it appears that a size-dependent mechanism may enhance NPs toxicity [7, 8].

A number of publications have detailed the toxicity of CuO NPs to multiple species of bacteria, yeast [9], annelids [10], and human cells [9]. A number of factors have been suggested to influence NPs toxicity including particle size [7], solubility [11], organic material present in the test media [12], and aggregation [13]. Therefore, defining the primary cause of toxicity from CuO NPs, that of the nanoparticle itself or the released Cuf ions, is frequently difficult and the ultimate cause of toxicity can remain elusive [14]. For MeO NPs, the dissolution of metal ions from the NP must be carefully measured as it has been suggested to be the primary toxic mechanism of silver (Ag) NPs [15] as well as zinc oxide (ZnO) NPs [16]. Several studies suggest the soluble ions released from NPs to be the sole source of MeO NPs toxicity [10, 17]. Other studies conclude that the CuO nanoparticle component itself also contributes to the observed inhibitory effects on important cellular functions [18, 19].

1.3 Copper as a micronutrient and as a toxin

Copper ions are an important micronutrient for *Saccharomyces cerevisiae* as these ions have distinct redox state wherein electrons can be donated or received [20]. This redox chemistry allows copper ions to be used in a multitude of necessary biological functions including oxidative stress defense, catecholamine biosynthesis, copper and iron homeostasis, and oxidative phosphorylation [10]. Alterations in the amount of bioavailable Cu^{+} (in excess or in deficiency) can result in severe effects on these biological functions.

The potential to induce redox reactions can result in increased prevalence of

oxidative stress due to the increased generation of reactive oxygen species (ROS) [21]. Cu^{+} is frequently found to produce hydroxyl radicals, which can cause lipid peroxidation in organelle membranes, oxidation of crucial proteins, and damage to both DNA and RNA [22]. Oxidative stress is an outcome of copper toxicity as the increase in ROS can result in depletion of protective antioxidant molecules [23]. Predki *et al* observed damage to proteins by the displacement of metal ions in the catalytic sites with Cu^{+} ions [24, 25]. Cu^{+} ions are crucial to cells but must be kept at balanced concentrations such that this redox-active metal won't interfere with intracellular functions and biochemical reactions [26].

The effects of CuO NPs in comparison to the bulk and ionic forms of copper are contradictory regarding the most toxic form of copper (ionic or nanoparticle) [27-30]. For example, the observed toxicity to aquatic organisms from CuO NPs exposure is observed to be caused by the released Cu ions [31]. In a study of the effect of CuO on duckweed, it was observed that a strong toxic effect was mediated by the nanoparticulate structure [32]. The major cause for increased toxicity of CuO NPs compared to bulk CuO particles was suggested to be the higher uptake rate of CuO NPs [32]. NPs are frequently more toxic than their bulk and ionic counterparts due to the large surface area to volume ration, which is suggested to result in greater number of reactive groups on the particle surface [33, 34] [35]. Different forms of the same metal can trigger different mechanisms of toxicity as Midander *et al* [8] observed CuO NPs to cause DNA damage while the released Cu^{2+} ions did not. I predict that several NPs characteristics will have varying degrees of impact on toxicity, supporting the need for detailed characterization of the NP physicochemical properties.

1.4 Copper oxide nanoparticle can induce oxidative stress

The NPs structure itself can also influence ROS production as the additional surface-reactive groups on the NPs surface act as active sites for interactions with molecular dioxygen. The interaction of oxygen with the NPs may lead to formation of superoxide radicals (O_2^-), hydrogen peroxide (H_2O_2), and hydroxyl radicals ($OH^\cdot$) [35]. ROS molecules are endogenously produced in cells as signaling molecules and metabolic byproducts [36, 37] and in normal conditions are neutralized by antioxidant enzymes. However, under conditions of excess ROS production the dynamic redox equilibrium is changed and can lead to toxicological outcomes [1, 38]. CuO NPs have been shown to induce oxidative stress in human cell cultures, aquatic organisms, bacteria and yeast [30, 39-43]. For CuO NPs, the release of Cu ions contributes to ROS generation and thus complicates mechanistic investigations [1].

1.5 Copper oxide nanoparticle internalization has been linked to toxicity

A number of toxicological studies suggest the internalization of NPs to be an important factoring in causing toxic effects [31]. The primary mechanism of NPs uptake has been shown to be facilitated via energy-dependent endocytosis in a number of human cell types including brain, cervical, and lung cancer cell lines [44, 45]. The internalization of CuO NPs into the cells of alga *Microcystis aeruginosa* was confirmed by TEM analysis [31]. Endocytosis was suggested as the primary mechanism for CuO NP uptake in the human cell line A549 [30]. In *Saccharomyces cerevisiae*, internalization of iron oxide (Fe_2O_3) aggregates and ‘quantum dot-glucose’ conjugates through endocytosis has been suggested [46, 47] but not confirmed. Currently there is no data are available to confirm CuO internalization in *S. cerevisiae*. Critical issues such as the relationship of NP size, surface charge, and aggregation and agglomeration can all

affect internalization. The confirmation of internalization of NPs is difficult as direct visualization via TEM is a methodology not accessible to all researchers.

1.6 Observation of copper toxicity in the single cell model organism Saccharomyces cerevisiae

S. cerevisiae is a promising unicellular eukaryotic model organism for the toxicological evaluation of NPs as the cellular structure and functional organization of NPs have many similarities to higher-level organisms. *S. cerevisiae* a well understood eukaryotic single cell organism with a short generation time, traceable genetics and the availability of systematic genome-wide mutant collections [48]. *S. cerevisiae* has been employed for toxicological evaluations of heavy metals, anti-cancer drugs and herbicides [49], fullerenes [50, 51], as well as nanomaterials (ZnO, CuO, TiO_2, FeO_2, [46, 52, 53] and cesium oxide (CeO_2) [50]. Previous studies involving CuO NPs exposure to *S. cerevisiae* mutant strains reported growth inhibition that was induced primarily through the action of released Cu ions [19]. This study also observed different mechanisms of growth inhibition as exposures performed in water suggest the Cu ions were the sole source of inhibition, whereas exposures in growth media indicated an effect from sources beyond the released Cu ions [19].

The molecular mechanism of several copper-related diseases can be observed using yeast as several mammal cells (liver, heart, intestine, and pancreas) contain proteins with high homology to yeast Cu homeostasis proteins, e.g., human high-affinity copper transporters Ctr1p (hCTR1)p and Ctr3p (hCTR3) [24]. Wilson's disease is a human disease shown to be linked to a defective Cu^+ transporter protein. This defective Cu^+ transporter in Wilson's disease has a high degree of homology with the Ccc2p in yeast, which is a Cu^+-transporting ATPase required for Cu^+ exocytosis [54]. *S. cerevisiae* is employed as a model for oxidative stress and ageing [55]. Additionally, several human

genes involved in the metabolism of metals have functionally homologous genes in yeast, making *S. cerevisiae* a model for understanding the impact of NPs on cellular copper homeostasis [56].

1.7 Pathways for copper homeostasis in Saccharomyces cerevisiae

The copper ion homeostasis mechanisms of *S. cerevisiae*, including Cu^{+} uptake, distribution, and detoxification, are well defined and understood [57]. This network of genes in yeast responsible for establishing copper homeostasis is described in (Figure 1). Transcription factors Ace1p and Mac1p are responsive to Cu^{+} levels and induce transcriptional regulation, in either Cu^{+} excess or starvation, respectively [58]. The dynamic reaction to the environment via Ace1p or Mac1p, results in the induction or inhibition of a variety of genes associated with Cu^{+} detoxification or Cu^{+} import, respectively [57]. The transcription factor Mac1p regulates the ferric and cupric reductases *Fre1* and *Fre7* whilst Aft1p transcriptionally regulates the four *FRE* genes *Fre2-Fre6* [59].

In *S. cerevisiae*, the uptake of Cu^{+} begins with Cu^{2+} becoming reduced to Cu^{+} by the Cu^{2+} reductases *Fre1* and *Fre7* after which the Cu^{+} ions will be internalized by the high affinity Cu^{+} transporters *Ctr1* and *Ctr3 [60]* . Several low affinity uptake systems have also been identified [24] which are encoded by the divalent metal ion transporters *Fet4*, *Smf1/2*, and *Ctr2* genes [61-63]. After internalization, several Cu^{+} chaperones deliver Cu^{+} to the mitochondria and secretory pathway through the actions of the Cu^{+} metallochaperones Cox17p and Atx1p, respectively [24]. The enzyme key to respiration, cytochrome oxidase C, requires Cu^{+} to function, which is incorporated via the mitochondrial COX protein and is mediated by the copper binding proteins *Sco1* and *Sco2* [64]. The Cu^{+} chaperone for superoxide dismutase, (*CCS1*), enables Cu^{+} incorporation into superoxide dismutase 1 (*SOD1*), an enzyme crucial for appropriate

response to oxidative stress [65]. Several cytoplasmic proteins are responsible for binding free Cu^{+} within the cytoplasm, such as the metallothioneines Crs5p and Cup1-1p that are upregulated via Ace1p to bind additional free ions within the cytoplasm [57].

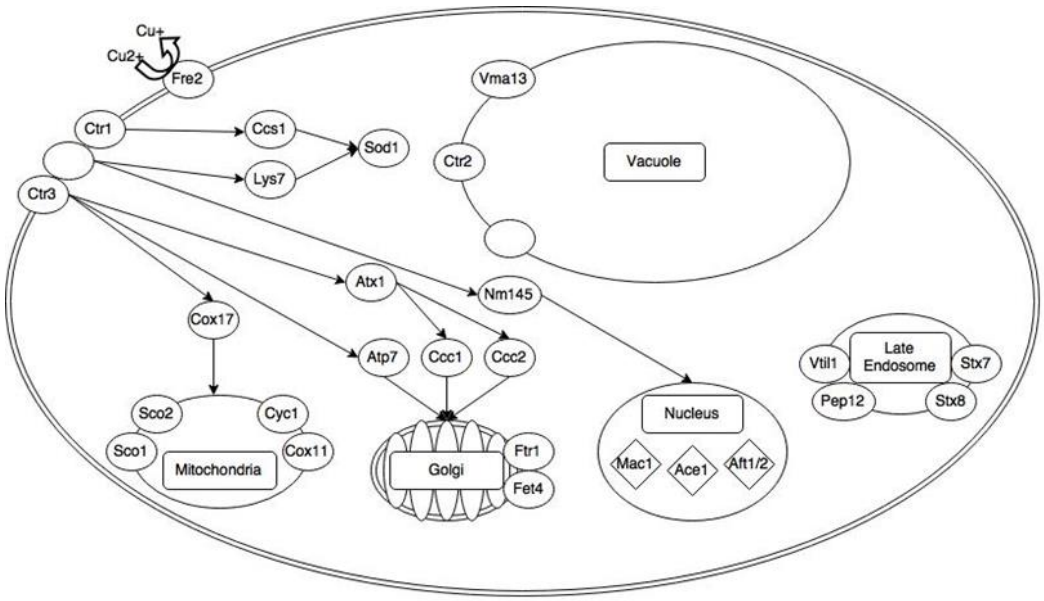

Figure 1. *S. cerevisiae* proteins involved in copper homeostasis pathway (an original figure, generated by Michael Mashock and Dan Van Blarcom).

1.8 *Observation of copper toxicity in the multicellular model organism* Caenorhabditis elegans

Caenorhabditis elegans (*C. elegans*) is employed as a model organism in many studies because of its small size, short lifespan, rapid maturation time, defined anatomy, and translucent body. Nematodes are a relevant environmental model as they decompose organic material within soil [66]. Excess levels of copper in *C. elegans* have resulted in decreases in reproduction [67, 68] and egg-laying [69]. Toxicity from copper

has led to changes in nematode cuticle structure and changes in chemotaxis behavior [69].

Neuronal health can be assayed with *C. elegans* as they have relatively conserved complex biochemical pathways compared with mammalian species. A number of genes associated with neurological disorders, including Alzheimer's Disease (AD), have homologs in *C. elegans* [70]. Excess copper has been associated with several neurological disorders including prion diseases, amyotrophic lateral sclerosis, and Parkinson's Disease (PD) [71]. However, there is a lack of studies addressing whether CuO NPs induce neurodegeneration in *C. elegans.* Damage or loss of dopaminergic (DA) neurons can occur if cells do not keep Cu ions under tight regulation [72]. Heavy metals, such as manganese, copper, cadmium, lead, and mercury, have been shown to affect neurons by depleting cellular energy, usually by decreasing mitochondrial function or activating the necrosis and apoptosis pathways [72]. Exposure to heavy metals has also been associated with extracellular oxidation of neurons that results in ROS generation and consequent lipid peroxidation [72].

1.9 Dissertation goals

The objective of this study is to further understand the underlying mechanisms of CuO NPs toxicity in both *S. cerevisiae* and *C. elegans*. This study operates on the following hypotheses:

1. The released copper ions from the copper oxide nanoparticles are a major source of the nanoparticles inhibitory effects on cellular and organismal functions.
2. Copper oxide nanoparticle inhibition is in part due to an effect from the nanoparticle structural component.

3. Exposure of yeast with copper oxide nanoparticles will result in gene induction different than those genes induced or reduced after released copper ion exposure.
4. The genetic differences between laboratory adapted nematode strains and wild nematode strains will influence their sensitivity to copper exposure.

CHAPTER 2

COPPER OXIDE NANOPARTICLES INHIBIT THE METABOLIC ACTIVITY OF *Saccharomyces cerevisiae*

2.1 Abstract

The interaction of CuO NPs with complex media and the impact on cell metabolism when exposed to sublethal concentrations are largely unknown. In the present study, the short-term effects of two different size manufactured CuO NPs on metabolic activity of *Saccharomyces cerevisiae* were studied. The role of released Cu^{2+} during dissolution of NPs in the growth media and the CuO nanostructure were considered. Characterization showed that the 28 nm and 64 nm CuO NPs used in the present study have different primary diameter, similar hydrodynamic diameter, and significantly different concentrations of dissolved Cu^{2+} ions in the growth media released from the same initial NPs mass. Exposures to CuO NPs or the released Cu^{2+} fraction, at doses that do not have impact on cell viability, showed significant inhibition on *S. cerevisiae* cellular metabolic activity. A greater CuO NP effect on the metabolic activity of *S. cerevisiae* growth under respiring conditions was observed. Under the tested conditions the observed metabolic inhibition from the nanoparticles was not fully explained by the released copper ions from the NPs.

2.2 *Introduction*

The acute toxicity of copper oxide nanoparticles (CuO NPs) has been studied in algae [73], bacteria [74], yeast [75, 76], protozoa [77], crustacean [78], and fish [79] species. The extensively used unicellular eukaryotic model organism, *Saccharomyces cerevisiae*, has similar cellular structure and functional organization to those of higher-level organisms [76] making it ideal in toxicity studies for nanoparticles. Copper

cytotoxicity and impact on cellular functions is of intrinsic interest. The adverse consequences of defective Cu homeostasis (Wilson's disease and Menke's syndrome in humans) or of changes in external copper concentration are well documented [80]. There is limited information of how dissimilarities in nanoparticles characteristics, different exposure conditions, and differences in the metabolic and cell cycle stage of *S. cerevisiae* cultures impact the toxicity metrics. For example, differential copper resistance has been associated with cell cycle stage and ageing in yeast [81]. Additionally, environmental factors such as ionic strength, pH, and the presence of organic material have an impact on how nanoparticles entering the environment would react in solution [82].

CuO NPs have been shown to both dissolve [75, 77] and aggregate [79] within solution depending on the conditions within the medium. Some studies have indicated that the acute toxicity observed is due to the release of copper ions from the nanoparticles [73, 77]. However, other studies suggest the presence of nanoparticle-specific effects [75, 83]. Kasemets *et al* [76] suggests that the observed CuO NP toxicity to *S. cerevisiae* was due to a cell surface localized increase in released Cu ions causing an increase in uptake. The authors also suggested in a separate study that the released Cu^{2+} from the CuO NPs could explain approximately half of the toxicity and structure component-related oxidative stress was the mechanism of toxicity [75]. These results demonstrate that the toxicity of NPs toward organisms is challenging to predict because of the difficulty of adequately linking the nano-material properties in a directly proportional relationship to the toxic mechanisms, thus further investigation remains necessary [84].

The current study investigates the impact of organic molecules-rich growth media on CuO nanoparticle dissolution, aggregation, and copper bioavailability on cellular metabolic activity of *S. cerevisiae*. Cells were exposed to two CuO NPs with identical

copper oxide composition but different primary particle size (Figure 2), crystal lattice structure, and dissolution rate/amount of released Cu^{2+} after incubation in the growth medium. These CuO NPs were applied as either fresh suspensions or aged NPs in the culture medium. To distinguish between the role of Cu^{2+} ions released from the NPs and the nanospecific effect, parallel exposures were carried out with the released Cu^{2+} fraction in the media from CuO NPs and the NP suspensions. Experiments performed in organic-rich media can represent the diverse and dynamic surroundings which may be encountered with accidental introduction of nanoparticles into the environment [17], thereby stressing the role of media on the cell-nanoparticle interactions.

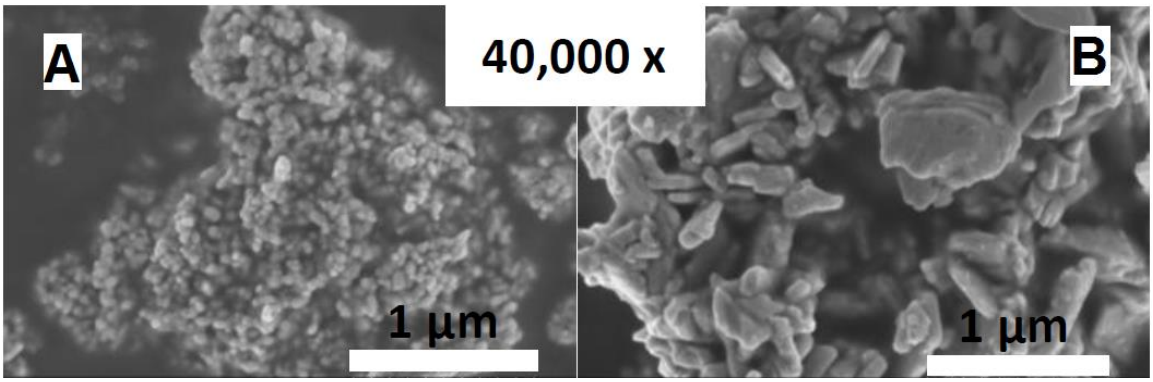

Figure 2. Scanning electron micrographs to observe the primary diameter of the copper oxide nanoparticles. The 28.4 nm (A) and 64 nm (B) copper oxide nanoparticles employed in this study.

2.3 Material and Methods

2.3.1 *Saccharomyces cerevisiae strains and cultivation conditions*

Saccharomyces cerevisiae W303-1A wild type (*MAT*a: *leu2-3,112 trp1-1 can1-100 ura3-1 ade2-1 his3-11,15*) was a kind gift of Dr. Rosemary Stuart (Marquette

University, WI). The strain was maintained on YP agar plates (pH 6.6) containing 1% yeast extract (Amresco), 2% Bacto peptone (Difco laboratories) and 2% of the respective carbon source at 30^{o}C overnight. To prepare starter cultures single colonies from the respective master plates were transferred in 5 ml YP media with ethanol, galactose, or dextrose as carbon source and grown overnight at 30^{o}C, 250 rpm in order to culture the cells under respiratory, respiratory/fermentative, or fermentative metabolism, respectively. YP media with dextrose or ethanol as a carbon source were employed to examine the influence of different types of metabolism (fermentation vs. respiration) on *S. cerevisiae* sensitivity to copper treatments while YP with galactose (YP-gal, fermentation/respiratory metabolism) was employed for all other experiments throughout the present study. *S. cerevisiae* experimental cultures were started from the overnight cultures. The turbidity of the cell culture was measured via absorbance at 600 nm using a spectrophotometer (Molecular Devices) and diluted with sterile YP media with respective carbon source to an OD_{600} 0.1. The cultures were grown until OD_{600} 0.3 was reached (approximately $4.0x10^{6}$ Colony Forming Units, CFU mL^{-1} determined by dilutions and plating on YP-galactose plates with colony counting after 72 hours at 30^{o}C incubation). Exposure to tested chemicals was performed in 96-well black with clear bottom, polystyrene plates (Costar) at 30^{o}C with continuous shaking at 250 rpm. This concentration of cells was consistently used in all toxicity assays.

2.3.2 *Nanoparticle physicochemical characterization*

NPs diameter and morphology. Bare, uncoated CuO NPs were purchased from Meliorum Technologies (28 nm CuO NPs) or Sigma Aldrich (64 nm CuO NPs). Transmission electron microscopy (TEM) was employed to characterize both CuO NPs morphology and primary particle diameter. Diluted CuO NPs suspensions in water or YP-gal media were deposited onto formvar coated copper 200 mesh grids and allowed

to settle for 10 min prior to removal of the excess liquid. TEM imaging was performed on a Hitachi H9000NAR Analytical High Resolution Transmission Electron Microscope, 300 KeV (dpr) and the primary particle diameters were assessed using ImageJ image processing and analysis software. Briefly, the measuring tool was employed, after altering the scale to nanometers, in order to assess dimensions of 100 individual NPs of both 28 nm and 64 nm CuO NPs in 15 or more images. Measurement of NPs diameter was performed only when well-defined individual nanoparticles could be observed. TEM micrographs of gold nanoparticles at established dimensions were analyzed in identical fashion with ImageJ to confirm validity of measurements (data not shown).

NPs dispersion. A stock solution of CuO NPs (8,000 mg/L) was prepared in sterile deionized H_2O and dispersed by using a 450 W probe sonicator (Branson Digital Sonifer) at 20% amplitude for 5 min on ice with pulsing on for 20 sec and off for 20 sec. The stock solutions were stored in dark at ambient temperature.

After 5 min dispersion, different volumes of the CuO NPs stock solution were aseptically added to yeast cultures (in YP medium containing different carbon source) to achieve different exposure concentrations.

NPs hydrodynamic diameter and zeta potential. To determine the average hydrodynamic diameters of CuO NPs agglomerates, NPs were diluted to 40 mg/L in sterile double distilled water (sterile) or YP-gal growth medium and injected using a sterile syringe into the viewing chamber of NS500 platform (Nanosight Ltd) equipped with a 640-nm laser. All measurements were taken at room temperature. Average diameters and standard deviations were measured using the Nanoparticle Tracking Analysis (NTA) 2.0 Build 127 analytical software for real-time dynamic nanoparticle visualization and measurement. The samples, in the respective solution, were measured for 30 sec with manual shutter and gain adjustments and six measurements of the same sample were performed for all of the respective time points. Although Nanosight has a

minimum limit of detection of 10 nm, the smaller CuO NPs employed in the present study have an average primary particle diameter, as measured by TEM, of 28 nm.

However, it should be noted that any populations of CuO nanoparticles or agglomerations smaller than 10 nm would not be detected by this analysis. To exclude artifacts from organic components within media, analysis of YP growth media without addition of CuO NPs was performed and run in batch processing as five separate runs to avoid introducing additional artifacts from altering fluidic flow. The data were combined and averaged to provide background intensity data which was then used to exclude organic matter from conflicting with the NPs/organic matter agglomeration measurements. This exclusion was accomplished through the use of the 'intensity comparison' tool in the NTA 2.0 build software which allows the user to establish intensity values as a cutoff for the minimal intensity necessary to be incorporated in the sample analysis. To determine Zeta potentials of CuO NPs in YP media, NPs in solution, at 69.5 mg Cu/L, were pipetted into Folded Capillary Cells (Malvern Instruments) and Zeta potential was measured using a Zetasizer Nano-ZS (Malvern Instruments).

2.3.3 *NPs aging in the growth media.*

Note that *S. cerevisiae* has a high copper tolerance, up to 480 mg/L CuO NPs for 12 hours of exposure in YP media without observing lethal effects (data not shown). In the current study, sub-lethal nanoparticle concentrations in the range of 40 – 240 mg Cu/L were employed in 1.5 hour exposure scenario to study the NPs effect on *S. cerevisiae* cell metabolism. To explore media component-NPs interactions, CuO NPs were dispersed into YP-galactose media as described above to 40, 80, or 240 mg/L initial mass in 4 mL volume in 15 mL polypropylene disposable centrifuge tubes (VWR). The NPs solutions were covered to prevent light exposure and placed at 30^{o}C in a table-top incubator at 250 rpm for 24 hour. A 2 mL aliquot of the 'aged' NPs were

ultracentrifuged at 45,000xg for 30 min (Optima MAX-E Ultracentrifuge) and supernatant was then removed and used as released fraction. The CuO NPs pellet was resuspended in sterile YP- galactose media and used as aged NPs in fresh media. The remaining 2 mL of aged NPs in released fraction was used as an additional treatment. Fresh suspensions of CuO NPs were prepared by diluting stock solution (8,000 mg/L) to 40, 80, and 240 mg/L and immediately added to cell suspensions for exposure.

In cases of NPs exposure with Cu^{2+} chelation, ethylenediaminetetraacetic acid (EDTA) in final concentration of 0.5 mM was added to CuO NPs or the released ionic copper fraction in YP- gal medium and incubated at 30^{o}C for 1 hour prior to the addition of *S. cerevisiae* cells. The *S. cerevisiae* cells used as the untreated control were pelleted and resuspended in growth media which was also supplemented with EDTA.

2.3.4 *NPs dissolution*

To define the amount of Cu^{2+} ions released from CuO NPs in the growth media, aliquots of each NPs suspension in YP-gal medium were collected immediately after dispersion in the media, after 1.5 hour, or 24 hours incubation at 30^{o}C with shaking (250 rpm) and ultracentrifuged (45,000 g for 30 mins) to remove cells and suspended CuO NPs. Aliquots were stored at 4^{o}C (up to one week) until Zincon analysis was performed. The Cu^{2+} ion concentration was measured using Zincon assay as described by [85] with modifications described herein. Prior to analysis, supernatants were examined for NPs presence using NTA and concluded that NPs were not detectable.

Nanoparticles with a diameter less than 10 nm were not detected due to the limit of detection by NTA but may be present. However even if a small NP fraction of <10 nm is present, experiments indicate that Zincon dye does not interact directly with CuO NPs (data not shown). Measurement of Cu^{2+} within the supernatant was performed on a Spectra Max® M2e spectrophotometer (Molecular Devices) using Zincon reagent (MP

Biochemicals). All samples were diluted in Tris-HCl buffer (20 µM, pH 7.2) containing Zincon (40 µM). A standard curve with Cu^{2+} (0 - 2.4 mg/L) was prepared from $CuSO_4$ in the same buffer. Samples were incubated at room temperature for 10 min and absorbance was measured at 615 nm. The relationship between absorbance at 615 nm and the known concentration of Cu^{2+} standard served to determine Cu^{2+} ion concentration. To observe the influence of organic material and anions, identical experiments were performed in double distilled water. To remove the pH as a potential variable, distilled water was adjusted to pH 6.4, identical to the growth media. All measurements were performed in triplicate.

To define the amount of total Cu released from CuO NPs in the growth media, aliquots of previously ultracentrifuged supernatant were digested with equal volume 70% (w/v) Nitric acid (HNO_3) at 65^{o}C for 2 hour and stored in acid-washed glass vials at 4^{o}C for no more than 1 week. Samples were then further diluted to 2% HNO_3 with sterile water, containing 0.5% HCL, prior to sample analysis using an ICP-MS system (7700x ICP-MS with autosampler, Agilent Technologies). ICP-MS detects total copper regardless of copper ion species, copper in strong-association with organic material, or copper in the form of nano-solids.

2.3.5 *Cell viability spot assay*

Overnight cultures of *S. cerevisiae* in YP-gal media were diluted to OD_{600} 0.1 and 150 µL of the cell suspensions were aliquoted to 0.6 mL in a 96-deep-well plate. Cell suspensions were mixed with 150 µL of CuO NPs and $CuSO_4$ solutions in YP-gal media. Plates were covered loosely with aluminum foil and incubated at 30^{o}C for 24 hours with shaking at 250 rpm. Cells were then serially diluted in PBS buffer (pH 7.2) and 2 uL of the cell solutions were spotted onto YP-gal agar plates in triplicate. The formation of

colonies was visually examined after 72 hours of incubation at 30^{o}C and was compared to colony formation of untreated cells.

2.3.6 *Metabolic activity assay*

The inhibitory effects of CuO NPs were determined by quantifying cellular metabolic activity using AlamarBlue (aB, Invitrogen), a cell-permeable redox-sensitive dye that turns from a non-fluorescent blue color to a highly fluorescent pink color upon reduction by metabolically active cells. Fluorescence detection of the reduced aB signal was performed in a Spectra Max® M2e spectrophotometer (Molecular Devices Inc.).

The metabolic activity assay was performed according to the following protocol: Copper treatments were generated by adding $CuSO_4$, or released Cu^{2+} fraction from NPs, or dispersed CuO NPs into YP-galactose media to achieve 300 uL volume at desired concentration. Freshly inoculated cultures of *S. cerevisiae* in YP-gal media were incubated at 30^{o}C for 3-4 hours until OD_{600} 0.3 was reached, centrifuged at 4,000 rpm for 2 min, supernatant removed, and cell pellets were then resuspended with YP-galactose media containing different copper treatment. Each experimental treatment was amended with 10% (v/v) AlamarBlue dye to achieve a final volume of 330 µL, which was then aliquoted to three separate wells to a final volume of 100 µL per well in a 96-well plate (Costar polystyrene flat bottom, non-treated, black sided, clear bottom). Cell free YP-galactose media was added to cell free control wells for background subtraction. Plates were covered with aluminum foil to prevent light exposure and incubated at 30^{o}C, with shaking at 250 rpm for 1.5 hour up to 4 hours. Fluorescence was recorded at 550/585nm excitation/emission with a 570 nm cutoff every 5 min at 1.5 hour and 4 hours. Cellular metabolic rate was determined by employing SpectraMax software to calculate rate of fluorescence at the linear portion of each curve. Each respective

treatment was performed in triplicate wells and the results were averaged per well. Data are mean of three independent experiments ± range of values.

2.3.7 *Preparing released fraction exposure scenario*

Copper oxide nanoparticles were less inhibitory to yeast metabolism compared to $CuSO_4$ (Figure 3). When $CuSO_4$ was used to mimic the released Cu^{2+} from CuO NPs, less metabolic inhibition was observed compared to exposure with the actual released fraction from NPs. This observation of soluble Cu salt treatments not being an adequate mimic of NPs-released Cu ion treatment has also been reported in other studies [17]. Only after incubation of $CuSO_4$ in YP-gal (to simulate the Cu ions released from CuO NPs) was the metabolic inhibition more similar to the metabolic inhibition observed with released Cu treatments (Figure 4). Instead of aged $CuSO_4$, the released copper ion-containing supernatant from the CuO NPs was used in the subsequent experiments

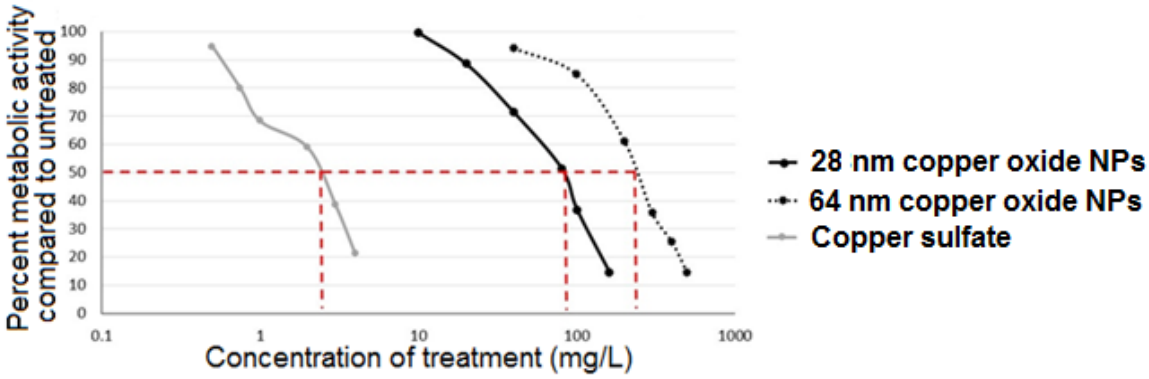

Figure 3. Comparison of IC_{50} values of metabolic activity rate for 28 nm and 64 nm copper oxide nanoparticles. Red lines indicate IC_{50} value for respective copper exposure scenarios.

to better represent the nature of the soluble copper within the YP-galactose media. To characterize the released copper from CuO in the growth media, total copper was measured with ICP-MS. Cu^{2+} is a dominant fraction in the 'released copper only' exposure scenario as the concentration of total copper, as measured with ICP-MS, was not significantly different than Cu^{2+} ions concentrations, as measured with zincon assay (Figure 5).

2.3.8 *Statistical analysis*

For all data, significant difference between samples was determined using pair-wise comparisons performed by Student's t-test (after confirming normal distribution) and $p<0.05$ were considered significant. IC_{50} toxicity values after 1.5 hour, i.e. concentration of chemical which reduced cell metabolic activity by 50%, were compared to the control and their confidence intervals (95%) were compared using Log-normal model in the Excel macro REGTOX [86].

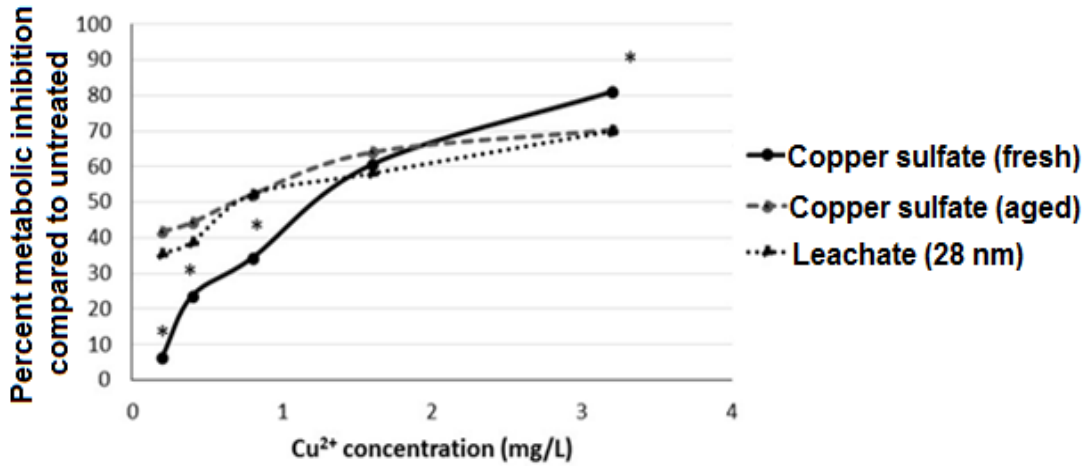

Figure 4. The influence of copper ions, from copper sulfate as well as released from CuO NPs, on *S. cerevisiae* metabolism. 28 nm CuO NPs and $CuSO_4$ were added to sterile YP-galactose media for 24 hours and then diluted to 0.2 - 3.2 mg Cu^{2+}/L and inhibition of metabolic activity was assayed after 1.5 hour exposure. Significant difference ($p<0.05$) is indicated by asterisks.

2.4 *Results*

2.4.1 *Copper oxide nanoparticle characterization*

Copper oxide (CuO) nanoparticles (NPs) from two different commercial sources were characterized for primary NP diameter and morphology by TEM (Figure 6 E-H). The Meliorum CuO NPs have an average primary particle diameter of 28.4 nm, herein referred to as 28 nm CuO NPs, while the Sigma CuO NPs had an average primary particle diameter of 64.2 nm, herein 64 nm CuO NPs (Figure 6G and 6H). The 28 nm CuO NPs displayed a rough surface, spherical shape, and a uniform size distribution (large black arrows, Figure 6E and 6F). TEM imaging of the 64 nm CuO NPs showed

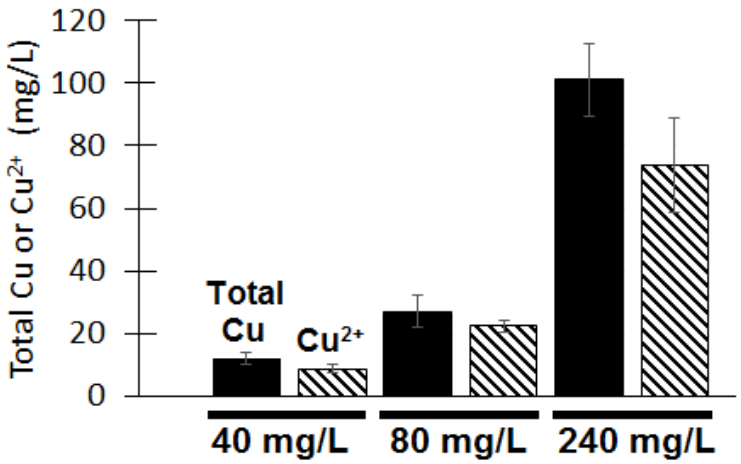

Figure 5. Characterization of the copper ions within the released from the copper oxide nanoparticles when incubated in growth media. CuO nanoparticle released fraction contains predominantly a population of Cu^{2+} ions. 28 nm CuO nanoparticles were aged for 24 hours in sterile YP growth media, nanoparticles were removed from solution by ultracentrifugation, and supernatant was then assayed for total copper (solid bars) or Cu^{2+} ions (stripped bars). There was no statistically significant difference between the total Cu and Cu^{2+} concentrations for 40, 80, and 240 mg/L treatments (*p* value 0.053, 0.061, and 0.098, respectively).

different morphologies with both small spherical particles and large irregular crystals being observed in the same sample (Figure 6G). The 28 nm and 64 nm CuO NPs exhibited purity of >99.8 % as reported by the manufacturers and determined by ICP-MS analysis (data not shown). High resolution TEM (HR-TEM, Figure 6F) images displayed a distance of 2.4 Å between parallel lattice fringes (parallel to solid black lines with small arrows) in the 28 nm CuO NPs, consistent to the spacing of the (2 0 0) crystal planes of CuO. The HR-TEM images of 64 nm CuO NPs had parallel lattice fringe spacing of 5.1 Å (Figure 6H) consistent with the interlayer separation of the (1 0 0) crystal plane of CuO.

Hydrodynamic diameter and zeta potential were measured to determine the propensity of the 28 nm and 64 nm CuO NP to form aggregates or agglomerates (Figure 6, Table 1). Both CuO NPs form similarly sized aggregates when suspended in double distilled water (sterile, Figure 6A, 6B) and similarly sized agglomerates when suspended in YP-galactose growth medium (Figure 6C, 6D). The CuO NPs suspended in water had significantly smaller hydrodynamic diameter compared to NPs suspended in growth media ($p<0.05$) at pH 6.4. While the pH was the same, the ionic strength was significantly higher within YP media compared to water (data not shown). Both increased ionic strength and organic matter have been implicated in increased nanoparticle dissolution [82, 87] which may partially explain the increased dissolution observed in YP media compared to water. The 28 nm CuO NPs had a smaller average hydrodynamic diameter ($p<0.05$) when suspended in water (94 nm) compared to the diameter range observed in YP-galactose medium (214.1 nm) and in both cases were smaller than the 64 nm CuO NPs (146.3 nm in water and 246.9 nm in YP-galactose, Figure 6, Table 1). All particles had low zeta potential values (-5.6 to -14.5 mV, Table 1) indicating

substantial instability and a high potential to form agglomerates in the growth media. Suspensions from both NPs did not alter the pH of the YP-galactose culture medium up to 24 hours of incubation (data not shown).

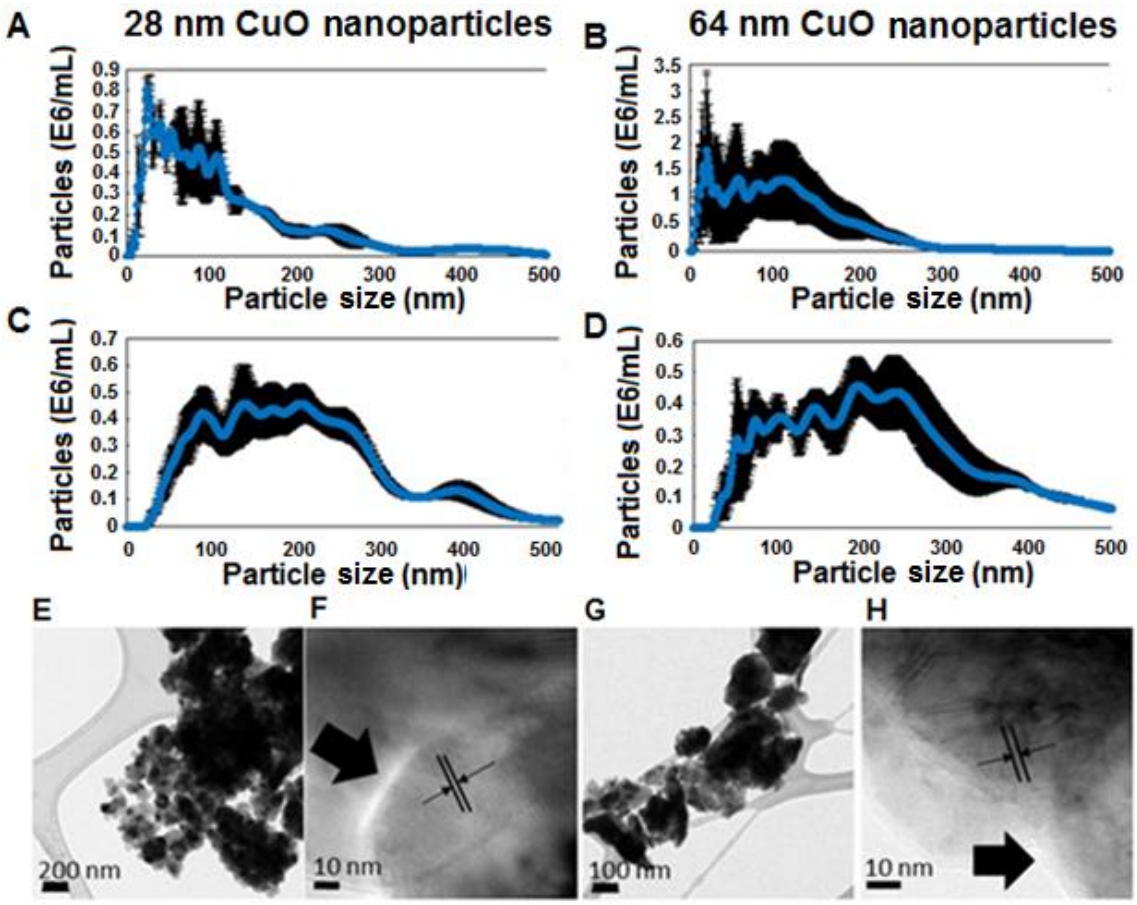

Figure 6. The primary diameters and average hydrodynamic diameters of the 28 nm and 64 nm copper oxide nanoparticles in growth media. The two types of copper oxide nanoparticles have similar agglomeration in culture medium but different primary particle diameter and crystalline structures. The hydrodynamic size distribution was performed in sterile water (A, B) and YP-galactose (C, D) using NTA. TEM images of the CuO NPs indicate rough surfaces (indicated by large arrows) and show the primary diameter of the particles is different from that suggested by the manufacturers (E-H). High resolution TEM images for 28 nm (F) and 64 nm (H) CuO NPs. The different lattice fringe width is highlighted for easier observation by parallel lines with small arrows.

2.4.2 *Copper oxide nanoparticle dissolution*

For nanomaterials, metal ion release is a critical physical parameter and as such NPs dissolution has been suggested to be just as important as surface dependent effects regarding potential toxicity of nanomaterials [88]. In our study, the culture media, YP-galactose, led to enhanced CuO NPs dissolution compared to water while the smaller 28 nm CuO NPs exhibited greater dissolution than the 64 nm CuO NPs. We observed that distilled water (pH 6.4) had no effect on NPs dissolution for most of the exposure doses employed (Table 1) except under prolonged incubation (25.5 hour) with higher initial mass of 64 nm particles. The 28 nm freshly resuspended CuO NPs showed higher release of Cu^{2+} in the YP-galactose medium in comparison to the Cu^{2+} released from the same initial mass of freshly resuspended 64 nm CuO NPs (Table 1). The 28 nm CuO NPs suspended in YP-galactose medium displayed up to 21.8% reduction of the initial particle mass after 4 hours, while the 64 nm CuO displayed significantly less particle mass loss (2%, $p<0.01$). The increased CuO NPs dissolution in YP-galactose is in agreement with previous reports indicating enhanced CuO NPs dissolution in culture media containing amino acid-rich components, such as tryptone and yeast extract, in comparison to dissolution in water [17, 89].

To observe the effects of prolonged media interactions with CuO NPs on dissolution, the 28 nm and 64 nm CuO NPs were suspended in YP-galactose medium for 24h at 30°C followed by separation of the remaining CuO solids (“aged” NPs) from the media (“released” Cu^{2+}). Aged 28 nm CuO NPs were pelleted and resuspended in fresh YP-galactose media resulting in significantly greater ($p<0.05$) Cu^{2+} release compared to fresh suspensions of CuO NPs (Table 1). The opposite trend was observed

for aged 64 nm CuO NPs in fresh media, which released less Cu^{2+} into YP-galactose compared to fresh suspensions of 64 nm CuO NPs (at 80 and 240 mg/L, Table 1).

Both CuO NPs used in the present study have different primary nanoparticle diameter and different crystal structure (determined by HR-TEM, Figure 2), similar hydrodynamic diameter (NTA, Figure 6), and released significantly different amounts of Cu^{2+} into the growth media from the same initial NPs mass (Table 1).

2.4.3 *Copper oxide nanoparticles inhibit* S. cerevisiae *metabolism*

The potential cytotoxicity of two different commercially available CuO NPs to *S. cerevisiae* was evaluated using a cell viability spot assay and cellular metabolic activity was assayed by alamarBlue (aB) fluorescence. After 1.5 hour and 24 hours of exposure no significant effects on cell viability were observed for the 28 nm and 64 nm CuO NPs up to the highest concentration tested (480 mg/L) (Figure 7). Susceptibility to CuO NPs or $CuSO_4$ exposures was greater in cell cultures undergoing respiratory than fermentative metabolism (Table 2). The 1.5 hour IC_{50} values for inhibition of metabolic rate of *S. cerevisiae* W303-1A exposed to 28 nm and 64 nm CuO NPs (fresh suspensions) in our study are 306 $\pm$ 67 and 467 $\pm$ 7 mg/L, respectively, when cultured on YP-dextrose.

These values are consistent with the range of the previously reported 24 h growth inhibition test IC_{50} for *S. cerevisiae* BY4741 of 643 $\pm$ 52 mg/L CuO NPs in YPD medium [76]. *S. cerevisiae* cells cultured with respiratory carbon sources, including YP-ethanol (YPE), were more sensitive to exposures than cells in fermentative conditions (p<0.05, Table 2). The metabolic rate IC_{50} for cells on respiratory carbon sources (ethanol and glycerol) are 2 to 5 times lower (p<0.01) compared to exposure to cells cultured on YPD (fermentative metabolism). The IC_{50} for $CuSO_4$ exposure was more than

Table 1. Characterization of copper oxide nanoparticles and their properties when suspended in media or water.

Average hydrodynamic diameter (nm)			
Experimental media	**1.5h[a]**	**5.5h**	**25.5h**
28 nm copper oxide nanoparticles			
YP-galactose	214 ± 112	184 ± 116	222 ± 141
YP-ethanol	200 ± 162	225 ± 117	236 ± 129
water	87 ± 7	191 ± 175	113 ± 82
64 nm copper oxide nanoparticles			
YP-galactose	240 ± 172	124 ± 48	211 ± 155
YP-ethanol	346 ± 177	232 ± 182	175 ± 104
water	144 ± 149	140 ± 90	160 ± 94
Zeta-potential (mV)			
Experimental media	**1.5h**	**5.5h**	**25.5h**
28 nm copper oxide nanoparticles			
YP-galactose	-14.5 ± 0.5	-10.5 ± 0.2	-7.8 ± 0.3
YP-ethanol	-14.5 ± 0.5	-10.4 ± 0.6	-9.2 ± 0.1
water	-13.9 ± 0.7	-15.2 ± 7.2	-21.2 ± 5.9
64 nm copper oxide nanoparticles			
YP-galactose	-12.8 ± 0.3	-5.6 ± 0.7	-8.6 ± 0.4
YP-ethanol	-12.8 ± 0.3	-9.7 ± 0.3	-8.9 ± 0.8
water	-12.7 ± 0.4	-16.6 ± 6.4	-11 ± 11.1

Data are mean of 3 replicates of 2 independent experiments ± range of values. [a] Period of time nanoparticles were incubated in media or water.

20 times lower compared to the IC_{50} for both CuO NPs under study. Cells cultured on YP-galactose (fermentative/respiratory carbon source) showed similar or slightly higher sensitivity to CuO NPs and Cu^{2+} exposures compared to cells cultured on YP-ethanol. YP-galactose was employed in the following experiments because of the higher *S. cerevisiae* w303-1A biomass yield on galactose compared to yield with YP-ethanol (data not shown). The metabolic state of *S. cerevisiae* had an impact on the degree of inhibition of metabolic activity by copper exposure. Regardless of the state of metabolism, Cu^2 ions (as $CuSO_4$) had greater inhibitory effect than 28 nm CuO NPs followed by the 64 nm CuO NPs.

2.4.4 *Effect of copper oxide nanoparticle aging on yeast metabolism*

To unravel the toxic effect of released Cu^{2+} from that of the CuO NPs, *S. cerevisiae* cells were exposed for 1.5 h to several Cu exposure scenarios: fresh suspensions of NPs in YP-galactose media, aged NPs resuspended in fresh media, aged NPs within YP-galactose containing the released fraction, or the released fraction in YP-galactose without NPs (Figure 8). Among all exposure conditions, 28 nm CuO NPs inhibited *S. cerevisiae* metabolism to a greater extent than 64 nm CuO NPs exposures (Figure 8). The increased inhibitory effect of the 28 nm compared to the 64 nm CuO NPs is consistent with previous studies which frequently show greater toxicity from NPs with smaller primary particle diameter [90, 91].

The aged 28 nm and 64 nm CuO NPs within released fraction and the released fraction in the absence of CuO NPs were significantly more inhibitory of *S. cerevisiae* metabolic activity ($p<0.05$) compared to exposure to the fresh suspensions of aged CuO NPs in YP-galactose media (excluding 64 nm CuO NPs at 40 mg/L). The higher inhibition of metabolic activity of *S. cerevisiae* were observed in exposure conditions with greater amounts of Cu^{2+}. These results suggest that the presence of greater amounts of

Table 2. *Saccharomyces cerevisiae* cell metabolic rate IC_{50} values in response to copper exposure.

IC_{50} (mg CuO/L)	28 nm copper oxide nanoparticles	64 nm copper oxide nanoparticles	Copper sulfate
YP-dextrose	305 ± 67.2	468 ± 27	10.3 ± 2.0
YP-glycerol	224 ± 30.4	304 ± 38	5.3 ± 2.0
YP-ethanol	96.0 ± 23	224 ± 52	2.7 ± 0.03
YP-galactose	88.0 ± 15.2	216 ± 18	2.4 ± 0.5

Cells were treated for 1.5 hour copper treatments exposure in YP media with selected carbon sources.

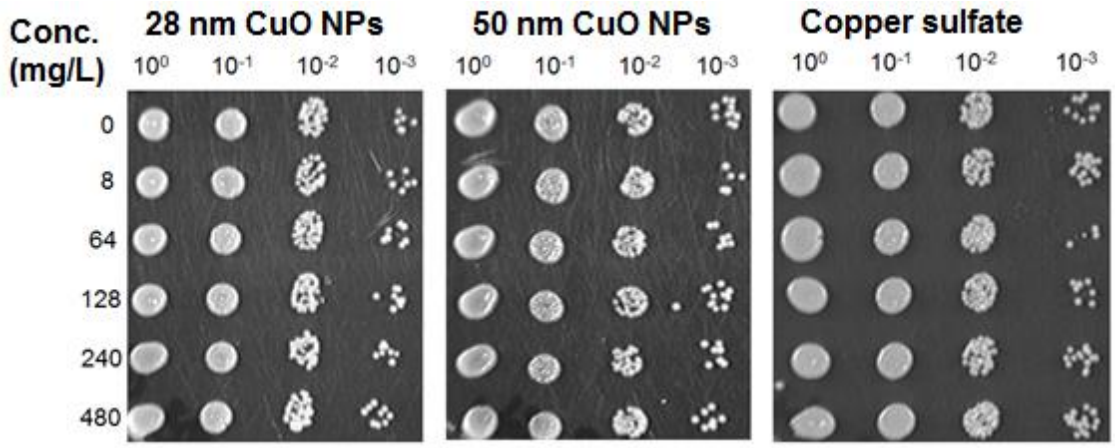

Figure 7. The effect of copper exposure on *S. cerevisiae* viability. Images are representative of spot assays performed on agar plates with all carbon sources (dextrose, glycerol, and galactose) and at different time of exposure (1.5, 24, and 48 hrs). Cell suspensions were serially diluted and incubated on agar plates for 72 hours at 30°C.

released Cu ions, including the measured Cu^{2+} form, had increased toxic effect on *S. cerevisiae* in the presence or absence of CuO NPs compared to freshly resuspended CuO NPs, containing lower amounts of Cu^{2+} (Figure 8). The aged 64 nm CuO NPs after resuspension in fresh YP-galactose showed significantly greater metabolic inhibition ($p<0.01$) at initial mass of 80 mg/L compared to 40 mg/L in the presence of similar concentrations of released Cu^{2+} (Table 3 and Figure 8). The observed dose dependent effect of aged CuO NPs at similar concentrations of released Cu^{2+} indicates the decrease in metabolic activity observed in aged 64 nm CuO NPs treatment is due to the NP component.

The difference in metabolic rate inhibition from freshly resuspended and aged NPs, and the presence of the released Cu^{2+} fractions suggest that both the released Cu ions as well as the CuO NP component have a role in the observed impact on *S. cerevisiae* metabolism.

2.4.5 Effect of chelating Cu ions in nanoparticle exposure scenarios

The CuO NPs employed released Cu ions when suspended in YP-galactose, an effect not observed in water (Table 3). Chelation of Cu^{2+} ions by EDTA addition significantly decreased the metabolic inhibition by aged 28 nm CuO NPs within the released Cu fraction ($p<0.05$) and the released Cu fraction in the absence of 28 nm or 64 nm CuO NPs ($p<0.05$, $p<0.01$, respectively, Figure 9). There was no significant difference of metabolic activity of *S. cerevisiae* in the presence of EDTA of freshly resuspended and aged 28 nm and 64 nm CuO NPs in fresh YP-galactose media nor the aged 64 nm CuO NPs within media containing the released Cu fraction. The observation that under low concentrations of Cu^{2+} present in the NPs exposure scenarios, the addition of EDTA caused no significant change in metabolic activity may suggest that the toxicity observed was due to the NPs structural component.

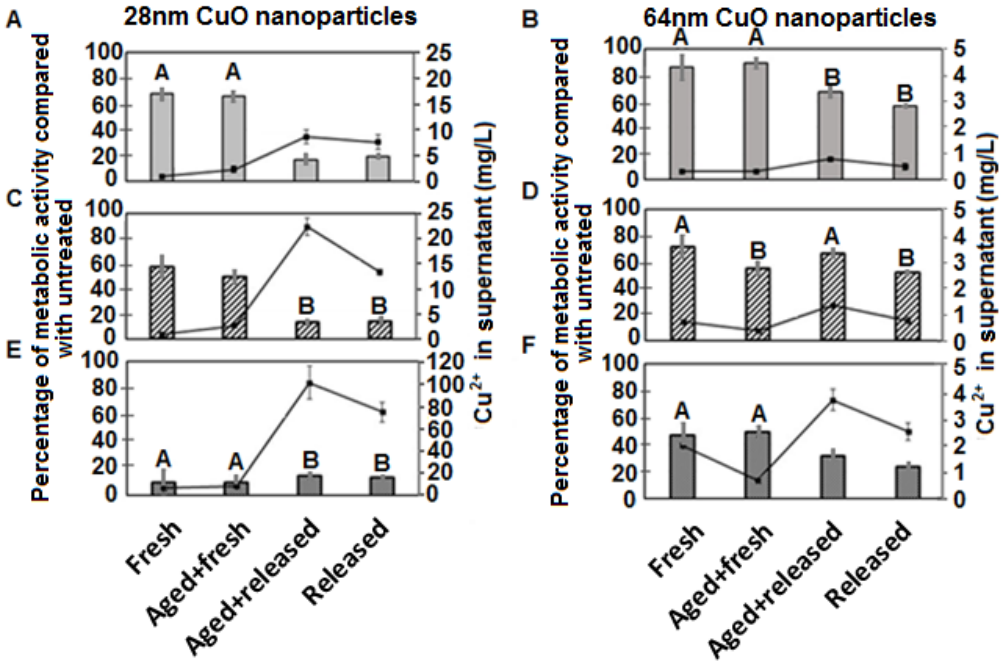

Figure 8. The inhibition of *S. cerevisiae* of metabolic activity after treatment with 28 nm and 64 nm copper oxide nanoparticles and associated copper exposures. Copper oxide nanoparticle effect was assessed using AlamarBlue assay at 40 mg/L (A, B), 80 mg/L (C, D) and 240 mg/L (E, F) after 1.5 hour exposure. The bar graph represents results expressed as percent metabolic activity compared to untreated cells. The line graph represents Cu^{2+} ions released into YP-galactose medium from each respective treatment. Results are presented as mean ± standard deviation of 3 independent experiments. Significant results as compared to the other treatments (bar graph, $p<0.05$) are marked with letters, values with the same letter indicate they are not significantly different from one another. Error bars represent standard deviation.

Chelation of copper ions with EDTA often resulted in a decrease in inhibition (10% to 30% decrease of metabolic inhibition with 28 nm and 64 nm CuO NPs exposure scenarios containing the released fraction), though not a complete recovery of cellular metabolic activity. This may in part be explained by the copper bioavailability, as the chelation of Cu^{2+} ions may not affect the bioavailability of Cu^{2+} ions towards *S. cerevisiae.* A study performed by Li *et al* [92] with ZnO NPs and Zn^{2+} ions suggests that

a decrease in free metal ions does not necessarily result in a subsequent decrease in the bioavailable ions that can interact with cells.

The chelation of Cu^{2+} did result in a dramatic reduction in toxicity of several CuO NPs exposure scenarios, though not a complete recovery, suggesting that both the released Cu ions as well as the CuO NP component have a role in the observed inhibition of cellular metabolic activity.

2.5 Discussion

The physiochemical properties of nanomaterials, such as aggregation, zeta-potential, crystal structure, roughness, primary particle size, agglomeration, and dissolution, have been shown to be a factor in relation to their potential cytotoxicity [82, 87, 88]. We examined the impact of CuO NPs with measured differences in primary particle size, crystal structure, and rate of dissolution in the growth media on *Saccharomyces cerevisiae* cellular metabolic rate.

The commercially available 28 nm and 64 nm CuO nanoparticles used in the present study were characterized utilizing Transmission Electron Microscopy (TEM), Zetasizer, and Nanosight Tracking Analysis (NTA). TEM has the advantage of providing a direct image of particle size and morphology at high resolution (Figure 6). The 28 nm CuO NPs appeared as spherical with an average primary particle diameter of 28.4 nm with a range from 17.3 nm to 39.5 nm and the 64 nm CuO NPs had irregular shapes with a small population of NPs showing spherical shapes with an average particle diameter of 64.2 nm within a range of 11.7 to 120.7 nm. Catalytic properties, specifically structure-sensitive reactions usually involving oxygen-oxygen bonds, are dependent on particle size [93, 94]. The CuO NPs used in the present study also demonstrated similar rough surfaces which has been associated with differences in the amount and identity of proteins absorbed on the nanoparticle surface [95]. The 28 nm and 64 nm CuO NPs

showed different orientations of crystal planes on the surface of the NPs which may have implications in the available catalytic sites, as implicated with TiO_2 nanoparticles [96, 97]. Both CuO NPs used in the present study had similar low zeta-potentials (Table 1), indicating the CuO NPs had equal potential to form aggregates and agglomerates in the growth media [98].

In complement to the TEM, NTA was used to measure particle size in solution in real time with the advantage of needing little to no sample preparation (Figure 6). NTA permits the measurement of single nanoparticles, aggregates, or agglomerates in solution greater than 10 nm in size [99]. Aggregation of CuO NPs, as determined in water after sonication, showed greater hydrodynamic diameter in both CuO NPs compared to the primary particle size. Aggregation of uncoated, unmodified oxide nanoparticles is considered to be an intrinsic property [100, 101]. The lack of dispersal of the CuO NPs by sonication suggests either fusion or strong bonding of the primary particles or reformation of aggregates after dispersal [100]. Agglomerations consist of interactions between NPs, aggregates of NPs, and media components generating formation of clumps or clusters of primary particles and organic molecules. The CuO NPs within the growth media used in the present study displayed hydrodynamic diameters greater than in water and greater than the primary particle diameter, indicating formation of agglomerates. The aggregation and agglomeration observed in our study has been reported elsewhere for CuO in water [76, 87], yeast growth media [76], in the presence of small amounts of organic material [94], and several different natural waters [87]. Aggregation and agglomeration are important attributes to measure as they decrease the available NP surface area that facilitates interaction with living cells and media components.

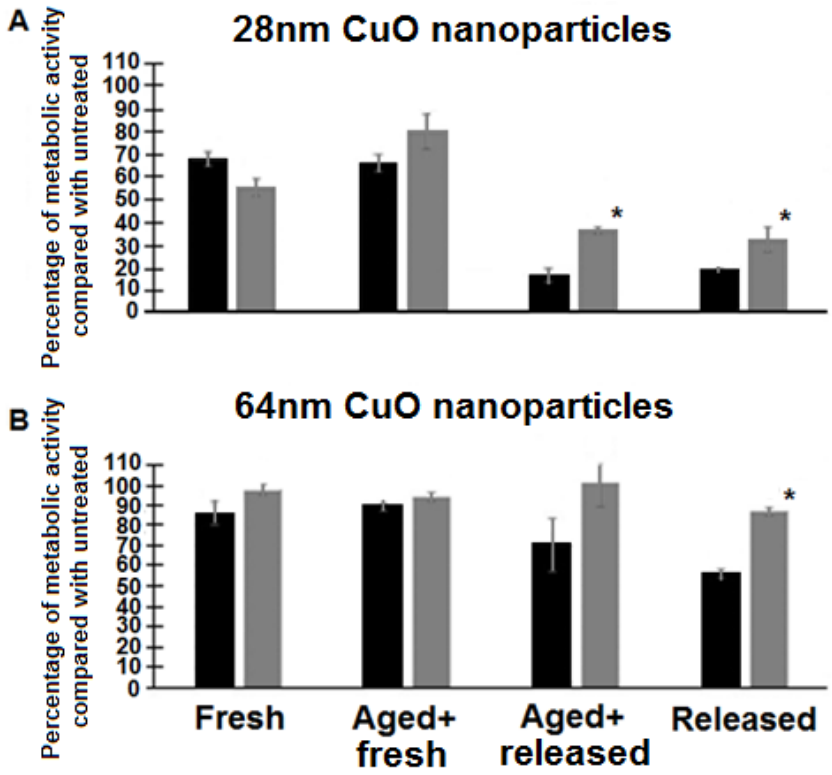

Figure 9. The inhibition of *S. cerevisiae* metabolic activity after chelating copper ions released from copper oxide nanoparticles. The copper oxide nanoparticles effect on *S. cerevisiae* metabolism after 1.5 hour exposure at 40 mg/L of 28 nm (A) or 64 nm (B) CuO NPs was assessed using AlamarBlue assay. Black bars represent treatment without chelation and grey bars represent treatment with the addition of EDTA at 0.5 mM. Data are expressed as percent metabolic activity compared to untreated cells. Error bars represent standard deviation of 3 independent experiments. Significant differences between treatments without chelation compared to treatment with EDTA are indicated with an asterisk ($p<0.05$).

The effect of particle size on dissolution was investigated by comparing Cu^{2+} ion release from 28 nm and 64 nm CuO NPs within double distilled water and the complex biological media used in the present study (Table 3). The dissolution of the CuO NPs showed that only a small fraction (3.6%) of the CuO NPs dissolute within the 1.5 hour after addition to the growth media. After 24 hour within the media, the dissolute concentration of the CuO

Table 3. The concentrations of Cu^{2+} ions released from copper oxide nanoparticles in growth media over time.

28 nm copper oxide nanoparticles				
	Conc. (mg/L)	**1.5h[a]**	**5.5h**	**25.5h**
YP-galactose	40	0.95 ± 0.11	2.54 ± 0.15	8.67 ± 1.40
	80	0.93 ± 0.51	5.35 ± 0.53	22.35 ± 1.7
	240	6.98 ± 1.0	10.62 ± 0.22	101.1 ± 15.0
sterile water	40	BDL	BDL	BDL
	80	BDL	BDL	BDL
	240	BDL	BDL	BDL
64 nm copper oxide nanoparticles				
	Conc. (mg/L)	**1.5h**	**5.5h**	**25.5h**
YP-galactose	40	0.34 ± 0.08	0.59 ± 0.07	0.79 ± 0.07
	80	0.71 ± 0.08	0.83 ± 0.02	1.36 ± 0.03
	240	1.96 ± 0.06	2.56 ± 0.13	3.66 ± 0.4
sterile water	40	BDL	BDL	BDL
	80	BDL	BDL	0.17 ± 0.02
	240	BDL	BDL	0.32 ± 0.04

Data are mean of 3 replicates of 2 independent experiments ± range of values. [a] Period of time nanoparticles were incubated in media or water. BDL = below detection limit of Zincon assay (0.24 mg/L).

NPs increased to as much as 52.7%. The observed dissolution of Cu^{2+} from CuO NPs was consistent with results reported elsewhere for growth media rich in organic material [102, 103]. The 28 nm CuO NPs showed greater dissolution than 64 nm CuO NPs. Differences in the amount of Cu ions released from different sized CuO NPs have been described elsewhere [17]. The Ostwald-Freundlich equation predicts that as particle size decreases the equilibrium solubility of particles increases, therefore, smaller nanoparticles would have a greater propensity for dissolution [104]. Factors such as surface curvature and roughness, in addition to size, may affect surface area and play a role in dissolution of nanoparticles [104]. The size dependent dissolution observed in the

present study may be related to the greater surface area with, and particle number of, the 28 nm CuO NP compared to 64 nm CuO NP at equal mass [105]. The difference in exposed crystal structures of 28 nm and 64 nm CuO NPs on the surface may be leading to different surface chemistries with more reaction sites and thus result in different amounts of Cu^{2+} ion release [97].

The IC_{50} for the acute inhibitory effect of CuO nanoparticles and $CuSO_4$ to *S. cerevisiae* metabolic activity were compared (Table 3). The exposure to increasing concentrations of CuO NPs and copper salt led to decrease in metabolic activity (Table 4). When exposure occurred in YP-galactose, Cu salt had significantly greater effect on metabolic activity (IC_{50}: 0.96 mg Cu/L) compared with the 28 nm CuO NPs (IC_{50}: 70.3 mg Cu/L) which were subsequently more toxic than 64 nm CuO NPs (IC_{50}: 172.6 mg Cu/L). *S. cerevisiae* under respiratory conditions were more sensitive to CuO NPs exposures compared to fermentative conditions which may implicate respiratory metabolism or the mitochondria in facilitating CuO NPs toxicity, as suggested with gold nanoparticles [106], however we have no direct evidence if this is the case.

The lower toxic effect of CuO nanoparticles compared to Cu salts has been shown in the gram-negative bacteria *Escherichia coli* [74] and *Vibrio fischeri* [107], the protozoa *Tetrahymena thermophila* [77], and the freshwater crustacean *Thamnocephalus platyurus* [107]. In our study, *S. cerevisiae* demonstrated greater resistance to the toxicity of the CuO NPs when compared to the reported EC_{50} of the microalgae *Pseudokirchneriella subcapitata* (0.57 mg Cu/L, [73]) and the crustacean *Thamnocephalus platyurus* (1.7 mg Cu/L, [107]). However, the range of concentrations used is similar to other studies as indicated by similar EC_{50} found in the protozoa *Tetrahymena thermophila* (127 mg Cu/L, [77]) and the bacteria *Bacillus subtillis* (48.8 mg Cu/L [102]) and *Streptococcus aureus* (52.5 mg Cu/L [73]) . The observed size dependent metabolic inhibition of smaller primary particle size yielding greater toxicity is

consistent among metal oxide nanoparticles [17, 90, 108]. The inhibitory effect due to differences in primary particle size is confounded by the release of Cu^{2+} ions through dissolution, which is greater in the 28 nm CuO NPs compared to the 64 nm CuO NPs which may explain the increase in impact on cellular metabolic activity.

To unravel the inhibitory effect of the released soluble Cu and that of the structural NPs component, the 28 nm and 64 nm CuO NPs were resuspended in the growth media for 24 hour prior to separation of the remaining nanoparticles and the released copper ions in solution. *S. cerevisiae* was then exposed to freshly resuspended CuO NPs, the aged CuO NPs within the growth media containing the released Cu^{2+}, the aged CuO NPs separated from the released Cu^{2+}, and the growth media containing the released Cu ions in the absence of nanoparticles. The 64 nm CuO NPs freshly resuspended in growth media, independent of aging, showed increased cellular metabolic inhibition with increased NPs mass between 40 and 80 mg/L despite similar release of Cu^{2+} indicating that the increased effect on metabolic activity was due to the presence of more nanoparticles. While 28 nm CuO NPs showed a similar increase in measured inhibitory effect with greater concentration of NPs at similar concentrations of Cu^{2+} released in the fresh media, the increase was not statistically significant. The soluble Cu ions released from CuO NPs did not fully explain the observed toxicity to *S. cerevisiae*, as observed also by [75].

Metabolic activity inhibited by CuO NPs was recovered by chelation of copper ions with EDTA (Figure 9). The recovered metabolic activity from chelation was more dominant in 64 nm CuO NP compared to 28 nm CuO NPs. However, the presence of EDTA did not remove the metabolic inhibition of the aged or freshly resuspended NPs in media with low amounts of soluble copper indicating that the NPs were the cause of the observed effect at the lower dose of exposure. Combined, these results suggest that the observed CuO NPs inhibition of *S. cerevisiae* cell metabolic activity is related to both the

nanoparticle, as well as, the released Cu ions. While the 28 nm CuO NPs showed greater inhibitory effect compared to 64 nm CuO NPs, this is most likely due to greater surface area and number of particles present at the same NPs mass [105].

The observed inhibition of cell metabolic activity rate but not impact on cell viability upon exposure up to 480 mg/L CuO NPs suggests that *S. cerevisiae* might utilize a mechanism such as cell cycle arrest, as found in human epithelial A549 cells [109], to escape cell death. Cu is a redox active chemical involved in reactions leading to oxidative stress in cells. At the same time copper is eliciting antioxidant activity by acting as a redox site in superoxide dismutase (SOD1) for dismutating superoxide radicals. *S. cerevisiae* is a great model to study how CuO NPs and the released Cu^{2+} influence these processes and further experimental work needs to be pursued. The specific pathways involved in *S. cerevisiae* response to sublethal concentrations of CuO NPs will be further studied by whole genome analyses.

2.6 Conclusion

The present study shows that under the tested conditions CuO nanoparticles had less effect on *S. cerevisiae* metabolic activity compared to copper salts, while the observed inhibition from the nanoparticles was not fully explained by the released copper ions from the dissolving nanoparticles. The presence of a nanoparticle size-related effect may be related to the different physicochemical characteristics rather than only size. The present study also demonstrated a greater CuO NP effect on the metabolic activity of *S. cerevisiae* grown under respiring conditions. Future work in yeast should focus on the possible different impacts on metabolic pathways involved in respiring and fermenting cells and determine differences in cell response related to the nanostructure compared to dissolved soluble metals.

Table 4. The change in rate of metabolism of *Saccharomyces cerevisiae* cells after copper exposure.

28 nm copper oxide nanoparticle exposure scenarios					
	Conc. (mg/L)	Fresh NPs in Fresh Media	Aged NPs in Fresh Media	Aged NPs in Released Fraction	Released Fraction
Without EDTA	**40**	68.1+/-9.2	66.0+/-3.8	16.7+/-2.9	19.2+/-0.5
	80	57.6+/-3.2	49.5+/-5.2	13.2+/-2.1	13.8+/-2.6
	240	9.9+/-5.1	9.3+/-0.6	14.3+/-0.5	13.2+/-1.2
With EDTA[a]	**40**	55.2+/-3.5	79.7+/-7.7	36.4+/-1.5	32.4+/-5.4
	80	36.0+/-1.1	66.2+/-6.6	13.1+/-1.2	13.9+/-1.3
	240	5.8+/-0.3	20.3+/-9.3	10.2+/-4.9	14.8+/-3.4
64 nm copper oxide nanoparticle exposure scenarios					
	Conc. (mg/L)	Fresh NPs Fresh Media	Aged NPs Fresh Media	Aged NPs in Released Fraction	Released Fraction
Without EDTA	**40**	85.8+/-5.6	89.2+/-2.0	70.0+/-13.0	56.3+/-2.1
	80	71.7+/-6.3	54.9+/-4.1	66.5+/-0.6	52.1+/-6.8
	240	46.8+/-1.8	49.3+/-6.9	31.7+/-7.8	23.5+/-0.4
With EDTA[a]	**40**	97.2+/-2.6	93.7+/-2.2	101.1+/-12	86.5+/-2.1
	80	82.3+/-2.9	80.3+/-2.6	79.6+/-2.5	84.9+/-2.5
	240	60.7+/-5.7	60.8+/-0.3	57.9+/-3.6	61.3+/-2.3

Results are expressed as percent metabolic activity of *S. cerevisiae* compared to untreated cells. Data are mean of 3 replicates of 2 independent experiments ± range of values. [a] 0.5 mM EDTA added 1 hour prior to addition of cells. NPs = nanoparticles.

CHAPTER 3

COMPARING THE EFFECTS OF COPPER OXIDE NANOPARTICLES TO THAT OF THEIR RELEASED COPPER IONS ON *Saccharomyces cerevisiae* GENE EXPRESSION

3.1 Abstract

The increasing use of copper oxide nanoparticles (CuO NPs) makes occupational and environmental exposure more likely. While the toxic effects of Cu ions on the gene expression of the model organism *Saccharomyces cerevisiae* is well studied, the effects of CuO NP on gene expression remain unknown. The mechanism of toxicity on *S. cerevisiae* from CuO NPs treatment remains complex as it may primarily be attributed to the released Cu ions but the nanoparticle itself might contribute to the previously observed inhibition of cell metabolic activity. To this end, the effect of both 28.4 nm CuO NPs and the nanoparticle released Cu ions in the growth media on *S. cerevisiae* gene expression was analyzed via microarray analysis.

After copper treatments a total of 137 genes displayed differential expression compared to untreated cells with 108 genes responding to both CuO and released Cu ion exposures while 26 genes were only altered compared to untreated after exposure with the CuO NPs. It was observed that both copper exposures resulted in an increase in carbohydrate storage, a decrease in protein production, protein misfolding, increased membrane permeability, and cell cycle arrest.

Exposure to the CuO NPs resulted in a difference in stress response as cells appeared to induce cell cycle arrest via a separate pathway, compared to the Cu ion exposure. Scanning electron microscopy revealed the 28.4 nm CuO NPs adsorbed to the cell exterior suggesting close proximity of Cu ion release that facilitates membrane damage. To the best of the author's knowledge, this is the first work to compare changes

in *S. cerevisiae* gene expression after CuO NPs compared to released Cu ions exposure.

3.2 Introduction

The incorporation of nanoparticles (NPs) in commercial and consumer goods has resulted in a billion dollar industry [1]. The large surface area to size ratio of NPs enable them to have useful material properties that may induce harm when these NPs interact with cells. Therefore, it is necessary to develop an understanding of the potentials of NPs to induce cellular stress response or cause toxicity. A review of many metal oxide nanoparticles and their toxicity on several model organisms revealed soluble copper to be more toxic to bacteria, algae, and aquatic organisms, while the CuO NPs were more toxic to mammalian cells and yeast [2]. The release of Cu ions from CuO NPs makes it difficult to differentiate the toxic effects of Cu ions from that of the NPs itself on molecular level [3]. To this end, the mechanism of toxicity of CuO NPs continues to remain in question with some in support of released Cu ions as the only source of toxicity [3] and others propose the NPs structural component may influence nanotoxicity [2, 4, 5].

A study observing changes in yeast gene regulation after copper sulfate exposure observed an increase in expression of genes related to binding free copper within the cell [6]. A majority of genes increased in expression were involved in to metabolism of methionine, lipid and fatty acids, carbon compounds, and carbohydrates. Additionally, many genes induced in expression were involved in the functional categories of ‘cellular transport’, ‘cell rescue, defense, and virulence’, and ‘cell cycle and DNA processing’ [6]. Copper exposure also resulted in changes in gene regulation related to metal ion homeostasis in a separate study [7]. Jin *et al.* also observed changes in regulation of genes coding for proteins involved in metabolism of both carbohydrates and fatty acids. Thus, identifying changes in yeast gene regulation after

CuO NPs exposure, as well as a separate exposure to the released copper ions, will help to further define the causative agent of CuO NPs toxicity as this currently remains in question.

An analysis of *Saccharomyces cerevisiae* (*S. cerevisiae*) transcriptomic response to copper and other heavy metals, including cadmium, chromium, and mercury, observed a number of genes altered in regulation [7]. Interestingly, copper exposed yeast were observed to drastically decrease expression of genes related to ribosomal functions and protein production. Exponentially growing yeast spend up to 50% of cellular energy in ribosome and protein production, therefore limiting this energy expenditure would enable that energy to be put into defensive mechanisms to deal with stress [7]. Toxic levels of Cu ions may have resulted in cell membrane damage in yeast as suggested by the increased expression of cell wall biosynthesis genes [6]. It is proposed that reactive oxygen species (ROS) generated from Cu ions may induce lipid peroxidation and results in damage to the yeast cell membrane. The induction of several ROS scavengers supports the suggestion of oxidative stress from Cu ions causing the membrane damage [6]. This ROS generation may in part also be responsible for the unfolded protein response suggested by the increased expression of heat shock proteins after copper exposure. The changes in *S. cerevisiae* gene expression observed in a separate study after copper sulfate exposure resulted in increased proteasome-related genes, suggesting damage to proteins [14]. The other major category of up-regulated genes was related to stress response, specifically genes encoding copper metallothioneines and other copper binding proteins.

S. cerevisiae contains several genetic pathways involved in copper homeostasis (Figure 1) and has a high degree of similarity to human genes [8]. The cupric reductase *FRE2* reduces Cu^{2+} into Cu^{+}, which is then taken into the cell. Several high affinity copper transporters, *CTR1* and *CTR3*, are primarily responsible for Cu^{+} uptake, which

are regulated based on the environmental copper concentration [9]. Several cytoplasmic proteins bind free Cu^+ ions, including the metallothioneines *CRS5* and *CUP1-1*, and are regulated via Ace1p in response to an increase in Cu^+ cellular levels [10]. The copper chaperone for SOD1p, *CCS1,* incorporates Cu^+ into superoxide dismutase 1 (Sod1p), a crucial enzyme required for appropriate response to oxidative stress [11]. There are several transcription factors that react to Cu levels and induce transcriptional regulation in either copper excess (Ace1p) or copper starvation (Mac1p) [12]. The vacuole is involved in excess Cu^+ ions storage and the transporter *CTR2* allows Cu^+ transport into the cytoplasm [13].

The present study investigates changes in *S. cerevisiae* gene expression after exposure to CuO NPs, as well as the effect of released Cu ions, to elucidate the CuO NPs effect on molecular level. DNA microarrays were employed to analyze the gene expression of *S. cerevisiae* after copper exposures. Pathways of significantly affected genes from both CuO NPs and Cu ion leachate treatments were identified and compared to differentially expressed genes after CuO NPs treatment.

3.3 Material and methods

3.3.1 *Nanoparticle physicochemical characterization*

NPs diameter and morphology. The copper oxide (CuO NPs) employed in this study have already been characterized in a previous study [15] by employing transmission electron microcopy (TEM) to establish primary particle size.

NPs dispersion. A fresh stock of CuO NPs, in sterile deionized water, were stored in a dark environment to prevent light exposure (8,000 mg/L). Prior to experiments, stock solutions of CuO NPs were sonicated using a Branson Digital Sonifer for 5 mins with pulse 30 sec on, 30 sec off and diluted to working concentrations (69.5 mg Cu/L, the IC_{50} for yeast respiratory metabolism based on previous study [15]).

NPs hydrodynamic diameter and zeta potential. The Nanosight instrument was used at room temperature with a 640-nm laser and data was collected as per the protocol described in [15]. Average diameter of nanoparticles when suspended in YPG-medium was determined using the Nanoparticle tracking analysis (NTA) 2.0 Build 127 analytical software. The Zetasizer Nano-ZS (Malvern Instruments) was used to determine the zeta potential of CuO NPs in YPG-medium.

NPs dissolution. The NPs suspended in medium were removed by centrifugation at 14,000 rpm for 30 min followed by filtration (0.1µm Supor® low protein binding syringe filter, Acrodisc® PALL Life Sciences) and stored at 4°C until Cu^{2+} concentrations were measured (within 24h-48h) by Zincon assay as described in [15].

3.3.2 *Released copper ion treatment procurement and exposure conditions*

In order to generate the released Cu ion treatment, CuO NPs at 800 mg/L were incubated for 24 hr, the suspended NPs were then centrifuged (14,000 rpm 30 min) and the supernatant was then filtered (0.1 µM syringe filter, Supor® low protein binding, Acrodisc® PALL Life Sciences). The supernatant was assayed using Zincon dye as per [15] and determined to contain 200 mg Cu^{2+}/L. This supernatant was considered the 'released Cu ion' treatment stock and was diluted to a working concentration of 0.95 mg Cu/L in the cell culture. A concentrated CuO NPs stock (100 mg Cu/L) in sterile double distilled water was added to the cell culture to achieve a working concentration of 69.5 mg Cu^{2+}/L CuO NPs. The *S. cerevisiae* cell cultures in exponential phase were exposed at 75 mL volume in 250 ml glass flasks in triplicate (3 separate 75 mL cultures per treatment), and then incubated at 30^{o}C under constant shaking at 250 rpm to keep the cells and the NPs suspended. Sterile techniques were employed to sample sub-cultures at 0.5, 1, 2, 4, and 8 hours after the initial exposure. Samples were centrifuged (4,000xg

for 2 min) followed by flash freezing in liquid nitrogen and immediately stored at -80ºC until RNA could be extracted.

3.3.3 *Saccharomyces cerevisiae strains and cultivation conditions*

Saccharomyces cerevisiae (*S. cerevisiae*) W303-1A wild type (*M.2AT*a: *leu2-3,112 trp1-1 can1-100 ura3-1 ade2-1 his3-11,15*) was a kind gift of Dr. Rosemary Stuart (Marquette University, WI). The strain was maintained on YP-galactose agar plates (pH 6.6) containing 1% yeast extract (AMRESCO), 2% Bacto peptone (Difco laboratories) and 2% galactose (AMRESCO). Starter cultures were prepared from the respective master plates in 5 ml YP media with galactose as a carbon source (YPG) and grown overnight at 30ºC, 250 rpm. *S. cerevisiae* experimental cultures were started from the overnight cultures. The turbidity of the cell culture was measured via absorbance at 600 nm using a spectrophotometer (Molecular Devices) and diluted with sterile YP-galactose to an OD_{600} 0.1. The cultures were incubated under the same conditions until exponential growth was achieved (OD_{600} 0.3) and cultures were then sequentially exposed to different copper treatments.

3.3.4 *RNA extraction and subsequent cDNA production*

The *S. cerevisiae* cell pellets from all treatment time points were removed from -80ºC storage and placed on ice immediately prior to RNA extraction. The freshly thawed cell pellet was homogenized using 0.2 um zirconium oxide beads in a 2 mL polystyrene microcentrifuge tube placed inside a Bullet Blender® bead beater (Braintree Scientific, Inc) at 4ºC. The Bullet Blender® was employed at power level setting 7 for 3 min followed by 5 min incubation on ice and another round of bead beating at power level 7 for 3 min. The cell lysate was centrifuged at 4,000xg for 2 min and supernatant was transferred to

PureLink® spin column cartridge. The PureLink® RNA mini kit (Ambion®, Life technologies®) was used as per the manufacturer's instructions using spin columns and table top centrifuge. The extracted RNA was treated with DNase as per the TURBO DNA-*free*™ kit (Ambion®, Life technologies®) instructions. The cDNA was generated by using the SuperScript® III First-Strand Synthesis kit with the DNase-treated RNA as per product recommendations (Invitrogen™). Briefly, 2 ug of RNA was used in a 20 uL reaction volume in a thermocycler and run with the following program: 25^{o}C for 10 min, 50^{o}C for 30 min, 85^{o}C for 5 min followed by 4^{o}C until placed on ice. RNase H was added for 20 min, at room temperature incubation, prior to storage at -20^{o}C.

3.3.5 *Scanning electron microscopy specimen preparation*

To visualize the interaction of CuO NPs with *S. cerevisiae* cells scanning electron microscopy (SEM) analysis was performed. *S. cerevisiae* cells were treated with 69.5 mg Cu/L CuO NPs for 1 hour, followed by primary fixation with 2.5% glutaraldehyde in PBS overnight at 4^{o}C. Solution containing fixed cells was dropped onto glass slides coated in Poly-L-lysine and cells were allowed to settle onto the coated surface. Secondary fixation was performed in 1% osmium tetroxide (OsO4) in PBS for 1 hour followed by dehydration in sequential stages of ethyl alcohol and double distilled water at 20%, 40%, 70%, and 100%. Sample drying was performed using Hexamethyldisilazane (HMDS; BASF SE) at a 1:1 dilution with 100% ethyl alcohol for 10 min followed by pure HMDS solution for 10 min. After drying, glass slides were attached to 15 mm aluminum stubs using double-coated carbon tape. The samples were then coated in 6 nm Iridium with K500X sputter coater (Quorum Technologies). Imaging was performed with a Hitachi S4800 ultra high resolution cold cathode field emission scanning electron microscope at 15,000 kV in scanning electron mode.

3.3.6 *Membrane damage Staining*

To detect changes in cell membrane permeability after treatment with CuO NPs and $CuSO_4$, *S. cerevisiae* cells at 1 mL volume were stained with 5 uL of 1 mg/mL propidium iodide solution in DMSO (Biotium), washed, and subsequently stained with 5 uL of 5 mM calcofluor white M2R (MP Biomedicals). To quantify total cell number, 5 uL of 5 mM calcofluor white M2R (MP Biomedicals), dissolved in water, was added to cells. Cell solutions were incubated with both dyes at room temperature for 10 mins protected from light. After staining, cells were washed twice in water and resuspended in 100 uL volume water. The cells were imaged with a Leica inverted microscope (DMI 6000B, Leica microsystems with Leica application suite AF). The DAPI filter set was used for calcofluor white detection, with an excitation at 405 nm and emission range of 425-475 nm, the Texas Red filter set was used for propidium iodide detection, with an excitation at 561 nm and emission range of 570-620 nm. Images were analyzed using Image-J software.

3.3.7 *Microarray data analysis*

The microarray was performed at the Genome center of University of Wisconsin Madison Biotechnology Center. The Affymetrix CEL files containing the expression data for the yeast 2.0 probe set were loaded into R with the Affy package where each chip was represented as an array. Background noise correction was performed on each chip by employing Affy and using the Robust Multichip Average expression measure. Each chip was then normalized to the geometric mean of the expression of housekeeping genes (*Alg9*, *Kre1*, *Taf10*, *Tfc1*, and *Ubc6*) as suggested by Teste [16]. Normalization to the geometric mean of these genes in each chip has been shown to be much more accurate than normalization to a single gene in the analysis of microarray data [17].

These correction measures were used to transform the raw expression data into corrected, normalized log expression values.

Annotation data (such as probeID and experimental information) was extracted from the CEL files using Bioconductor's a4 package [18]. This package was also used to extract gene name, description of function, ORF, Gene Ontology numbers, and KEGG pathways from probe IDs in conjunction with the Affymetrix Yeast 2.0 chipset database, available through Bioconductor.

Linear models were fitted to each chip's logarithmic expression values with the Limma package [19]. A contrast matrix was constructed from the arrays in order to compare two different treatments (e.g. untreated and nanoparticle treatments). The package was then used to calculate the $\log_2$ fold differences in gene expression and the probability of differential expression for each probe using an empirical Bayes approach. The a4 package was used to adjust the calculated *p* values in order to account for the family wise error rate using the Benjamini Hochberg method and to generate a table of the calculated values.

Genes were considered differentially regulated after copper exposures with greater than/less than 1.5/-1.5 Log_2 Fold Change (LogFC) and an adjusted $p<0.05$. These genes were further separated into up and down-regulated categories. These genes were then submitted to Princeton University's Gene Ontology Mapper and the resulting ontologies were used to observe patters of altered gene expression [20].

The probe ID, fold change data, and KEGG pathway number annotations were also extracted from the list of differentially expressed genes. Probe IDs were converted into Entrez Gene IDs using DAVID, and further converted into KEGG gene numbers on their website [21, 22]. The fold change data for each probe in the Yeast 2.0 set associated with that KEGG pathway was then submitted to the KEGG pathway mapper tool [23].

3.4 Results

3.4.1 *Copper oxide nanoparticles and released copper ion exposures affect regulation of similar genes*

Changes in yeast gene expression were measured in order to differentiate the cellular pathways affected after CuO NPs exposure compared to released Cu ions exposure. The released Cu ions treatment contains 0.95 mg Cu^{2+}/L, which is equal to what would be released from the CuO NPs treatment after 1 hour (0.95+/-0.05 mg Cu^{2+}/L). The microarray expression results were confirmed by using qPCR as an independent gene expression profiling method, which was found to have good correlation (Table 5). The 1 hour exposure changed the regulation of 132 genes with the upregulation of 55 genes and downregulation of 53 genes.

Most of the differentially regulated genes in response to the copper treatments, 108 of the total 137 genes, were affected by both CuO NPs (69.5 mg Cu/L) and the released Cu ions treatments (0.95 mg Cu^{2+}/L). The up-regulated and down-regulated genes with 1.5 log cutoff can be found in Table 6 and Table 7, respectively. Of the 108 genes altered in regulation after CuO NPs and released Cu ion exposures, 55 genes were up-regulated and assigned to 13 pathways (Table 6) and 53 genes in 9 pathways were down-regulated (Table 7).

The effect of CuO NPs exposure on *S. cerevisiae* cells, based on changes in the regulation of genes, is suggested in section *3.4.2* that increased environmental stress is occurring. Damage from copper exposure may have resulted in lipid peroxidation (*3.4.3*), increased glycogen and trehalose accumulation (*3.4.4*), and DNA damage or replication stress (*3.4.5*). The physical interaction of the NPs-media agglomerates with the cell surface could result in damage to the cell wall. DNA damage or replication stress can

Table 5. Measured changes in regulation of genes, in the form of Log_2 fold change, with microarray and qPCR methods.

Log_2 Fold Change	**Copper oxide nanoparticle**		**Released copper ions**	
Gene Name	*Microarray*	*qPCR*	*Microarray*	*qPCR*
Hsp30	5.1	5.37	5.9	5.26
Hxt13	3.7	2.02	2.1	2.04
Crs5	3.1	2.09	2.4	1.86
Gad1	2.2	2.23	1.8	1.29
ctt1	1.7	1.9	1.4	1.67
Alg9	-0.1	0.08	-0.2	0.09
Ccs1	-0.4	0.1	-0.3	-0.06
Ctr2	-0.7	-0.42	-0.6	0.06
Act1	-2.2	-0.31	-1.4	-0.21
Clb5	-2.8	-2.3	-2.7	-1.82
Ctr1	-4.3	-3.25	-3.9	-2.89

result in cell cycle arrest through the action of cyclins. Additionally, increase in carbohydrate storage molecules, glycogen and trehalose, are related to prolonged cell cycle arrest [24].

3.4.2 *Cells respond to copper exposure by altering regulation of genes related to copper homeostasis*

Exposure to CuO NPs and released Cu ions resulted in numerous gene changes associated with the environmental stress response (ESR) pathway. A number of copper detoxification genes were changed in regulation after exposure to both CuO NPs and released Cu ions. The copper-resistant suppressor protein *CRS5* was found to be one of

Table 6. *S. cerevisiae* up-regulated genes and their pathways after copper oxide nanoparticle, copper sulfate, or both the nanoparticles and copper sulfate exposures.

Copper oxide nanoparticle specific processes	**# of genes**	**Mutually affected processes**	**# of genes**	**Released copper specific processes**	**# of genes**
Cellular processes	2	Cytokinesis	1	Protein sorting	1
Mercury resistance	1	Meiosis	1	Autophagy	1
Transporters	2	Membrane	2	Transcription	1
Signal transduction	3	Protein kinase (Signal transduction)	5		
Response to Chemical stress	2	Response to stress	11		
Metabolism	4	Protein folding and degradation	2		
		Signal transduction	1		
		DNA repair	1		
		Glycogenesis	11		
		Transporters	3		
		Transcription factors	3		
		Metabolism	7		
		Unknown	6		
Total number of genes affected	14		54		3

the most up-regulated genes. These copper metallothioneines are considered one of the main copper defense molecules [25]. Two genes required for copper import, the ferric reductase *FRE1* and the high-affinity copper importer *CTR1*, were significantly down-regulated. Proteins involved in glutathione production, related to the response to

Table 7. *S. cerevisiae* genetic pathways down-regulated in response to copper oxide nanoparticle exposure or both the nanoparticles and copper sulfate treatments.

Copper oxide nanoparticle specific processes	# of genes	Mutually affected processes	# of genes
Transportation	1	Membrane	1
Translation (Ribosome biogenesis)	2	Cell cycle-related (Cell cycle)	2
Response to chemical stress	1	Peroxisome	1
Meiosis	1	Ubiquitin mediated proteolysis	1
Unknown	1	mRNA degradation and Ribosome biogenesis	41
		Response to stress	2
		Copper transport	2
		Diphthamide synthesis	2
		Unknown	1
Total number of genes affected	**7**		**53**

Genes were assigned Gene ontology and separated based on whether gene regulation was altered by both treatments (shared) or 28.4 nm CuO NPs only.

oxidative stress, were found to be up-regulated including the glutamate decarboxylase encoded by *GAD1* and the phospholipid hydroperoxide glutathione peroxidase *GPX1*.

Cellular signaling was affected as genes related to signaling and transcriptional regulation were up-regulated after copper exposure. The protein kinases 'Mid-two like' *MTL1,* 'Viable in Hal3 Sit4 background' *VHS1,* the protein kinase *KIN82,* and 'yet another kinase' *YAK1* were all up-regulated. Several transcription factors were up-regulated including 'chromosome instability' *CIN5,* 'expression dependent on Slt2' protein *EDS1,* heat shock protein-related *MGA1,* 'up in starvation' *USV1,* and 'Zinc finger protein' *ZNF1*.

3.4.3 *Copper exposure may be causing damage to cellular proteins*

A number of genes coding for proteins usually involved in heat stress response were differentially up-regulated after both CuO NPs and released Cu ions exposures. These heat shock proteins (HSP) were up-regulated, 'Stress-inducible yeast Mpv17' protein *SYM1,* and the *HSP26* and *HSP42,* serve as protein chaperones to prevent protein misfolding. Several of the highly up-regulated genes were HSP including *HSP30*, a critical regulatory molecule and chaperone protein, and 'Stationary phase genes' *SPG1* and *SPG4*, which are required for high temperature survival (Table 8). The HSP30p is of particular importance as this transcription has been shown to be induced in response to a multitude of stressors including heat shock, osmostress, weak acid exposure, and even glucose limitation [26]. The stress-induced expression of HSP30 has been suggested to play an energy conservatory role as it limits unnecessary ATP consumption by regulating the activity of the H^+-ATPase PMA1p [26]. The transcription factor *MGA1* is similar to a heat shock transcription factor and was found to be up-regulated, suggesting damage to proteins may be occurring (Table 8). Protein damage may be the result of divalent metal ion replacement or lipid peroxidation from increased oxidative species [27, 28]. Increased generation of oxidative stress at the periphery of the cell can also result in lipid peroxidation of the cell wall [29].

3.4.4 Copper oxide nanoparticles interact with cell surface and may induce damage to cell wall

The interaction of NPs with the *S. cerevisiae* cell surface may be facilitating damage to the cell. SEM imaging of yeast cells after exposure to CuO NPs reveals nano-sized particles bound to the yeast cell surface (Figure 10A), which were absent in untreated cells (Figure 10B). The NPs agglomerates bound to the cell's exterior were

Table 8. *S. cerevisiae* top 10 up-regulated genes in response to both copper sulfate and copper oxide nanoparticles.

Systemic name	Standard name	Log_2FC CuO NP	Log_2FC Cu ions	Adj. *p* value CuO NPs	Adj. *p* value Cu ions	Basic description
YGR249W	HSP30	5.13	5.88	0.001	0.003	Stress response protein
YEL069C	SPG4	3.93	2.68	<0.001	0.003	Required for high temp survival
YGL096W	MGA1	3.72	4.37	0.009	0.029	Heat shock transcription factor
YGR236C	HXT13	3.65	2.57	0.001	0.003	Hexose transporter
YEL069C	TOS8	3.38	2.95	0.001	0.007	Putative transcription factor
YER054C	SPG1	3.24	2.1	0.001	0.003	Required for high temp survival
YER150W	SPI1	2.95	2.75	0.004	0.019	Involved in weak acid resistance
YBR147W	GIP2	3.15	2.63	0.001	0.004	Involved in glycogen synthesis
YGR249W	CRS5	3.10	2.45	<0.001	0.003	Cu-binding metallothionein
YEL069C	RTC2	3.10	2.61	0.001	0.004	Cationic amino acid transporter

examined using energy-dispersive x-ray spectroscopy (EDS) (Figure 10D). The EDS spectrum confirms the presence of copper within the nanoparticle agglomerates attached to cell surface (Figure 10E). Damage to the cell wall by the attached NPs at the exterior of the cell is suggested by increased expression of genes related to cell wall

biosynthesis. The transcription factor *USV1* is related to regulation of cell wall biosynthesis genes and *RTN2*, a reticulon-like protein involved in stabilizing membrane curvature, were both up-regulated after copper exposure. The gene with the most up-regulation, *HSP30*, also acts as an activator for *PMA1,* which is an H^+- ATPase that is responsible for ion homeostasis. Changes in ion homeostasis are a frequent problem encountered in cells after cell membranes have become permeable from damage.

To directly examine the effect of Cu exposure on cell membrane integrity, the DNA-binding fluorescent dye propidium iodide (PI) was employed. Cells were stained with PI after exposure to both CuO NPs and $CuSO_4$ for 4 hours (Figure 11). Cells exposed to 28 nm CuO NPs as well as $CuSO_4$ displayed significantly greater fluorescent dye intake ($p<0.01$) compared to untreated yeast. This cell staining data further supports membrane damage suggested by the gene expression data.

3.4.5 *Cells increase energy reserves by altering ribosome biogenesis and increased carbohydrate storage*

When cells enter a state of stress, energy is frequently conserved through the storage of carbohydrates as well as a decrease in protein synthesis [30]. Several up-regulated genes were in response to both CuO NPs and released Cu ions were involved in the synthesis and accumulation of the energy storage carbohydrate molecules, glycogen and trehalose (Table 9). There were 11 up-regulated genes in the glycogenesis pathway including glycogen branching enzymes, glycogen synthases, and several subunits of the main trehalose synthase molecule.

Over 30 genes involved in various stages of protein production were significantly down-regulated (Table 10, Table 11), suggesting a decrease in cellular transcription. Among these were genes involved in various aspects of protein synthesis including mRNA processing, mRNA degradation, 18s rRNA maturation, and 60S ribosome

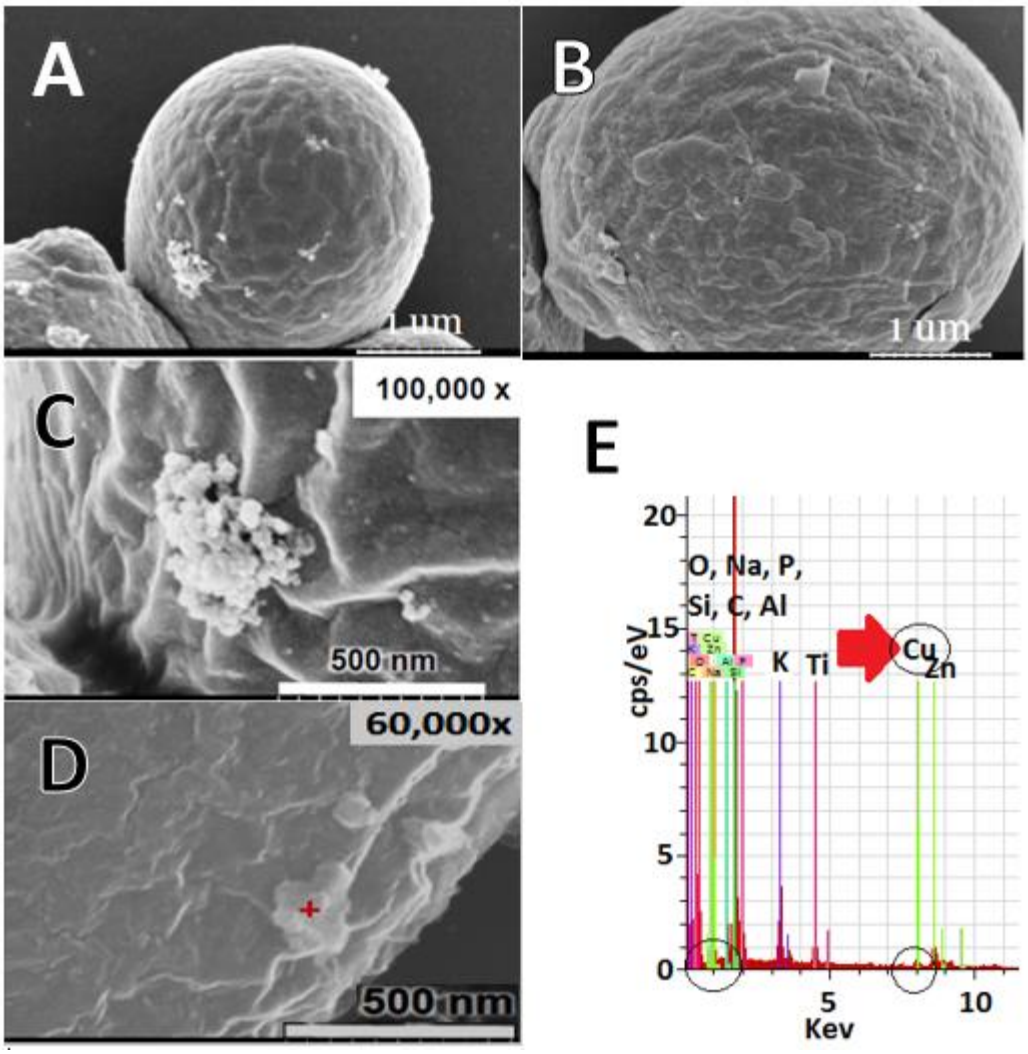

Figure 10. Scanning electron micrographs of *S. cerevisiae* cells after exposure to copper oxide nanoparticles. Scanning electron micrographs depicting yeast cells were exposed to 28.4 nm copper oxide nanoparticles and subsequently found to be adsorbed to the cell membrane (A, C) which is not observed without the addition of nanoparticles (B). To confirm the attached particles are indeed the copper oxide energy-dispersive X-ray spectroscopy was performed (D) which identified spectrum peaks at locations which confirm copper in the attached nanoparticles (E).

components. Several of the genes most down-regulated were involved in ribosome biogenesis. These ribosome-related down-regulated genes include 'ribosomal RNA processing' protein *RRP36*, necessary for early cleavage of 35S pre-rRNA and 'Brefeldin A resistance' protein *BFR2*, involved in pre-18S rRNA processing. Additional genes

Table 9. Up-regulated *S. cerevisiae* genes related to the glycogenesis and trehalose synthesis pathways.

System Name	Standard Name	Basic description
YEL011W	GLC3	Glycogen branching enzyme
YDL079C	MRK1	Glycogen synthase kinase 3 homolog
YFR015C	GSY1	Glycogen synthase
YKR058W	GLG1	Glycogenin glucosyltransferase
YFR017C	IGD1	Cytoplasmic, inhibits glycogen debranching activity
YDR074W	TPS2	Phosphatase subunit of the trehalose-6-P synthase
YML100W	TSL1	Large subunit of trehalose 6-phsphate synthase complex
YER054C	GIP2	Regulatory subunit of protein phosphatase Glc7p
YIL045W	PIG2	Type-1 protein phosphatase targeting subunit
YOR178C	GAC1	Regulatory subunit for Glc7p type-1 protein phosphatase
YBR050C	REG2	Regulatory subunit of the Glc7p type-1 protein phosphatase

include the ‘Exit from G1’ protein *EFG1*, ‘Translation initiation factor Four A Like’ *FAL1,* ‘Lethal with conditional Pap1’ *LCP5,* and ‘U three protein’ *UTP5*. The 18S rRNA was not the only ribosome component affected as genes coding for components of the 60S ribosome were also down-regulated such as nulceolar G-protein *NOG2*. Other ribosome protein *RSA4*. Genes found to be down-regulated included the ‘Arginine methyltransferase-interacting RING finger’ protein *AIR1*, for RNA processing and degradation, and ‘Ribosome assembly’ protein *RSA4,* used in 60S maturation and transport (Table 11). Several RNA helicases dead box proteins *DBP2* and *DBP7* and the and thus is considered a key regulatory molecule for mitotic and meiotic cell up-regulated genes include the ‘Arx1 little brother’ protein *ALB1*, ribosome assembly cycle

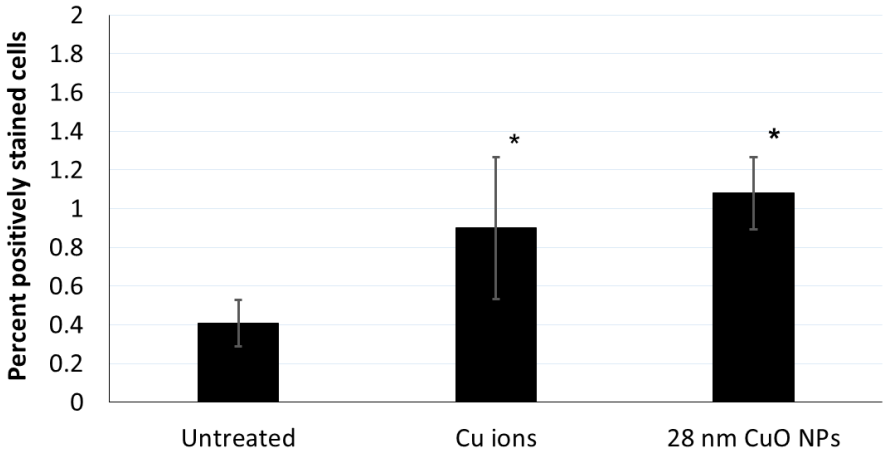

Figure 11. The percent of stained cells, as a measure of membrane damage, after exposure to CuO NPs or Cu ions (in the form of copper sulfate). Cells were exposed to 69.5 mg Cu/L copper oxide for 4 hrs and membrane damage, as measured by intake of propidium iodide dye.

progression [32]. *PCL1*, another important Pho85 cyclin, was down-regulated after copper exposure and is responsible for regulating cell cycle progression by interacting with the cyclin-dependent kinase Pho85p [33]. Cell cycle arrest may also be occurring through the up-regulation of *YLR149C*, which can induce cell cycle arrest and often increases in abundance in response to DNA replication stress [34]. DEAH-box RNA helicase *DHR2* were observed to become down-regulated after copper exposure. Genes involved in metabolic functions were also up-regulated after exposure to both copper exposures including genes involved in pyrimidine, leucine biosynthesis, and the pentose phosphate pathway. Metabolite transporters were up-regulated including hexose transporter *HXT13* and maltose transporter *MAL11*.

3.4.6 *Yeast cells undergo cell cycle arrest in response to copper exposure*

Genes related to cell cycle progression were changed in regulation including Pho85 cyclin *PCL1*, cyclin B *CLB6*, and yeast homeobox *YOX1*, which suggests cells are beginning to induce cell cycle arrest (Table 12). Clb6p is an important cyclin responsible for activating the cyclin-dependent kinase Cdc28p, which is responsible for a variety of cellular functions including transcription, growth, and morphogenesis [31].

Cell cycle arrest might explain the observed significant effects on *S. cerevisiae* cell metabolic activity after both CuO NPs and copper sulfate exposures in our previous study [15]. The employed copper concentrations significantly inhibited cell metabolism but did not affect yeast cell viability, which could be explained by cell cycle arrest.

3.4.7 *Copper oxide nanoparticles induce changes in gene regulation not observed after released copper ion exposure*

To differentiate the effects from the nanoparticle structure from those of the released Cu ions, genes that were up or down regulated only in response to CuO NPs exposure were organized into pathways and compared to genes regulated after released copper ion exposure. Yeast displayed a different response to stress, as observed as changes in the regulation of genes, after CuO NPs exposure compared to released Cu ions exposure. CuO NPs exposure resulted in 14 up-regulated genes and 7 down-regulated genes that were not changed in regulation after exposure to released Cu ions. Among these are genes encoding several proteins involved in energy production and cell cycle progression.

The CuO NPs exposure resulted in up-regulation of genes in 7 pathways including energy production, transporter activity, and amino acid metabolism. Contrary to changes in gene regulation from both CuO NPs and released Cu ions, several of the genes up-regulated only from CuO NPs exposure were involved in energy production

Table 10. The down-regulated *S. cerevisiae* genes in response to both copper sulfate and copper oxide nanoparticles.

Systemic name	Standard name	Log_2FC CuO NP	Log_2FC Cu ions	*p* value NPs	*p* value Cu ions	Basic description
YPR124W	CTR1	-4.34	-3.86	<0.001	0.001	High-affinity Cu transporter
YLR214W	FRE1	-4.29	-3.90	<0.001	0.002	Ferric/Cupric reductase
YJR097W	JJJ3	-3.44	-3.18	0.001	0.009	Involved in dipthamide synthesis
YOR287C	RRP36	-2.88	-2.29	0.001	0.034	Component of 90S pre
YNL289W	PCL1	-2.88	-3.00	0.001	0.019	Cyclin, regulates growth and cell cycle progression
YGR109C	CLB6	-2.83	-2.70	0.001	0.014	Cyclin, involved in DNA replication (Sphase)
YDR299W	BFR2	-2.78	-2.38	0.001	0.004	Component of SSU, 90S preribosome
YIL079C	AIR1	-2.75	-2.37	0.002	0.014	Component of TRAMP complex
YML027W	YOX1	-2.60	-2.23	0.001	0.007	Homeobox transcriptional repressor
YCR072C	RSA4	-2.59	-2.43	0.001	0.006	Involved in ribosome biogenesis

instead of energy storage. As an example, the external NADH dehydrogenase *NDE2* is up-regulated after CuO NPs exposure. This up-regulation of *NDE2,* the first component of the electron transport chain, suggests cells may require additional energy input and thus are shifting metabolism towards respiration. This shift in energy requirements may also explain the up-regulation of 'deletion suppressor of mptFive mutation' *DSF1*, a putative mannitol dehydrogenase.

Table 11. *S. cerevisiae* down-regulated genes involved in protein synthesis and ribosome biogenesis.

Categories Ribosome Biogenesis	System Name	Standard Name	Basic description
General Transcription	YML113W	DAT1	DNA binding protein
	YBL054W	TOD6	PAC motif binding protein
	YOL080C	REX4	Putative RNA exonuclease
	YKR024C	DBP7	Putative ATP-dependent RNA helicase (DEAD-box family)
	YDL167C	NRP1	Putative RNA binding protein
	YMR179W	SPT21	Role in transcriptional silencing
	YCL037C	SRO9	RNA-binding protein
	YOR078W	BUD21	Component of small ribosomal subunit processosome
	YBR141C	BMT2	Nucleolar rRNA methyltransferase
mRNA processing and RNA degradation	YIL104C	SHQ1	Chaperone protein involved in pre-rRNA processing
	YNL299W	TRF5	Poly(A) polymerase
	YNL112W	DBP2	ATP-dependent RNA helicase
	YIL079C	AIR1	protein in TRAMP complex
	YOR359W	VTS1	DNA/RNA-binding protein
Required for 18s rRNA maturation	YKL078W	DHR2	Nucleolar ATP-dependent RNA helicase
	YGR271C-A	EFG1	Maturation of 18S rRNA
	YDR021W	FAL1	Maturation of 18S rRNA
	YER127W	LCP5	Maturation of 18S rRNA
	YHR196W	UTP9	18S rRNA pre-processing
	YDR398W	UTP5	Production of 18S rRNA
	YKL099C	UTP11	Production of 18S rRNA
	YMR093W	UTP15	18S rRNA pre-processing
	YMR014W	BUD22	Required for rRNA maturation
	YJL069C	UTP18	SSU protein, pre-18S maturation
Component of 60S ribosome	YHR085W	IPI1	Processes ITS2 sequences from 35S pre-RNA
	YNL182C	IPI3	Processes ITS2 sequences from 35S pre-RNA
	YNR053C	NOG2	Putative GTPase
	YJL122W	ALB1	Shuttling pre-60S factor
	YCR072C	RSA4	Involved in maturation and transport of pre-60S subunit

SSU = small subunit processome complex.

Table 12. *S. cerevisiae* regulated genes encoding cyclins of interest.

Standard Name	Log_2FC		Adj. *p*Value		Complexation induces:
	CuO	$Cu^{2+/+}$	**CuO**	$Cu^{2+/+}$	
*PCL1******	**-2.87**	-3.00	**0.001**	0.019	Cell-cycle progression
*PCL2******	**-1.17**	-0.39	**0.022**	0.52	Cell-cycle progression
*CLN1***^**	**-1.07**	-0.98	**0.004**	0.55	Cell-cycle progression
*CLN2***^**	**-0.95**	-0.73	**0.006**	0.084	Cell-cycle progression
*CLB6***^**	**-2.83**	-2.69	**0.001**	0.014	Activates Cdc28
*PCL8******	**1.07**	0.69	**0.004**	0.085	Glycogen accumulation
*PCL10******	**0.75**	0.70	**0.01**	0.091	Glycogen accumulation
*PCL5**	**2.13**	1.36	**0.001**	0.091	Protein production

Bold values are associated with exposure to CuO NPs. An (*****) indicates relation to Pho85 regulation and interaction. An (**^**) indicates association with Cdc28.

The suggestion of differential response to stress from CuO NPs exposure compared to treatment with released Cu ions culminates in the changes in regulation of two cell cycle related genes, *XBP1* and *MCD1.* The *XhoI* site-binding protein *XBP1* was up-regulated only from CuO NPs exposure, which is important as this transcriptional repressor has been linked to inhibition of 15% of all yeast genes [35]. Up-regulation of *XBP1* has been linked to cell cycle arrest at G1 phase after the cell encounters stress such as DNA damage. The mitotic chromosome dominant protein *MCD1* encodes an essential subunit of the cohesion complex required for proper sister chromatid cohesion during mitosis and meiosis [36]. The *MCD1* gene was found to be down-regulated only after CuO NPs exposure, which is suggestive of decreased mitosis and meiosis that was not observed with released Cu ion exposure. Together the differential expression of these cell cycle related proteins suggests cell cycle arrest may be induced by other regulatory systems including *YLR149C*.

3.5 *Discussion*

3.5.1 *Proposed mechanism for* S. cerevisiae *response to released copper ions and copper oxide nanoparticles*

A majority of changes in the regulations of genes were observed after both the CuO NPs treatment as well as the released Cu ion exposure (Figure 12). The mutually-changed gene pathways from the two copper exposures are considered an effect caused by the Cu ions released from the CuO NPs. The regulation of many of the genes is most likely related to the yeast environmental stress response (ESR), which can result in over 900 different genes becoming induced or inhibited in order to overcome environmental stress [37]. The ESR in yeast induces up-regulation in genes involved in scavenging of reactive oxygen species, protein folding and degradation, and DNA-damage repair [38]. It has been proposed that the up-regulation of ESR genes primarily serve a protective role for critical cellular functions [37].

The Cu ions released from CuO NPs resulted in cellular damage, as suggested by increased expression in genes involved in scavenging of reactive oxygen species, protein folding and degradation, and DNA-damage repair. A decrease in protein production is suggested as many genes related to ribosome biogenesis were decreased in regulation. The reduced protein production allows the cells to conserve energy and thereby allows cells to more appropriately adapt and respond to the stress. Numerous genes involved in glycogenesis were also up-regulated, including glycogen debranching enzymes and glycogen synthases. Increased abundance of glycogen and trehalose after exposure to stress can establish energy reserves for improved response to stress.

Alongside the afore mentioned gene changes, multiple genes involved in cell cycle progression were changed in regulation after both CuO NPs and released Cu ions exposures.

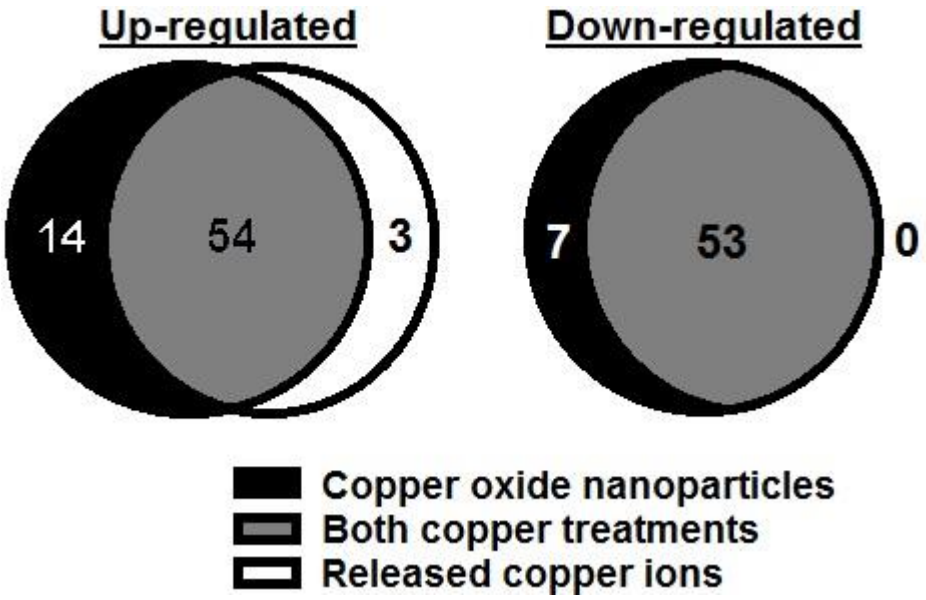

Figure 12. Changes in regulation of *S. cerevisiae* genes after exposure to either copper oxide nanoparticles, released copper ions, or both treatments.

The observed cell cycle arrest is consistent with previous results [15] wherein a significant inhibition of cellular metabolic activity was observed (80% reduction with 208 mg Cu/L CuO NPs) without any effect on cell viability. The delay of cell cycle progression is a defense mechanism employed by *S. cerevisiae* cells to prevent cell death, similarly as was observed after linoleic acid hydroperoxide treatment [39]. The up-regulation of genes related to glycogen and trehalose storage is further evidence of cell cycle arrest as this has been linked with arrest at G1 phase [40]. Cell cycle arrest at G1 would be in agreement with previous experiments with both CuO NPs and Cu ions exposure to human A549 cells in which cell cycle arrest was also observed [41]. Exposure of *S. cerevisiae* to both CuO NPs and released Cu ions may have resulted in cell cycle arrest as demonstrated by up-regulation of *YLR149C*. The gene product of

YLR149C induces cell cycle arrest and often increases in abundance in response to DNA replication stress [34].

Yeast cells that encounter cell cycle arrest may have increased DNA replication stress as suggested by Niu *et al* [34]. DNA replication stress may be occurring after copper exposure as indicated by the expression of a number of genes 'Phosphoglucomutase' *PGM2,* 'Trehalose synthase long chain' *TSL1,* 'Suppressor of Los-1' *SOL4,* 'Restriction of telomere capping' *RTC3,* 'homolog of *S. pombe* SDS23' *SDS24,* 'Reticulon-like' *RTN2,* 'Found in mitochondrial proteome' *FMP16,* 'Heat shock protein' *HSP42,* 'Inhibitor of glycogen debranching' *IGD1*, as an increase in abundance of these genes has previously been suggested to occur in response to DNA replication stress [35]. The effect on *S. cerevisiae* DNA replication from copper exposure was also observed in Bayat *et al*, based on the GreenScreen and comet assays [42], from CuO NPs at only 8 mg/L concentration. Prolonged DNA replication stress results in cells being more sensitive to further DNA damage and the cell can become arrested leading to poor binding of initiation complexes or limited dNTP pools [38].

Many genes related to ribosome biogenesis were down-regulated after both copper treatments (Table 11). A reduction in biogenesis-related genes is frequently observed during the ESR wherein almost 70% of the down-regulated genes are involved in protein synthesis [37, 43]. This reduces protein levels and conserves energy to allow cells to more appropriately adapt and respond to the stressor [44]. Numerous genes involved in glycogenesis were up-regulated after exposure to CuO NPs and released Cu^{2+} ions, including glycogen debranching enzymes, glycogen synthase, glycogenin glucosyltransferase, and several subunits of the Glc7p phosphatases (Table 10). Recent literature suggests yeast cells can increase abundance of glycogen and trehalose storage molecules upon exposure to stress in order to have established energy reserves for appropriate stress response [45, 46]. Trehalose synthesis was induced as 2 subunits

of trehalose-6-p-synthase were also up-regulated, which provides further evidence of an increase in carbohydrate levels. Trehalose can assist in osmolyte balance [47] as well as to prevent protein misfolding [48] and as such has been found to increase in abundance in cells encountering protein damage [30].

In our study the pyruvate kinase *PYK2* was found to be up-regulated after both CuO NPs and released Cu ions exposure, suggesting cells may be entering the glycolytic shunt. *PYK2* maintains control of the relative flux of glycolytic intermediates and ATP within yeast cells by regulating the glycogen shunt. The glycogen shunt is a process by which cells can couple the metabolism of glycolysis, futile cycling, and the synthesis of glycogen and trehalose in order to establish ATP and glycolytic intermediate homeostasis in steady-state conditions [45]. It has been proposed by Gasch *et al* that the paradoxical induction of both catabolic and synthetic genes enables the cell to rapidly control corresponding enzymes, thereby increasing the ability for the cell to regulate its energy reserves [37]. The systems responsible for regulation of both glycogen and trehalose have been shown to be very dynamic and capable of swift response [48, 49]. The ability to sustain osmotic instability and buffer energy reserves is proposed to be regulated by a similar mechanism, which induces the regulation of both synthetic and catabolic functions of gene networks.

Damage to the cell membrane may be occurring as increased membrane permeability is suggested by up-regulation of *HSP30*, which regulates the plasma membrane H^+-ATPase *PMA1*. *PMA1* is suggested to stay steadily regulated but the activity of Pma1p has been found to be increased in order to help maintain intracellular homeostasis after a drop in intracellular pH [50]. A drop in intracellular pH has been observed to occur after exposure to toxic levels of copper which caused membranes to become permeable to ions [51]. The occurrence of membrane permeability is also suggested by the increase in expression of the v-SNARE binding protein *BTN2*, which is

involved with specific protein transfer from late endosome to the golgi. The up-regulation of *BTN2* has been shown to occur in order to counteract changes to vacuolar pH [52], observed in yeast after copper toxicity from an increase in membrane permeability [51]. The upregulation of *BTN2* in our study occurred only in yeast cells exposed to released Cu ions.

Up-regulation was observed in the transcription factor *USV1*, that specifically influences genes involved in cell wall biosynthesis. Further evidence of cell wall biosynthesis may be present in the significant up-regulation of the reticulon protein *RTN2*, which acts to stabilize membrane curvature. Previous studies have observed increased damage to cellular membranes after copper exposure and thus up-regulation of genes involved in cell wall biosynthesis [53]. The membrane damage observed after exposure to Cu ions is suggested to occur from ROS induced lipid peroxidation [54, 55].

3.5.2 *Exposure to CuO NPs changed regulation of additional genes*

Treatment with CuO NPs resulted in a number of genes whose regulation was not changed after treatment with released copper ions, suggesting differential stress response. These CuO NPs changed gene regulation encoding several critical proteins involved in cell cycle progression, environmental information processing, and energy production. Treatment with CuO NPs may have affected the metabolism of the yeast cells, as suggested by the up-regulation of genes related to oxidative phosphorylation, that were not changed after exposure to released Cu ions. The expression of a mitochondrial protein that plays the role of Complex I in the electron transport chain, NDE2p, was significantly up-regulated after CuO NPs exposure. This result is similar to the up-regulation of NADH-dehydrogenase Fe-S protein 4 in the nematode *Lumbricus rubellus* (NDE2p in yeast) after CuO NPs exposure [53].

Additional evidence of altered energy production can be found in the increased expression of the PHO85 cyclins *PCL8* and *PCL10*, involved in metabolic regulation via the cyclin-dependent protein kinase Pho85p [56]. PHO85p can negatively regulate glycogen accumulation by interacting with PCL8/10p [32], which also suggests a shift towards energy production. CuO NPs exposure also induced increased expression of the PHO85 cyclin *PCL5*, which interacts with PHO85p to increase cellular protein production. *GCN4* is a transcription factor involved in decreasing protein production under starvation conditions. PHO85p negatively regulates *GCN4* through the action of PCL5p, which subsequently induces protein production. This suggests a differently induced stress response from CuO NPs exposure as no indication of protein production occurred after released Cu ions exposure. The shift in energy state and protein production suggests that the stress induced by CuO NPs triggers additional stress response networks resulting in the need for additional energy via oxidative phosphorylation.

The cell cycle arrest in CuO NPs exposed cells may be induced by a separate pathway, i.e. the transcriptional repression from the up-regulated *XBP1* and reduced DNA replication from down-regulated *MCD1*. *MCD1* is a cell cycle specific gene that codes for an essential subunit of the cohesion complex needed for proper sister chromatid cohesion during mitosis and meiosis [36]. The decreased expression of *MCD1* after CuO NPs exposure would seriously inhibit progression of the cell cycle from improper sister chromatin adhesion. The increased expression of *XBP1* would lead to the cell cycle inhibition as it is a transcriptional repressor, expressed during stress, which is involved in maintaining cells in an arrested state at G1 phase. This transcriptional repressor is not normally expressed during logarithmic growth as it is responsible for inhibiting up to 15% of all yeast genes [57]. Increased expression of *XBP1* has been linked to stress from high osmolarity, oxidative stress, excessive heat, and DNA damage

and has been shown to inhibit cell cycle progression at G1 [58]. Indication of differential stress reaction after CuO NPs exposure is supported by the regulation of genes related to cell cycle arrest.

3.6 Conclusion

Exposure of *S. cerevisiae* cells with either CuO NPs or released Cu ions altered the regulation of a number of genes related to functions similarly affected by the environmental stress response (ESR). Among the genes changed in expression, more than half are involved in the ESR and play a protective role by reducing general protein production and increasing stress-related protein production. This decrease in protein production enables yeast cells to overcome a variety of stressors in order to reestablish homeostasis. The response after treating yeast with CuO NPs or released Cu ions was down-regulation of ribosome biogenesis and protein biosynthesis and up-regulation of glycogen synthesis to reduce cellular energy use. Along with reduction in cellular energy use, changes in gene expression suggest yeast may be encountering DNA replication stress, damage to cell membranes, and cell cycle arrest. We propose that the cell cycle arrest may be induced by the copper ions released from the CuO NPs through the up-regulation of *YLR149C*, as well as down-regulation of *CLB6* and *PCL1* that act in unison to induce cell cycle arrest. This is in contrast to exposure with CuO NPs that may be inducing cell cycle arrest via the additional up-regulation of *XBP1*. The observed changes in the regulation of genes only after CuO NPs exposure suggests yeast cells are experiencing differential stress response compared to exposure with released copper ions. It is significant that several mitochondrial proteins involved in energy production or oxidative phosphorylation were only up-regulated after exposure to CuO NPs.

CHAPTER 4:

COPPER OXIDE NANOPARTICLES IMPACT SEVERAL TOXICOLOGICAL ENDPOINTS AND CAUSE NEURODEGENERATION IN *Caenorhabditis elegans*

4.1 Abstract

Engineered nanoparticles (NPs) are increasingly becoming incorporated into technology and consumer products. In 2014, over 300 tons of copper oxide (CuO) NPs were manufactured in the United States. The increased production of NPs raises concerns regarding the potential introduction into the environment or human exposure. The toxicological endpoints of CuO NPs and copper sulfate were quantified in *Caenorhabditis elegans.* A laboratory-adapted *C. elegans* strain (N2) and three wild strains were utilized to examine differences in the toxicological responses of strains with diverse genetic backgrounds. All strains exhibited greater sensitivity to CuO nanoparticles compared to copper sulfate, as indicated by reduction of average population body length and feeding behavior. The reproduction of *C. elegans* strains was significantly reduced only at the highest copper concentration exposures, though still more pronounced with CuO NPs compared to copper sulfate treatment.

In transgenic *C. elegans* with neurons expressing a GFP reporter protein, neuronal degeneration was observed in up to 10% of the population after CuO NPs exposure. Nematode mutant strains containing gene knockouts in the divalent-metal transporters *smf-1* and *smf*-2 showed increased tolerance to copper exposure, and thus implicates both transporters in copper-induced neurodegeneration. These results demonstrate greater toxicological effects of CuO NPs compared to exposure with copper sulfate on several strains of *C. elegans*.

4.2 Introduction

Nanoparticles (NPs), particles with at least one dimension less than 100 nm, are increasingly employed in commercial products. NPs have high surface area to size ratios, which confer unique material properties compared to micron particles with the same chemical composition. Copper oxide (CuO) NPs are frequently employed for their superconductive properties and as such are found in many different consumer electronics including gas sensors, batteries, and solar cells [9]. As manufacturing output increases for any material, an associated increase in the risk of accidental exposure to humans or introduction into the environment occurs. Consequently, it is important to determine the toxicity of these commonly employed NPs to human, aquatic, and terrestrial organisms.

Previous studies have reported several toxicological endpoints of CuO NPs to many organisms including bacteria [163], yeast [19], *Oligochaeta* [27], and human cell lines [112]. Defining the mechanism of nanoparticle toxicity is difficult as released metal ions might also cause toxicity, making it difficult to define the ultimate cause of toxicity [14]. The released copper ions from CuO NPs has been suggested as the sole source of toxicity in earthworms, several algae and crustacean species, *Escherichia coli*, and human cell lines [9]. By contrast, other studies suggest the NP component also contributes to inhibition of cellular metabolic activity [18] and observed cytotoxicity in yeast [19] and plants [164].

Nematodes are an environmental model to study NP toxicity as they assist in decomposition of organic matter within soil. *C. elegans* is employed as a model organism in many studies because of low culture cost, short lifespan, conserved genome, and a translucent body, which enables the use of fluorescently labeled reporter

molecules. Although CuO NPs toxic effect on nematodes wasn't studied extensively (except one report), copper ions from copper salts have been shown to be toxic to several species including *Caenorhabditis elegans [72]*, *Panagrellus redivivus*, and *Pristionchus pacificus* [68]. Exposure of *C. elegans* to toxic levels of copper sulfate was observed to reduce brood size and life span while slowing development [67, 165]. It has been suggested that the mechanism of heavy metal toxicity in *C. elegans* can involve disruption of the cell membrane or competition and subsequent displacement with other necessary cations bound by proteins [166].

The effect of CuO NPs on *C. elegans* neurodegeneration is critical to investigate as it is a very sensitive and important toxicological endpoint but currently is understudied compared to the copper ion effect. *C. elegans* has been used as a tool to probe for mechanisms of numerous neurodegenerative diseases. This use has been exploited to study neurodegeneration induced by metals. *C. elegans* is an excellent model to study neuronal health, as it offers ease of genetic manipulation, the ability to fluorescently label neuronal subtypes, and the relative simplicity of the nervous system [72] . It is critical for cells to maintain strict regulation and control of copper homeostasis for normal neurological development [167]. Heavy metals, including Cu^{2+}, have been shown to affect neurons by depleting cellular energy through decreased mitochondrial function, increased oxidative stress, or activation of the necrosis or apoptosis pathways [72]. Exposure to copper, or mercury ions has resulted in morphological changes in dorsal and head GABA motor neurons in *C. elegans* [168]. Disrupted copper homeostasis has been associated with several neurological disorders, including prion diseases, amyotrophic lateral sclerosis, and Parkinson's Disease (PD) [71]. Death in the dopaminergic neurons is a known consequence of Parkinson's disease [72]. *C. elegans* has dopaminergic neurons that allow investigation of the effect of CuO NPs on this class

of neurons. Damage or loss of these neurons in *C. elegans* can cause changes in behavior and possibly even alter their responses to environmental stimuli [72].

Numerous studies in the last decade have observed that *C. elegans* N2 Bristol strain, along with a number of other model organisms, have become genetically modified from domestication over the many years of culturing in the laboratory [169-171]. Several newly derived alleles adapted in the laboratory N2 strain have altered nematode physiology and behavior, compared to wild strains, which subsequently affect experimental interpretations [172]. Thus, species and strain genetic variability has to be considered in toxicological studies. For example, the amphipod *Hyalella azteca* is a commonly used environmental monitoring organism for testing the toxicity of water and sediment. A recent study, amongst three laboratory cultures and seven wild populations of *H. azteca,* showed that more than 550-fold variation in sensitivity to pyrethroid insecticides exists [173]. When addressing the effects of copper exposure on reproduction and life span traits within five populations of brine shrimp (*Artemia)*, the environmental component was found to be the major factor for variance in effect [174]. Evidence of clonal variation in sensitivity to toxicants is found in a study examining several clones of *Daphnia magna*, isolated from different lakes, in response to the fungicide azoxystrobin [175]. These studies highlight the importance of interspecies and strain variation in toxicological studies.

Genomic variation has been observed amongst different wild *C. elegans* isolates from a genome-wide assessment of 202 strains revealing 97 distinct genome-wide haplotypes [176]. A recent study has revealed unexpectedly variation in both fertility and oocyte function in wild strains of *C. elegans* upon exposure to high temperature [177]. New high-throughput phenotypic assays were recently developed using the COPAS BIOSORT large particle nematode sorter. Using these assays and a collection of recombinant inbred strains, the quantitative trait loci involved in fecundity and growth

under normal growth conditions and after exposure to the herbicide paraquat were identified [171]. Thus, the effect of environmental and chemical stressors to *C. elegans* wild strains in comparison to a lab-adapted strain is important to consider [171].

The goal of the present study was to evaluate CuO NPs inhibitory effects on the model organism *C. elegans*. In order to explore the influence of genotypic background regarding the response to copper challenge, we examined three wild *C. elegans* isolates together with the Bristol N2 laboratory strain. We hypothesized that the established dissimilarities in the genotypes of these wild strains will result in differential sensitivity to copper when compared to the laboratory-adapted N2 strain. Several toxicological endpoints were analyzed via a high-throughput screening process to quantify the effects of CuO NPs in comparison to soluble copper salt. Potential physiological effects of CuO NPs on *C. elegans* were investigated also through the use of strains with dopaminergic neurons expressing GFP to visualize neuron degeneration after copper exposure. The CuO NPs employed showed a detrimental effect on the neuronal degeneration in *C. elegans*. Two genetic knockout mutants of the divalent-metal ion transporters *smf-1* and *smf-2* were employed to investigate if the effect of CuO NPs on *C. elegans* is SMF transporter dependent. To examine the potential effect of copper as stressor, a reporter strain with a GFP expression driven by a *hsp-16.2* stress inducible promoter was examined after CuO NPs and copper sulfate exposure. This work represents one of the first to address and quantify CuO NPs effects in *C. elegans*.

4.3 *Materials and Methods*

4.3.1 Caenorhabditis elegans *strains and cultivation conditions*

All *Caenorhabditis elegans* strains were routinely cultured on Nematode Growth medium (NGM) plates seeded with the *Escherichia coli* strain OP50. Strains were

transferred twice a week and stored at 20ºC according to the standard method previously described by Brenner [178]. Three wild strains and N2 mutants were also employed in addition to the N2 wild-type strain. The N2 strain was a kind gift of Dr. R. Stuart (Marquette University, Milwaukee, WI, USA). The wild strains CB4856, DL238, and JU258 were kind gifts of Dr. E. Andersen (Northwestern University, Evanston, IL, USA) and their genetic characteristics were described previously [176]. Strains CB4856 and DL238 are among the most highly diverged wild strains in the species [176, 179, 180]. The wild strain, JU258, is more related to N2 strain than the other two wild strains but nonetheless divergent [176]. The transgenic strains RJ907 (P_{dat-1}*::*GFP; *smf-1(eh5)*) and RJ938 (P_{dat-1}*::*GFP*; smf-2(gk133)*), each containing GFP expression controlled by the *dat-1* promoter, were kind gifts of Dr. R. Nass (Indiana University School of Medicine, Indianapolis, Indiana, USA). The BY250 strain (P_{dat-1}*::*GFP; N2 wild-type) was a kind gift of Dr. R. Blakely (Vanderbilt University, Nashville, TN, USA). Specifics on the construction of these transgenic *C. elegans* lines can be found in Nass *et al* [181]. The reporter strain KC136 with GFP expression controlled by the heat-shock protein (HSP) *hsp-16.2* promoter, which was a generous gift of Dr. K. L. Chow (Hong Kong University of Science and Technology, Clear Water Bay, Kowloon, Hong Kong) [182]. Nematodes were exposed to copper sulfate or CuO NPs for 96 hours in K medium [68] with HB101 bacterial lysate suspended within the medium to prevent nutrient deprivation [171].

4.3.2 *Nanoparticle physicochemical characterization*

[See above 2.3.2, 3.3.1]

4.3.3 *High-throughput endpoint assays for nematodes*

A note: these experiments and any further experiments involving the wild strains and the reproduction, feeding, and population body length toxicological endpoints were performed by Prof. Erik C. Andersen in the department of molecular biosciences, Northwestern University, Evanston. The analysis of these data and the subsequent hypotheses and conclusions were generated by myself.

A Complex Object Parametric Analyzer and Sorter (COPAS) BIOSORT was employed to assay the physiological endpoints after 96-hour treatment as per the previous protocol described in Andersen *et al* [171]. Body size was measured as 'time of flight' while the paralyzed animals passed through the flow cell. Reproduction was measured by quantifying the total number of objects that pass through the flow cell. These objects are assumed to be nematode progeny with 99.97% accuracy as per the support vector machine described previously [171] and were normalized to number of adults initially transferred to each well of the 96-well plate. Brood size was considered the amount of offspring generated by a nematode within the 96-hour experiment. Feeding behavior was assayed as pharyngeal pumping based on red fluorescence signal within each nematode after red fluorescent beads (Polysciences) were added to the food source. The COPASutils R package was used to process the data [183].

4.3.4 *Neuron degeneration and stress induction scoring*

The transgenic reporter strains used (BY250, RJ907, and RJ938) contain a green fluorescent protein (GFP) that is expressed under control of the *dat-1* promoter within dopaminergic neurons. Additionally, the transgenic strain KC136 contains GFP reporter which expression is driven by a *hsp-16.2* stress inducible promoter. Transgenic nematode populations were synchronized using standard alkaline hypochlorite method

[184] and allowed to enter L1 stage during overnight incubation. L1 nematodes were suspended in 1 mL K medium (supplemented with 5 mg/mL cholesterol and HB101 bacterial lysate prepared as in Andersen *et al* [171]) containing the respective copper treatment at desired concentration and were incubated at 20°C on a rotational shaker at 250 rpm for 24 hours. Due to the impermeable nature of the cuticle of *C. elegans*, a 24 hour exposure was necessary to observe any effect [185, 186]. After copper exposure, animals were gently pelleted at 1,500 rpm for 60 seconds. Supernatant was removed, and nematodes were washed twice with K medium (pH 6.5, with no cholesterol or lysate added) prior to plating onto K medium agar with OP50 bacteria. After a 72 hour recovering period, adult animals were picked onto agar stubs and scored on a fluorescent Nikon microscope (Nikon te2000) for any abnormal neuron formation. For neuronal degeneration nematodes were considered positive if neurons were malformed or completely absent. For stress response, KC136 nematodes were imaged (Leica DMI 6000B inverted microscope, Leica microsystems with Leica Application Suite AF), and GFP expression was measured as voxel volume and normalized to length using Metamorph 5.5 software (Molecular devices). Data represent three independent experiments and at least 40 nematodes were scored for each treatment.

4.3.5 *Statistical Analysis*

Significant differences between strains or treatments were determined using R statistical analysis program using the analysis of variance (AOV) followed by Tukey's Honestly Significant Difference (HSD) test. For neurodegeneration, comparisons between N2 and the wild strains were considered significantly different when a greater than a 10 percentage point difference between the phenotype values were measured and a Tukey's HSD $p<0.05$. For endpoint analysis, the wild-type laboratory-adapted *C.*

elegans strain N2 had significantly different untransformed, not normalized toxicological endpoint values (p<0.04) compared to all three wild strains (CB4856, DL238, and JU258). As such, statistical comparisons were made based on data normalized to untreated nematodes of the respective strain and represented as percent of untreated.

4.4 *Results*

4.4.1 *CuO nanoparticles aggregate and release copper*

The amount of ions released from metal oxide NPs depends on the physicochemical properties (such as size, surface charge, and crystal structure) and is an important factor in the measured toxicity to *C. elegans* [10]. The copper oxide (CuO) NPs used throughout this study have been previously characterized by transmission electron microscopy and were observed to be predominantly spherical with a rough surface and an average primary particle diameter of 28.4 nm [18] with parallel crystal lattice fringe spacing of 2.4 Å. When dispersed in nematode growth medium, the CuO NPs undergo changes in the hydrodynamic diameter, reported in Figure 13. The present within K medium as well as with other CuO NPs, and thus forming larger and more complex aggregates and agglomerates. CuO NPs may be interacting with the bacterial lysate components and these agglomerates might be subsequently ingested by the nematodes. After suspending the CuO NPs in K medium, the concentration of released Cu^{2+} ion corresponds to 22% of the NPs initial mass after 24 hours incubation and up to 68% of the NPs initial mass after 96-hours (in K medium pH 6.4, Figure 14). No Cu^{2+} was detected when the CuO NPs were suspended in water (pH 6.5, data not shown), suggesting the CuO NPs were not dissolving in water.

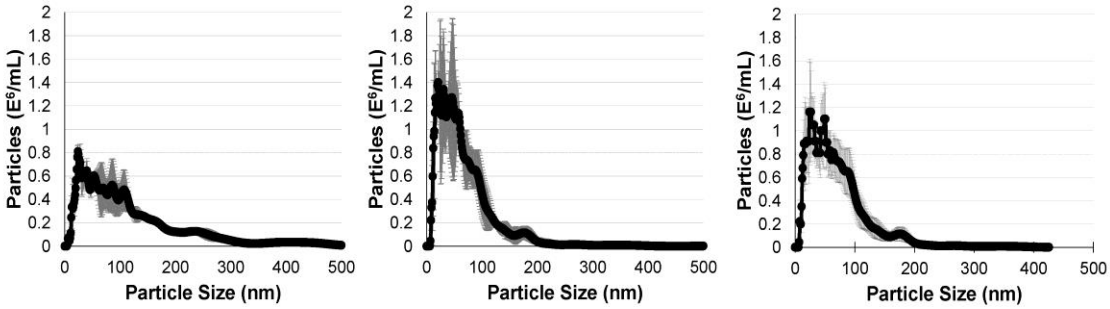

Figure 13. The hydrodynamic diameter of copper oxide nanoparticles suspended in nematode growth medium. The hydrodynamic size distribution was observed immediately after suspension of CuO NPs (A), 24 hours after suspension (B), and 96 hours after suspension (C) at 20°C and 250 rpm shaking. Black points and lines represent the mean particle concentration (10^6 per mL) and the error bars in grey represent the standard deviation from the mean. The copper oxide nanoparticles decrease in average hydrodynamic diameter with time as observed in the left-shift in peak indicating a gradual reduction in agglomerate and aggregate size.

4.4.2 *Nanoparticles have a stronger impact on C. elegans reproduction and development compared to released copper ions*

This study addressed the inhibitory effects of CuO NPs on the physiology of different *Caenorhabditis elegans* strains. In addition to N2, three wild strains, JU258, CB4856, and DL238, representing diverse genetic backgrounds of *C. elegans,* were also assayed. All *C. elegans* strains were exposed to copper in the form of CuO NPs or copper sulfate at 3.8, 7.9, and 15.9 mg Cu/L for 96 hours. Several endpoints were assessed after copper exposures including average population body length as a determinate of developmental stages, the brood size as a quantification of reproduction success, and fluorescent bead ingestion as a measure of feeding behavior of the nematodes (Figure 15, Table S1). Values for each toxicological endpoint were normalized to the untreated animals of the same strain, *e.g*. CB4856 treated with copper is normalized to untreated CB4856, and represented as a percentage of the untreated

traits (Figure 15). It is important to observe that the CuO NPs suspensions contain significantly less Cu^{2+} (p<0.04, Figure 14) compared to copper sulfate exposures used throughout this study (Figure 15, x-axis). The greater sensitivity of *C. elegans* to CuO NPs exposure compared with copper sulfate highlights the importance of an effect specific to the CuO NPs.

The average body length of a nematode population can be considered a measure of development as stressors can delay development of nematodes at early L1 or L2 stages [187]. A nematode population consisting of younger animals would be shorter in average body length. A population consisting primarily of adult nematodes or L4 animals would be much longer in average body length. Untreated *C. elegans* N2 populations had an average body length of 226.4 ± 9.5 µm.

Treatment with CuO NPs led to a significant decrease in average body length at all concentrations compared to untreated animals (p<0.001, Table S1). In contrast, the exposed populations displayed decreased average body length at only the highest copper sulfate treatment (p<0.001, 15.9 mg Cu/L). Significantly shorter body lengths were measured in the *C. elegans* N2 populations exposed to CuO NPs compared to animals exposed to copper sulfate (p<0.015 at all tested concentrations, Table S2).

Three wild *C. elegans* strains were also exposed and the population body length was analyzed to observe if a genetically broad selection displayed similar trends to CuO NPs sensitivity. Indeed, the trend of significantly greater effect (p<0.001) from CuO NPs compared to copper sulfate treatment on the average population body length was also observed in the three wild strains (7.9 and 15.9 mg Cu/L, Figure 15A and 15B). The wild strain average population body length decreased when the populations were exposed to moderate concentrations of CuO NPs 7.9 mg Cu/L while copper sulfate exposure was only inhibitory at the highest tested concentration (15.9 mg Cu/L). The wild strains

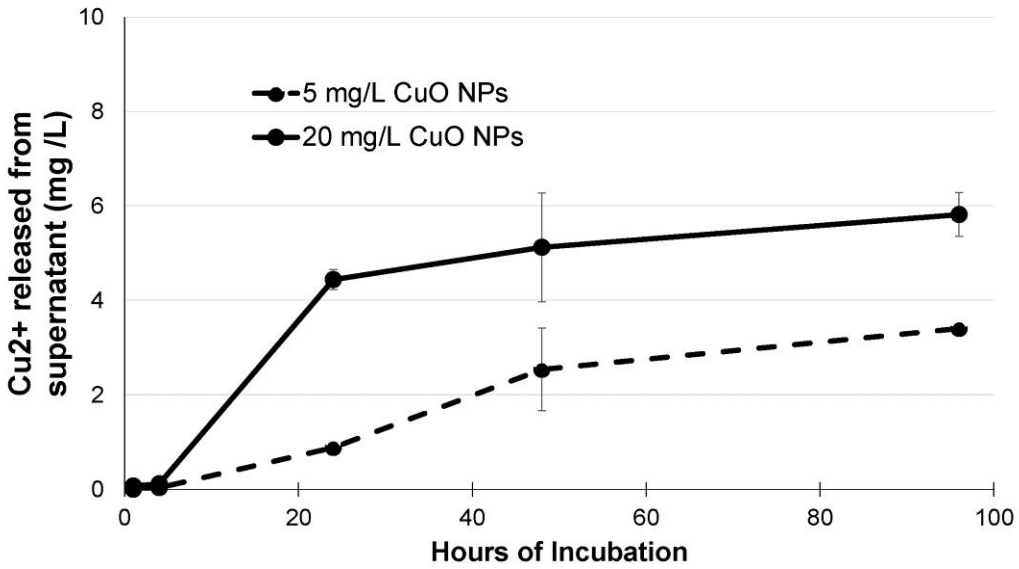

Figure 14. The concentration of copper ions released from copper oxide nanoparticles over time into nematode growth. The concentration of Cu^{2+} released over time was determined via zincon colorimetric assay at different time points. Cu^{2+} ion concentration plateaus after 48 hours of nanoparticle incubation in media with a small increase thereafter. Error bars represent standard deviation from the mean of three samples.

displayed increased resistance to CuO NPs exposure compared to strain N2, as no significant reduction in average population body length was observed at the 3.4 mg Cu/L treatment (Figure 15B).

Feeding behavior has been shown to be of particular importance regarding nematode physiology and behavior [172]. To observe changes in feeding behavior brought about by copper challenge, red fluorescent beads were introduced into the nematode growth medium (Figure 15). As the nematodes feed on bacterial lysate they also ingest the fluorescent beads, and the amount of relative fluorescence can therefore be quantified to represent feeding behavior. Sufficient amount of food as bacterial lysate has been supplied to the nematodes during the exposure time to ensure that the

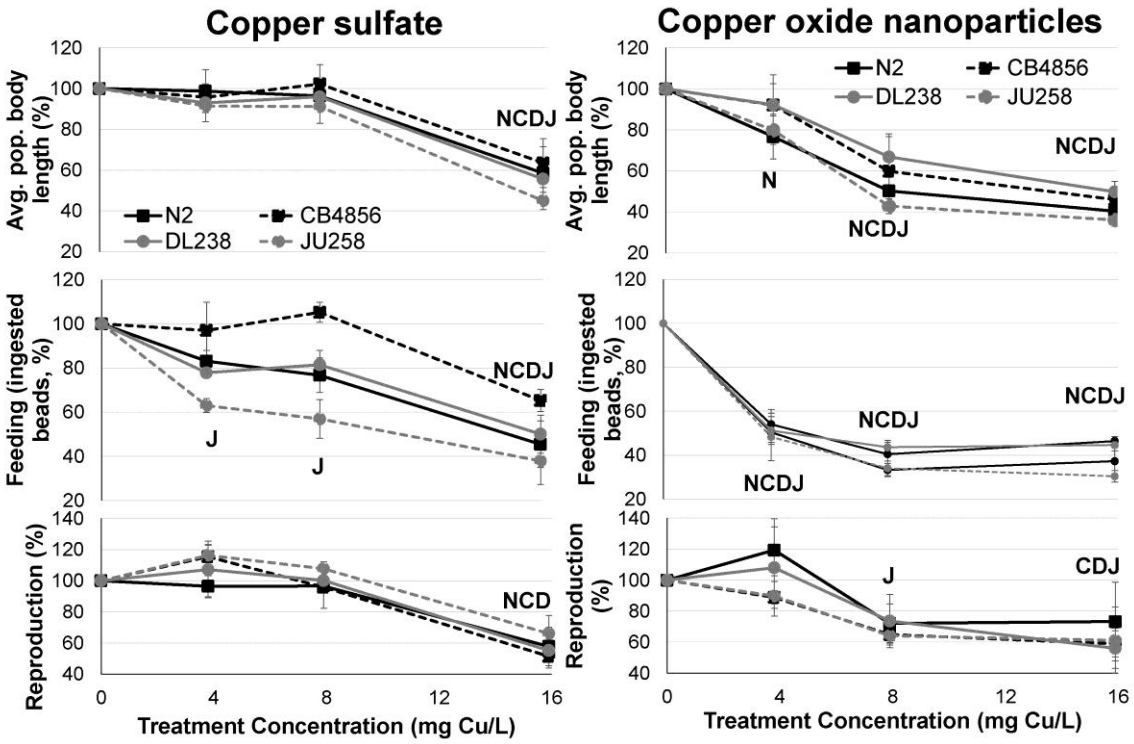

Figure 15. The inhibitory effects of copper oxide and copper sulfate on toxicological endpoints of *C. elegans*. The effects on body size (A, B), feeding behavior (C, D), and brood size (E, F) were assayed via the COPAS BIOSORT, and raw data were normalized to percentage of untreated for each respective strain. Data representing endpoint changes after copper sulfate (A, C, E) and copper oxide NPs (B, D, F) exposures. Significant differences of data prior to transforming into percentages compared to untreated (p<0.05) are designated by the first letter of each strain (N for N2 strain, C for CB4856 strain, D for DL238 strain, and J for JU258 strain). Results are presented as mean of four technical replicates, and error bars represent standard deviation.

animals are not starved. The N2 strain showed significant decreases in fluorescent red signal at all exposures of CuO NPs compared to untreated animals (Figure 15D) but was only significantly affected by copper sulfate at the highest concentration (Table S1, Figure 15C). CuO NPs exposure impacted the feeding behavior of N2 strain more, measured by a decrease in fluorescence (p<0.001), than copper sulfate exposure alone (all concentrations; Table S2).

A similar trend of increased sensitivity to CuO NPs was observed when assessing feeding behavior in the wild *C. elegans* strains. These wild nematode strains displayed significantly greater reduction in red fluorescent signal (p<0.001) after CuO NPs exposure compared to equal molar treatment with copper sulfate (3.8 and 7.9 mg Cu/L). However, we also observed some differences in the response to copper of two strains when assessing their feeding behavior. Strain JU258 was more resistant to copper sulfate exposure (Figure 15C and 15D) while the CB4856 strain was more sensitive compared to N2 strain at all concentrations examined (Table S3).

To test if exposure to CuO NPs have inhibitory effects on *C. elegans* reproduction, the brood size of all studied strains was quantified after 96 hours of exposure. The average number of progeny in the untreated N2 nematodes was 192±11, similar to results reported by Calafato *et al* [165]. Exposure to CuO NPs resulted in a rather variable decrease in N2 brood size that is not statistically different compared to untreated. The number of progeny decreased significantly (p<0.035) only after exposure of N2 to the highest concentration of copper sulfate (15.9 mg Cu/L). The wild strains had significantly decreased brood size compared to strain N2 at the highest exposure concentration of 15.9 mg Cu/L (p<0.015; Table S3), thus indicating that reproduction of the three wild strains displayed increased sensitivity to CuO NPs.

These measurements of the toxicological endpoints for all studied strains collectively indicate a greater sensitivity to CuO NPs compared to copper sulfate despite the genetic and phenotypic differences between *C. elegans* N2 and the wild strains. The observed differences in the degree of sensitivity of the wild strains to copper treatment, compared to N2 at some toxicological endpoints, requires a more in-depth investigation in order to determine the genetic causes.

4.4.3 *CuO nanoparticles affect nematode neuronal morphology*

The effect of copper exposure on neuronal health was examined using several transgenic nematode strains. The neuron morphology of a transgenic *C. elegans* strain with dopaminergic neurons expressing GFP [32] was assayed after exposure to both CuO NPs and copper sulfate. In addition, two mutant strains containing knockouts of either *smf-1* or *smf-2* were used to examine whether these metal transporters are involved in Cu^{2+} induced neurodegeneration after exposure to CuO NPs and copper sulfate.

Neurodegeneration was observed after copper treatment resulting in alterations in normal neuronal morphology (depicted in Figure 16A) in the form of absent neurons or partially formed ("blebbed") neurons (Figure 16B and 16C). The neurodegeneration observed in treated animals occurred in a dose-dependent manner in 3-10% of the population examined (total number of animals examined at each experiment is reported in Table S4). Exposure to CuO NPs resulted in a greater amount of neurodegeneration (in 6.4% and 10.4% of the scored animals; n=203 and 181, respectively) compared with copper sulfate (in 3.2% and 5.3% of the scored animals; n=213 and 266, respectively) at equal molar concentrations (3.8 and 7.9 mg Cu/L, Figure 16). After copper exposure, the *C. elegans* transgenic strains *smf-1* and *smf-2* containing a deletion in divalent metal transporter gene homologs displayed neurodegeneration in significantly smaller percent of the population compared to wild-type (BY250) ($p<0.001$ and $p<0.021$ respectively, Figure 16D). Neuron degeneration was absent and not detected in the untreated animals for any transgenic strain (Untreated, Figure 16).

The response of *C. elegans* to CuO NPs and copper sulfate exposures was assayed using reporter strain with GFP expression driven by a heat-shock inducible stress promoter (*hsp-16.2)*. Exposure to both CuO NPs and copper sulfate resulted in

stress response in *C. elegans* as indicated by the increased GFP expression of the *hsp-16.2* reporter strain in comparison to untreated nematodes (Figure 17; Table S5). Increased GFP expression may be considered organismal stress response from protein damage and unfolding as HSP-16.2 is a small heat-shock induced chaperone protein and is considered a general stress indicator reacting to temperature and oxidative stresses [182].

4.5 *Discussion*

The laboratory-adapted N2 strain and three wild strains were analyzed for copper sensitivity using reproduction, feeding behavior, and average population body length as toxicological endpoints. We observed an increased sensitivity to CuO NPs exposure compared to copper sulfate in all *Caenorhabditis elegans* strains examined (Figure 15, Table S2). The use of wild strains with more genetic variability enabled an initial, simplified but more realistic assessment of the toxicological effects of CuO nanoparticles on nematodes. The importance of strain variation in toxicological studies has been highlighted previously [171, 175, 180]. *C. elegans* N2 strain has been employed for decades in the laboratory, and yet the N2 strain has several phenotypic and genetic differences when compared to wild strains [172, 188] [169]. Some known phenotypic differences in the N2 strain compared to other *C. elegans* strains have been linked to changes in feeding behavior [172]. The differences in physiology and behavior of wild *C. elegans* strains compared to the N2 strain can include aggregation behavior observed during feeding [170], the stage of embryos during egg-laying , and the strength of mating ability in males [189]. The wild strain CB4856 used in our study has genomic differences averaging a SNPs once every 835 bp [190], yet the CB4856 strain displays greater sensitivity to CuO NPs compared to copper sulfate. This increased sensitivity of CB4856

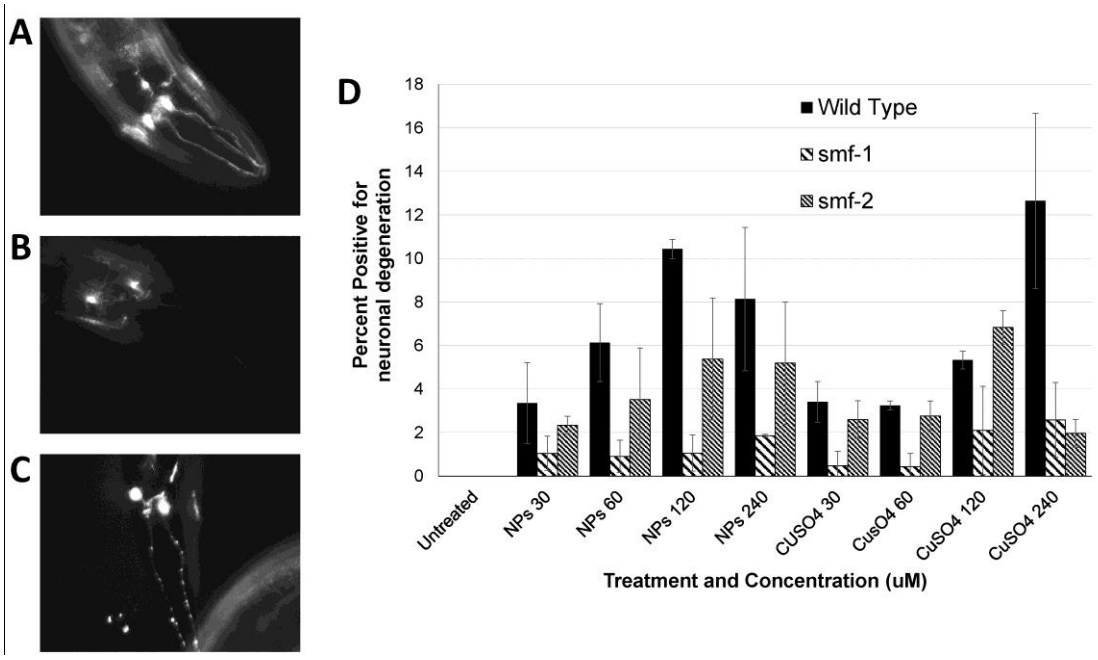

Figure 16. Induction of dopaminergic (DA) neuron degeneration in *C. elegans* from copper oxide nanoparticles and soluble copper exposure. Fluorescent images depicting healthy DA neurons (A) compared to deformed neurons which were either never formed (B) or partially formed ('beaded' or 'blebbed') (C). The bar graph represents neuron degeneration, which increases from both copper oxide and copper sulfate treatments (D). "Unt" represents untreated *C. elegans* that showed no observable neuron degeneration (n=203). Results are presented as mean of three independent experiments with a minimum of 40 nematodes observed per experiment. Significant results as compared to untreated (p<0.05) are marked with an asterisks (*). Error bars represent standard deviation.

feeding behavior could be an example of genetic variance affecting toxicity or could also be random chance or due to an environmental factor, thus supporting the need for future studies.

A reduction in the average population body length, *i.e.* a larger population of animals with smaller sizes, was observed after copper exposure, suggesting greater portion of the nematodes population is at earlier stages of development. In our study, the

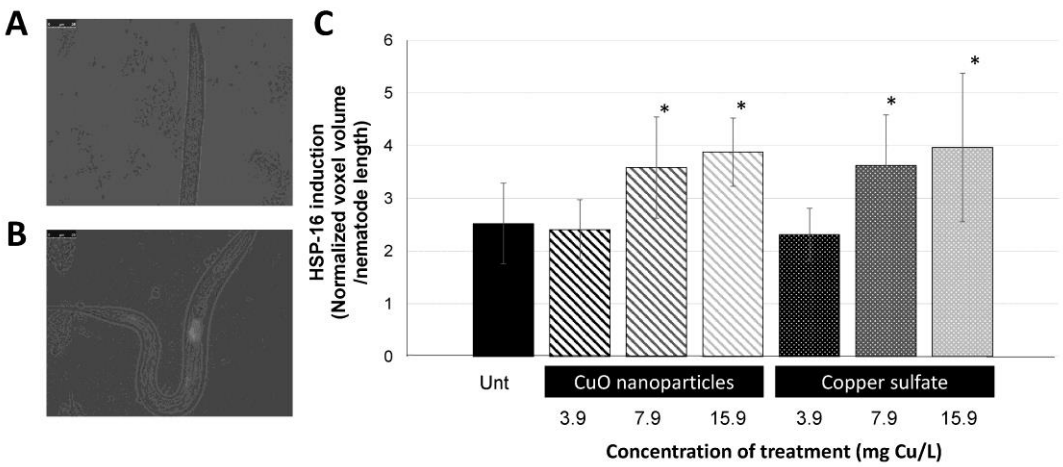

Figure 17. Oxidative stress induction, as observed by GFP fluorescence induction behind the HSP16-2 promoter, in a transgenic *Caenorhabditis elegans* strains. Treatment with both copper oxide nanoparticles and released Cu ions induced significantly increased levels of HSP16-2. Fluorescent images depicting endogenous HSP16-2 induction (A) and an increase in the induction of HSP16-2 (B). The bar graph is representative of experiments with at least 25 nematodes examined per treatment. The graph depicts increased HSP16-2 after both copper oxide nanoparticles and copper sulfate at the two highest concentrations employed (C). Significant results as compared to untreated (p<0.05) are marked with an asterisks (*). Error bars represent standard deviation.

of copper sulfate when assaying the *C. elegans* laboratory-adapted N2 strain average population body length. This trend of increased sensitivity to CuO NPs treatment compared to copper sulfate was also observed in all three wild strains. An increased resistance to the effects of copper in the wild strains could represent the impact of altered traits that have changed over time in the laboratory-adapted N2 strain. We observed variation in effect among the different *C. elegans* strains examined, such as a significant reduction in body size at 3.9 mg Cu/L in the N2 strain that wasn't observed in the wild strains until 7.9 mg Cu/L.

The developmental delay of *C. elegans* is a common physiological response to stress and has been observed after exposure to copper sulfate [186], titanium dioxide

(TiO_2), and zinc oxide (ZnO) NPs [191]. Wu *et al* observed the ZnO NPs to be more toxic than TiO_2, which may in part be due to greater metal ion release measured in the ZnO NPs suspensions compared to TiO_2 NPs [191]. Previous studies have shown that *C. elegans* displayed similar phenotypes, *e.g.* both growth delay and reduced lifespan, after exposure to copper ions from copper salt [165]. Changes in the body lengths of individual nematodes have been linked to decreased food intake, as well as effects from perturbation of insulin IGF-1 signaling [192]. Subsequently, a portion of the reduced average population body length observed in this study might be a consequence from the smaller individual body length as a result of diminished feeding. Additionally, a portion of the nematode population could be entering the dauer stage after encountering the copper stress, further complicating the interpretation of these data. Thus, multiple physiological effects triggered by the CuO NPs and copper ion exposures might be contributing to the observed *C. elegans* developmental delay.

Food ingestion and thereby energy uptake is essential for every animal and impairment can decrease survival and fitness. A reduction in red fluorescent bead intake, a measure of nematode feeding behavior, has been suggested to be both a response to environmental stress through neurotransmitters or changes in pharyngeal activity [193]. The feeding behavior endpoint was the most sensitive toxicological endpoint as the CuO NPs at every tested concentration displayed a significant effect (Table S1). The intake of fluorescent beads of N2 strain was significantly reduced by all concentrations of CuO NPs ($p<0.001$) but only significantly reduced by copper sulfate exposure at the highest concentration ($p<0.005$, Table S1).

A similar trend of increased sensitivity to CuO NPs compared to copper sulfate was observed when assessing feeding behavior in the wild *C. elegans* strains. Reduced feeding in *C. elegans* is critical because it has been linked to increased sensitivity to

stress and a reduction in motility [194]. Food-borne exposure of copper chloride has been shown to be the primary, and most toxic, route of exposure in *C. elegans* [195]. CuO NPs ingestion is most likely the point of entry of the NPs in *C. elegans* in our study, because the nematode cuticle has been shown to be generally impermeable to chemicals [186]. The ingestion of NPs is a frequent route of exposure in *Daphnia magna.* After exposure to CuO NPs, as well as TiO_2 NPs, it was observed that NPs were accumulating within the midgut of the *Daphnia* [196]. Once ingested, pH changes and enzymatic activity from the stomach/midgut could result in increased NPs dissolution and ion release [197]. An effect on *C. elegans* feeding behavior has also been observed after exposure to other toxins including silver NPs [198], methyl mercury [199], salicylate, high heat, and sulfhydryl-reactive compounds. This reduction of feeding may in part be a defense mechanism of the animal in order to reduce toxin intake as this has been observed after treatment with heavy metals [195].

Reproduction is a critical endpoint to analyze as it has been shown to be sensitive to lower concentrations of chemical stressors compared to concentrations that affect *C. elegans* behavior and viability [166]. However, within our study the observed reduction in brood size after 96 hours of exposure to CuO NPs and copper sulfate proved to be rather variable, which resulted in no significant difference compared to untreated animals (Figure 15E, 15F). The N2 strain reproduction declined with CuO NPs exposure but not significantly (Figure 15), while exposure to copper sulfate at the highest concentration only had a significant effect on brood size (p<0.035). A decrease in the reproductive capabilities of *C. elegans*, in the form of decreased rate of egg laying or decreased embryo survival, has been observed after exposure to fullerene NPs [200] and silver NPs [201]. Elevated levels of copper ions have been observed to induce

paralysis [194], which may reduce feeding and stress the animal to the point of affecting reproduction.

All of the wild strains exposed to CuO NPs and copper sulfate displayed reduced brood size at the highest concentration (15.9 mg Cu/L, Table S3). However, the brood size of the three wild strains tested were significantly more reduced after exposure to CuO NPs exposure compared to copper sulfate (p<0.013, Table S3). The increased effect on reproduction from CuO NPs in the *C. elegans* wild strains was not observed in the laboratory-adapted N2 strain, supporting the use of a genetically broad selection of strains for toxin evaluations.

The potential of CuO NPs to influence the nematode neuronal morphology was assayed utilizing transgenic strains of *C. elegans* with dopaminergic neuron-specific proteins tagged with GFP to visualize neuron degeneration after copper exposure. The association of Cu ions with neuronal degeneration has been established in *C. elegans* and humans [14, 71]. Transgene expression of genes of interest can provide more specific information regarding bioavailability and the phenotype of the NPs effect compared to conventional endpoint assessment [168, 181]. The CuO NPs induced morphological changes to neurons in a small portion of the *C. elegans* populations in a concentration-dependent manner. The neurodegeneration caused by CuO NPs compared to copper sulfate exposure was not statistically different, suggesting the released Cu ions may be the sole source of neuron damage (Table S5).

As the CuO NPs suspensions contained significantly less Cu^{2+} (p<0.04) compared to copper sulfate exposure but caused equal or greater neurodegeneration; these data support the greater sensitivity of *C. elegans* to CuO NPs exposure compared with copper sulfate. The concentration of copper sulfate employed in this study were two-fold greater than the Cu^{2+} concentration released from the CuO NPs after 24 hour

incubation in K medium (Figure 14). It is unlikely that the CuO NPs are being internalized into cells of *C. elegans* to directly interact with neurons. It is probable that the neurons are more sensitive to the highly localized and concentrated release of Cu ions from the surface of the CuO NPs after being ingested by the animal. Copper treatment of the *smf-1* and *smf-2* knockout strains resulted in reduced percent of the population with neurodegeneration (Figure 16) and was significantly different when compared to N2 ($p<0.001$ and $p<0.021$, respectively). The observed resistance to copper exposures of strains containing *smf-1* or *smf-2* deletion suggests this transporter may play a role in copper-related neurodegeneration. Combined, these data indicate equal effect on neuron morphology from exposure to CuO NPs compared to copper sulfate, suggesting that this physiological effect of copper toxicity is independent of the copper form, and in the case of CuO NPs is most likely due to the released copper ions.

A transgenic reporter strain for general stress in *C. elegans,* containing GFP expression under control of the *hsp-16.2* promoter, was used to observe stress pathway induction after a 24 hour copper exposure. Toxicity from copper sulfate exposure has been shown to be mediated by HSP-16.2p [72]. Exposure of the reporter strain with CuO NPs and copper sulfate at the two highest concentrations (Figure 17) resulted in significantly greater GFP expression when compared to untreated nematodes ($p<0.01$). The equal induction of GFP that was observed in the *C. elegans* population after CuO NPs and soluble copper exposures may reflect an equal response of *hsp-16.2* mediated protection to copper stress. Analogous to the observed effect on neuronal health, the similar stress response to CuO NPs compared to copper sulfate suggests the induction of *hsp-16.2* is due to the released Cu ions and not a NPs specific effect.

4.6 *Conclusion*

This study describes the physiological effects of copper oxide nanoparticles (CuO NPs) to *Caenorhabditis elegans* N2 and a genetically diverse selection of wild nematode strains as observed by inhibitory effects on feeding, reproduction, development, and neuron morphology. The results support an increased sensitivity to CuO NPs compared to copper sulfate in a genetically broad selection of *C. elegans* strains. CuO NPs sensitivity was a phenotype observed in all *C. elegans* strains assayed despite their different genotypes suggesting this effect is not due to laboratory domestication of the N2 strain. Neuronal deformation in similar portion of the *C. elegans* population occurred after exposure with either CuO NPs or copper sulfate at equal molar concentrations. Similarly, an equal response of *hsp-16.2* mediated protection to copper stress was observed in the *C. elegans* population after CuO NPs and soluble copper exposures. This implicates the released Cu ions from CuO NPs as major factor contributing to the observed NPs effect on neuronal health and organism stress response.

CHAPTER 5
FINAL CONCLUSIONS

5.1 Final conclusions

This work highlights the role of copper (Cu) ions released from the copper oxide nanoparticles (CuO NPs) when they dissolve in certain aqueous media on the observed toxicological endpoints in *S. cerevisiae* and *C. elegans*. These released Cu ions may be important as they can have inhibitory effects similar to those observed after exposure to CuO NPs. The present study shows that under the tested conditions CuO NPs had a smaller effect on *S. cerevisiae* metabolic activity compared to equal molar concentrations of Cu^{2+} in the form of copper sulfate or released Cu ions. Yeast metabolism was significantly more sensitive to exposure with 28 nm CuO NPs compared to exposure with larger 64 nm CuO NPs. Interestingly, the observed inhibition of metabolic activity rate from the 28 nm NPs was not completely due to the released Cu ions. The addition of the metal chelator EDTA significantly reduced the effect on yeast respiratory metabolism with both CuO NPs, but did not completely restored metabolic function after 28 nm CuO NPs exposure. Experiments addressing the aging of CuO NPs, i.e. prolonged incubation of NPs in sterile growth medium to facilitate interaction with media components, resulted in no difference in inhibitory effect when compared to freshly resuspended CuO NPs. It was observed that yeast have differential sensitivity based on the carbon source employed, with a greater CuO NP effect on metabolic activity when yeast were cultured under respiring conditions. This knowledge of sensitivity based on the cell metabolic state (respiratory vs. fermentative) may assist future studies in further defining the mechanism of CuO NPs inhibition on cell metabolism.

The copper ions that were released from the CuO NPs are a major factor for molecular effects on the *S. cerevisiae* cells. Interestingly, the observed inhibition from the nanoparticles was not fully explained by the released Cu from the dissolving nanoparticles. Treatment with either CuO NPs or released copper ions resulted in differential gene expression associated with cell cycle arrest. The copper ions may induce damage and result in up-regulation of YLR149C, as well as down-regulation of *CLB6, PCL1*, and other cyclins, which act in unison to halt cell cycle progression. XBP1p is a transcriptional repressor expressed during stress and is involved in maintaining cells in an arrested state at G1 phase. Exposure with CuO NPs resulted in changes in gene regulation that may lead to cell cycle arrest through the up-regulation of XBP1. The CuO NPs exposure resulted in up-regulation of several mitochondrial proteins involved in energy production and oxidative phosphorylation. In addition, CuO NPs exposure resulted in increased PHO85p activity from the up-regulation of regulatory cyclins *PCL8/10*, which was not observed from copper sulfate exposure. The change in regulation of genes observed to specifically occur after CuO NPs exposure suggests a differential response to stress compared to treatment with released Cu ions.

5.2 Proposed mechanism of copper oxide nanoparticle interactions with S. cerevisiae cells

Within this study, the CuO NPs were observed to adsorb to the exterior of *S. cerevisiae* cells in scanning electron microscopy images. This interaction of the CuO NPs with the cell's exterior surface may be a result of NP-peptide adsorption, as previously was proposed by others [19]. The CuO NPs are most likely bound with a strong affinity to the cell surface as they are still bound even after electron microscopy sample preparation [see section *3.3.4*]. Copper might induce oxidative stress within close proximity to the cell surface that could result in lipid peroxidation and subsequently

damage to the membrane (Figure 18). Damage to the cell exterior (cell wall and membrane) is suggested within our study from the increased expression of genes involved in cell wall biosynthesis. Increased activity in the plasma membrane ATPase (*PMA1*) was also observed as a response to damage that resulted in increased membrane permeability. Experiments with yeast deletion mutants also suggest oxidative stress as a driving factor in CuO NPs toxicity, as deletions in oxidative stress defense proteins were particularly sensitive to CuO NPs exposure [19].

The action of the CuO NPs inhibitory effect may be a two stage process, beginning with the cell interacting with the copper ions released from the CuO NPs. The first 'stage' of exposure results in a stronger influence from the released copper ions compared to CuO NPs exposure. The second 'stage' occurs as the CuO NPs interact with peptides, thereby facilitating interaction with the surface of the cell (Figure 18). The NPs are continuing to release copper ions while the NPs are within close proximity to the cell membrane. This highly localized and concentrated release of Cu ions can induce oxidative stress, including hydroxyl radicals, causing lipid peroxidation near the source of attachment. This process leads to further damage to the membrane that allows internalization of unbound Cu ions as well as any ROS within close proximity.

The increased internalization of Cu ions results in cellular damage, as suggested by increased expression in genes involved in scavenging of reactive oxygen species, protein folding and degradation, and DNA-damage repair. A decrease in protein synthesis is suggested as many genes related to ribosome biogenesis were decreased in regulation. Reduced protein synthesis allows the cells to conserve energy and thereby allows cells to more appropriately adapt and respond to the stress. Numerous genes

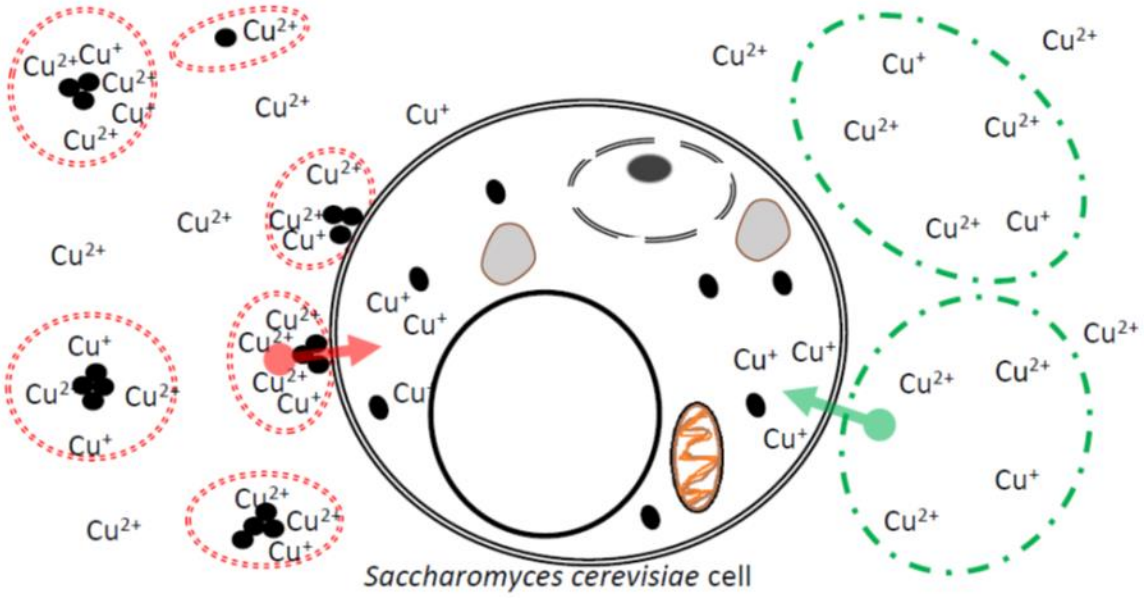

Figure 18. Proposed mechanism of copper oxide nanoparticle interactions with *S. cerevisiae cells.*

involved in glycogenesis were also up-regulated, including glycogen debranching enzymes and glycogen synthases. Increased abundance of glycogen and trehalose after exposure to stress can establish energy reserves for improved response to stress. The increased expression of genes related to glycogen and trehalose storage is further evidence of cell cycle arrest as this has been linked with arrest at G1 phase.

There remains further work to be performed regarding the interactions between CuO NPs and yeast cells. Future experiments can be conducted that will lend credence to the suggestion of cell cycle arrest. It is established that the budding yeast cell cycle at G1 phase is strictly linked to the initiation of budding [208]. That is, the degree of budding that a cell is undergoing closely corresponds to progression through the cell cycle. Therefore, microscopic observation of yeast cells can determine the stage of replication that a cell is undergoing. Copper treatment of yeast could result in a shifting

in the percent of the yeast population arresting cell cycle progression compared to untreated yeast.

Changes in gene regulation have been suggested based on a single time point microarray analysis. Additional qPCR experiments addressing gene changes over time, (at 0.5, 1, 2, 4, and 8 hrs) would improve the understanding of the overall effect of CuO NPs exposure on yeast cells. DNA and RNA samples from the exposure experiment for the microarray analysis are currently available and thus qPCR analysis based on specific genes of interest would further evaluate differentially regulated pathways during the CuO NPs exposure. Proteins involved in copper homeostasis can be further assessed to observe changes over time throughout the length of exposure. Additionally, the importance of increased oxidative stress can be addressed by observing changes in regulation of genes involved in oxidative stress defense.

The inquiries into oxidative stress-related damage in yeast after CuO NPs exposure can be further examined through the use of ROS-sensitive mutant strains. While a number of antioxidant single-gene deletion mutants were assayed within this work, double-mutations are often required to obtain responses strong enough to be studied. This work has highlighted the critical nature of the released Cu ions regarding the toxicity of CuO NPs. One can deduce the internalization of these Cu ions causes a portion of the observed toxicity after exposure to CuO NPs. Copper homeostasis within yeast is dynamic as the rate of Cu^{+} uptake, Cu^{+}-binding, and Cu^{+} export can all be controlled individually to maintain homeostatic levels of C^{+}. Thus, in-depth analysis of the internal cellular Cu concentration overtime, after varying copper exposure concentrations, would facilitate a better appreciation of the relationship between CuO NPs and yeast cells. Indeed, the CuO NPs may be becoming internalized into yeast via endocytosis. Therefore, establishing cellular Cu concentrations with or without endocytosis inhibitors, such as cytochalasin A or nocodazole, could clarify if CuO NPs

are becoming internalized. The use of transmission electron microscopy alongside the use of smaller and larger diameter CuO NPs exposures, would further support if internalization of the CuO NPs may be occurring at certain critical diameters.

5.3 Proposed interactions of copper oxide nanoparticles with nematodes

This study describes the inhibitory effects of CuO NPs to *C. elegans* N2 strain, as well as in a genetically diverse selection of wild nematode strains. Exposure to CuO NPs resulted in inhibitory effects on nematode population body length, feeding behavior, and reproduction. In the current study, CuO NPs were found to affect development and feeding behavior more than equal molar concentrations of copper sulfate. It is of interest to note that feeding behavior was very sensitive toxicological endpoint, as CuO NPs exposure at every tested concentration had a significant inhibitory effect. Exposure with copper sulfate was significantly less inhibitory towards feeding compared to exposure with CuO NPs, suggesting that ingestion of CuO NPs may be occurring. NPs may be ingested and subsequently dissolving internally, as was observed with silver NPs exposure to *C. elegans* [202].

The CuO NPs sensitivity is a strong phenotype as all of the *C. elegans* strains assayed were less sensitive to exposure to copper sulfate. Though the laboratory domesticated N2 strain has known differences in both behavior and physiology compared to wild strains, all strains assayed displayed increased sensitivity to CuO NPs compared to copper sulfate. The CuO NPs affected neuronal health as treatment with CuO NPs resulted in dopaminergic neuron degeneration. This neurodegeneration may be occurring via the metal ion transporters SMF-1 and SMF-2, as experiments with knockout deletion mutations in *smf-1* and *smf-2* were less sensitive to copper exposure. The CuO NPs were observed to induce neuron degeneration in an equal percent of the exposed population of *C. elegans* compared to the population exposed with copper

sulfate at equal molar concentrations. The induction of stress, as measured by *hsp 16.2* expression, was observed to occur equally by the CuO NPs and copper sulfate exposures. The damage to neuronal cells and inhibition of reproduction from exposure to CuO NPs appears to be related to released Cu ions, as these assays resulted in an equal effect from CuO NPs compared to exposure with released Cu ions. This is in contrast to effects observed on the feeding and development of *C. elegans*, which appear to be inhibited specifically by the nanoparticles as the CuO NPs exposure was more inhibitory than the soluble copper ion exposure.

CHAPTER 6

APPENDIX – DETAILED PROTOCOLS AND SUPPLEMENTARY INFORMATION

6.1 Nematode cultivation protocols

6.1.1 Caenorhabditis elegans *strains and cultivation conditions*

All *Caenorhabditis elegans* strains were routinely cultured on Nematode Growth medium (NGM) plates seeded with the *Escherichia coli* strain OP50. Strains were transferred twice a week and stored at 20ºC according to the standard method previously described by Brenner [178]. Three wild strains and N2 mutants were also employed in addition to the N2 wild-type strain. The N2 strain was a kind gift of Dr. R. Stuart (Marquette University, Milwaukee, WI, USA). The wild strains CB4856, DL238, and JU258 were kind gifts of Dr. E. Andersen (Northwestern University, Chicago, IL, USA) and their genetic characteristics are detailed in [176]. Strains CB4856 and DL238, are considered to differ the most in gene content compared to N2 [179]. The CB4856 and DL238 strains contain on average 3,613 SNPs which differed from N2 [176]. The other wild strain employed, JU258, is also considered dissimilar to N2 strain and is further described in [203]. The transgenic strains RJ907 ($P_{dat\text{-}1}$*::*GFP; *smf-2*(*eh5*)) and RJ938 ($P_{dat\text{-}1}$*::*GFP*; smf-2*(*gk133*)), each containing GFP expression controlled by the *dat-1* promoter, were kind gifts of Dr. R. Nass (Indiana University School of Medicine, Indianapolis, Indiana, USA) . The BY250 strain ($P_{dat\text{-}1}$*::*GFP; N2 wild-type) was a kind gift of Dr. R. Blakely (Vanderbilt University, Nashville, TN, USA). Specifics on the construction of these transgenic *C. elegans* lines can be found in Nass *et al* [181]. The reporter strain KC136 with GFP expression controlled by the heat shock protein (HSP) *16.2* promoter (Hsp-16 *him-5*(*el490*)), which was a generous gift of Dr. K. L. Chow (Hong Kong University of Science and Technology, Clear Water Bay, Kowloon, Hong Kong)

[182]. Nematodes were exposed to copper sulfate and CuO NPs for 96 hours in K medium with bacterial lysate to prevent nutrient deprivation.

6.1.2 High-throughput endpoint assays of development, brood size, and feeding behavior

A Complex Object Parametric Analyzer and Sorter (COPAS) BIOSORT was employed to assay the physiological endpoints after 96 hour treatment as per the previous protocol described in Andersen *et al* [176]. Body size was measured as 'time of flight' while the paralyzed animals passed through the flow cell. Reproduction was measured by quantifying the total number of objects that pass through the flow cell. These objects are assumed to be nematode progeny with 99.97% accuracy as per the support vector machine described in [176] and were normalized to number of adults initially transferred to each well of the 96-well plate. Brood size was considered the amount of offspring generated by a nematode within the 96 hour experiment. Feeding behavior was assayed as pharyngeal pumping based on red fluorescence signal within each nematode after red fluorescent latex beads (Polysciences) were added to the food source. The COPASutils R package was used to process the data as per [183].

6.1.3 Dopaminergic neuron degeneration and heat shock protein induction scoring

The transgenic reporter strains used (BY250, RJ907, and RJ938) contain a green fluorescent protein (GFP) that is expressed under control of the *dat-1* promoter within dopaminergic neurons. Additionally, the transgenic strain KC136 contains GFP reporter which expression is driven by a *hsp-16.2* stress inducible promoter. Transgenic nematode populations were synchronized using standard alkaline hypochlorite method [184] and allowed to enter L1 stage during overnight incubation. L1 nematodes were

suspended in 1 mL K medium (supplemented with 5 mg/mL cholesterol and HB101 bacterial lysate) containing the respective copper treatment at desired concentration and were incubated at 20°C on a rotational shaker at 250 rpm for 24 hours. Due to the impermeable nature of the cuticle of *C. elegans*, a 24 hour exposure was necessary to observe any effect [185, 186]. After copper exposure, animals were gently pelleted at 1,500xg for 60 seconds. Supernatant was removed, and nematodes were washed twice with K medium (pH 6.5, with no cholesterol or lysate added) prior to plating onto K medium agar with OP50 bacteria. After 72 hour recovering period, adult worms were picked onto agar stubs and scored on a fluorescent Nikon microscope (Nikon te2000) for any abnormal neuron formation. For neuronal degeneration nematodes were considered positive if neurons were malformed or completely absent. For stress response, KC136 nematodes were imaged and GFP expression was measured as voxel volume and normalized to length using Metamorph 5.5 software (Molecular devices). Data represent three independent experiments and at least 40 nematodes were scored for each treatment.

6.1.4 Decontamination of C. elegans *strains*

Prepare bleaching solution by adding 25 uL of 1M NaOH and 2 mL of standard commercial bleach to 6 mL ddH_2O. Mix solution by shaking. Transfer 10 uL of the NaOH/bleach solution to the side of a non-contaminated NGM petri, making sure to avoid adding bleach solution to the bacterial lawn. Using a worm pick, transfer 4-6 adult nematodes (gravid hermaphrodites) to the NaOH/bleach solution. The adults transferred should have eggs; this will be obvious upon observation at increased magnification. The NaOH/bleach solution must be present on the surface after the adults are added, if it has soaked into the plate another 5-10 uL should be added on top of the adults. The animals

should immediately react and thrash for a few seconds and then completely stop moving. Gently transfer NGM petri dish to 20^{o}C incubator and incubate overnight. Observe the following day to ensure L1 larvae have begun to hatch from the eggs and are beginning to crawl on the plate and enter the bacterial lawn.

6.1.5 Cryopreservation of C. elegans *strains*

Protocol adapted from Brenner *et al* 1977, Genetics 77. Seed several small NGM plates and transfer 4-6 adults per plate as per normal strain upkeep protocols. Incubate plates for 3-4 days or until food supply is exhausted as starved L1 and L2 animals survive the freezing and thawing conditions best. Do not allow more than a day to pass once food supply is exhausted or nematodes may enter dauer stage. Label 3 screw cap 2 mL cryotubes per each stock. Prepare S-basal with cholesterol added at a final concentration of 0.1 mg/mL. Use the S-basal media to gently wash the nematodes from the plate. Collect the nematodes in a 15 mL centrifuge tube, centrifuge at 1,500xg for 60 seconds (do not exceed 2,000 rpm as this will damage the worms). Toss supernatant and resuspend nematodes in 1.8 mL S-basal media, add 0.6 mL 30% glycerol and mix gently by flicking the tube. Aliquot 0.6 mL to each 2 mL cryotube, move cryotubes to Styrofoam box which will slow down the freezing process. Move Styrofoam box containing cryotubes to -80^{o}C freezer.

6.2 Saccharomyces cerevisiae *protocols*

6.2.1 Yeast cultivation and exposure protocols

Saccharomyces cerevisiae (*S. cerevisiae*) W303-1A wild type (*MAT*a: *leu2-3,112 trp1-1 can1-100 ura3-1 ade2-1 his3-11,15*) was a kind gift of Dr. Rosemary Stuart

(Marquette University, WI). The strain was maintained on YP agar plates (pH 6.6) containing 1% yeast extract (Amresco), 2% Bacto peptone (Difco laboratories) and 2% of the respective carbon source at 30^{o}C overnight. To prepare starter cultures single colonies from the respective master plates were transferred in 5 ml YP media with ethanol, galactose, or dextrose as carbon source and grown overnight at 30^{o}C, 250 rpm in order to culture the cells under respiratory, respiratory/fermentative, or fermentative metabolism, respectively.

S. cerevisiae experimental cultures were started from the overnight cultures. The turbidity of the cell culture was measured via absorbance at 600 nm using a spectrophotometer (Molecular Devices) and diluted with sterile YP media with respective carbon source to an OD_{600} 0.1. The cultures were grown until OD_{600} 0.3 was reached (approximately $4.0x10^{6}$ Colony Forming Units mL^{-1} determined by dilutions and plating on YP-galactose (YP-gal) plates with colony counting after 72 hour at 30^{o}C incubation). Exposure to tested chemicals was performed in 96-well black with clear bottom, polystyrene plates (Costar) at 30^{o}C with continuous shaking at 250 rpm. This concentration of cells was consistently used in all toxicity assays.

6.2.2 Determining cell viability spot assay

Overnight cultures of *S. cerevisiae* in YP-gal media were diluted to OD_{600} 0.1 and 150 µL of the cell suspensions were aliquoted to 0.6 mL 96-deep-well plate. Cell suspensions were mixed with 150 µL of CuO NPs and copper sulfate solutions in YP-gal media. Plates were covered loosely with aluminum foil and incubated at 30^{o}C for 24 hour with shaking at 250 rpm. Cells were then serially diluted in PBS buffer (pH 7.2) and 2 uL of the cell solutions were spotted onto YP-gal agar plates in triplicate. The formation of colonies was visually examined after 72 hour of incubation at 30^{o}C and was compared to colony formation of untreated cells.

6.2.3 Cell growth inhibition assay

S. cerevisiae experimental cultures were started from the overnight cultures. The turbidity of the cell culture was measured via absorbance at 600 nm using a spectrophotometer (Molecular Devices) and diluted with sterile YP media with respective carbon source to an OD_{600} 0.05. The cultures were grown until OD_{600} 0.2 was reached to ensure logarithmic growth was achieved. Experiment is performed in sterile clear 96 well clear bottom black plate, plates are sterilized by spraying with 70% ethanol followed by 60 mins incubation under UV light. Add 200 uL cell suspension into wells as is required based on triplicate analysis and dependent upon the number of exposures and concentrations to be employed. Plates should have the following controls: untreated (no treatment), cell free control (media as a blank for background), kill control (high temperature pre-treatment or high concentration of chemical confirmed to kill or inhibit growth).

Cover the plate with clear hard plastic cover, followed by aluminum foil to prevent light exposure. Place plate in a box with a moist paper towel inside to prevent dehydration, incubate plate at 30^{o}C for 4 hours or 24 hours dependent on time point of interest. After desired time point, use a multi-channel pipette, aliquot 50 uL from the plate and add to 250 uL water for a 1:6 dilution, subsequent dilutions can be performed for 24 hour experiment as OD will be greater than 1.0. Read plate in spectrophotometer at OD_{600}, calculate initial OD prior to dilution to determine reduced growth. Compare treatments to untreated control wells and ensure the triplicates are averaged. NOTE: The CuO NPs refract visible light and as such will interfere with this type of experiment and thus should be avoided or only performed with very low concentrations which must also have an additional cell free control with only CuO NPs.

6.2.4 Separation of cells from nanoparticles via Nycodenz assay

To separate CuO NPs from cell solution, nycodenz solution (30%) should be added to a 1.5 mL microcentrifuge tube prior to cell solution addition. Cell solution should be gently pipetted onto nycodenz solution and extra effort should be made to not perturb the nycodenz solution. Centrifuge at 4,000 xg for 3 mins, observe tube which should have an obvious separation of the cell culture medium and the clear nycodenz solution with a visible layer of cells suspended in between. If the cells still remain in the upper layer, increase speed to 7,000 xg for 5 mins. The CuO NPs should be visibly deposited on the side of the tube and should not be suspended in the cell layer. Carefully remove the cell layer as well as cell culture medium, if nycodenz solution is removed this will not interfere with other protocols. Two additional washes with culture medium, phosphate buffered saline, or water to remove any residual nycodenz solution.

6.2.5 Endocytosis inhibition protocol to investigate internalization of nanoparticles

S. cerevisiae experimental cultures were started from the overnight cultures. The turbidity of the cell culture was measured via absorbance at 600 nm using a spectrophotometer (Molecular Devices) and diluted with sterile YP media with respective carbon source to an OD_{600} 0.1. The cultures were grown until OD_{600} 0.3 was reached to ensure logarithmic growth was achieved. Endocytosis inhibitors were added to the following working concentrations: Chlorpromazine HCl 14 uM, Cytochalasin D 1 ug/uL, Dynasore 80 uM, and Nocodazole 20 uM. Incubate inhibitors for 20 mins at 30^{o}C, cultures are now ready for NPs exposure. The NPs inhibitory effect can now be analyzed via alamar blue, propidium iodide staining, growth inhibition, or other assay.

The following controls should also be run alongside experiments: inhibitor control (no NPs exposure), untreated control (no NPs exposure, no inhibitor), warm treatment control (30^{o}C incubation, NPs exposure, no inhibitor), cold treatment control (4^{o}C

incubation, NPs exposure, no inhibitor). Note: for the cold and warm treatment control, cultures should be pre-incubated for 20 mins prior to addition of NPs. The cold control should limit active endocytosis \without chemical endocytosis inhibitor.

6.2.6 Determination of Intracellular and membrane-bound copper

To determine the total Cu content of yeast cells after CuO and copper sulfate treatment, 0.5 mL of cell culture were removed and gently added on top of 0.4 mL 80% (w/v) Nycodenz solution (Progen Biotechnik GmbH, Heidelberg, Germany) and centrifuged at 4,000*g* for 5 minutes. The cellular fraction was removed and added to 1.0 mL PBS (pH 7.2). These solutions were then centrifuged at 8,000x*g* for 5 minutes, supernatant removed and cell pellet was washed twice in 1 mL PBS containing 20 mg L^{-1} EDTA and washed once with 1 mL PBS containing 20 mg L^{-1} Bathocuprionedisulfonic acid disodium salt (Sigma-Aldrich) to remove any residual membrane bound copper. A final wash with 1 mL PBS was performed and cell pellet re-suspended in 200 µL PBS. A 10 µL aliquot of cells was collected for cell count with a hemocytometer. The cell solutions were digested with equal volume 70% (w/v) HNO_3 at 65ºC for 2h and stored at 4ºC. Samples for ICP-MS analysis were further diluted to 2% HNO_3 with ddH_2O, containing 0.5% HCL, prior to sample analysis using an ICP-MS system (7700x ICP-MS with autosampler, Agilent Technologies, Santa Clara, CA).

6.2.7 Scanning electron microscopy specimen preparation

To observe interaction of *S. cerevisiae* cells and CuO NPs, scanning electron microscopy (SEM) analysis was performed after exposure. *S. cerevisiae* was treated with 69.5 mg Cu/L CuO NPs for 1 hour, followed by primary fixation with 2.5% glutaraldehyde in PBS overnight at 4ºC. Solution containing fixed cells was dropped onto glass slides coated in Poly-L-lysine and cells were allowed to settle onto the coated

surface. Secondary fixation was performed in 1% Osmium tetroxide (OsO_4) in PBS for 1 hour followed by dehydration in sequential stages of ethyl alcohol and double distilled water at 20%, 40%, 70%, and 100%. Sample drying was performed using Hexamethyldisilazane (HMDS; BASF SE) at a 1:1 dilution with 100% ethyl alcohol for 10 mins followed by pure HMDS solution for 10 mins. After drying, glass slides were attached to 15 mm aluminum stubs using double-coated carbon tape. The samples were then coated in 6 nm Iridium with K500X sputter coater (Quorum Technologies).

6.2.8 RNA extraction and subsequent cDNA production

The *S. cerevisiae* cell pellets from all treatment time points were removed from -80ºC storage and placed on ice immediately prior to RNA extraction. The freshly thawed cell pellet was homogenized using 0.2 um zirconium oxide beads in a 2 mL polystyrene microcentrifuge tube placed inside a Bullet Blender® bead beater (Braintree Scientific, Inc) at 4ºC. The Bullet Blender® was employed at power level setting 7 for 3 mins followed by 5 mins incubation on ice and another round of bead beating at power level 7 for 3 mins. The cell lysate was centrifuged at 4,000xg for 2 mins and supernatant was transferred to PureLink® spin column cartridge. The PureLink® RNA mini kit (ambion®, Life technologies®) was used as per instructions using spin columns and table top centrifuge. The extracted RNA was treated with DNase as per the TURBO DNA-*free*™ kit (ambion®, Life technologies®) instructions. The cDNA was generated by using the SuperScript® III First-Strand Synthesis kit with the DNase-treated RNA as per product recommendations (Invitrogen™). Briefly, 2 ug of RNA was used in a 20 uL reaction volume in a thermocycler and run with the following program: 25ºC for 10 mins, 50ºC for 30 mins, 85ºC for 5 mins followed by 4ºC until placed on ice. RNase H was added for 20 mins prior to storage at -20ºC.

6.2.9 Microarray data analysis and related statistical techniques

The microarray was performed at the Genome center of Wisconsin at the University of Madison Biotechnology Center. The Affymetrix CEL files containing the expression data for the yeast 2.0 probe set were loaded into R with the Affy package where each chip was represented as an array. Background noise correction was performed on each chip by employing Affy and using the Robust Multichip Average expression measure. Each chip was then normalized to the geometric mean of the expression of housekeeping genes recently analyzed and confirmed as appropriate (*ALG9*, *KRE1*, *TAF10*, *TFC1*, and *UBC6*) [121]. Normalization to the geometric mean of these genes in each chip has been shown to be much more accurate than normalization to a single gene in the analysis of microarray data [122]. These correction measures were used to transform the raw expression data into corrected, normalized log expression values.

Annotation data (such as probeID and experimental information) was extracted from the CEL files using Bioconductor's a4 package [123]. This package was also used to extract gene name, description of function, ORF, Gene Ontology numbers, and KEGG pathways from probe IDs in conjunction with the Affymetrix Yeast 2.0 chipset database, available through Bioconductor.

Linear models were fitted to each chip's log expression values with the Limma package [124]. A contrast matrix was constructed from the arrays in order to compare two different treatments (e.g. untreated and nanoparticle treatments). The package was then used to calculate the log two fold differences in gene expression and the probability of differential expression for each probe using an empirical Bayes approach. The a4 package was used to adjust the calculated *p* values in order to account for the family wise error rate using the Benjamini Hochberg method and to generate a table of the calculated values.

Genes were considered significantly altered in expression after copper exposure with greater than/less than 1.5/-1.5 Log_2 Fold Change (LogFC) and an adjusted $p<0.05$. We chose a 1.5 LogFC cutoff, e.g. 3 fold difference compared to the untreated cell cultures [18]. These genes were further separated into up and down-regulated categories. These genes were then submitted to Princeton University's Gene Ontology Mapper and the resulting ontologies were used to observe patters of altered gene expression [125].

The probe ID, fold change data, and KEGG pathway number annotations were also extracted from the list of differentially expressed genes. Probe IDs were converted into Entrez Gene IDs using DAVID, and further converted into KEGG gene numbers on their website [126, 127]. The fold change data for each probe in the Yeast 2.0 set associated with that KEGG pathway was then submitted to the KEGG pathway mapper tool [128].

6.2.10 Determining oxygen consumption of yeast using Seahorse Flux analyzer

The Seahorse XF96 was equilibrated at 30°C for 4 hours prior to experiment. Yeast at 1 x 10^5 cells/mL (OD_{600} 0.3) were added to each well of the XF96 plate at a volume of 160 µl in YP-gal; as well as CuO NPs, menadione, oligomycin, FCCP, and Antimycin A which were added to wells at specified time points throughout experiment. The XF plate, each well containing enough yeast to completely cover the bottom, was centrifuged for 1 min at 1,000 rpm in a swinging bucket rotor (Eppendorff, CA 5810R) followed by addition of 140 µl of substrate containing 1 × MAS was added to each well. Fresh stock solutions of Oligomycin, FCCP, and antimycin A were made in DMSO. The cartridge was calibrated by the XF machine, and following calibration the XF plate with yeast attached to the bottom was introduced into the machine. The injections for electron

flow experiment were prepared as follows: Port A, Oligomycin; Port B, FCCP; Port C, Antimycin A. The final concentrations were 10 ug/mL Oligomycin, 10 mM FCCP and 10 µM Antimycin A. Throughout experiment the a 1 min/1 min/2 mins time period was employed for the mix/wait/measure cycles at every read point for a total of 5 mins per read. Experimental reads were as follows: 5 basal reads, introduction of copper treatment with 5 reads post exposure, Oligomycin injection followed by 5 reads, FCCP injection followed by 3 reads, and Antimycin A injection followed by 4 reads.

6.2.11 *Determining oxygen consumption of yeast using Clark electrode*

Yeast were suspended at 1 x 10^7 CFU/mL (OD_{600} 0.3) in a YP media with galactose as a carbon source. The consumption of oxygen was assayed in a 300 uL volume using the Digital Model 10 clark electrode (Rank Brothers, LTD) to determine the rate of oxygen consumption within the chamber. The silver electrode is prepared for measurement by removing any oxide layer present by gently scrubbing with ascorbate using water and a cotton swab. An PTFE Teflon membrane was placed over the silver electrode at the base of the chamber, in such a way as to prevent air bubbles, prior to fully assembling the chamber. The ‘Stir’ function was employed at speed 7 with a magnetic glass stir bar within the chamber to ensure cells remained in suspension at room temperature. Water was added to chamber and measurements taken while adjusting sensitivity to attain 99.9 ± 1.0 as the output for 2 min to ensure steady state of gradual decline in oxygen (<2% over 5 mins) indicating membrane covering electrode remains intact. This cell free oxygen consumption was treated as background and removed from sample reads. Cells with or without treatment were added to chamber and read for 5 mins, followed by 2 additional reads after re-introducing O_2 into the chamber using a pipetter.

6.3 Fluorescence staining protocols

6.3.1 Determining membrane damage with propidium iodide staining

To detect changes in cell membrane permeability due to treatment with CuO NPs or copper sulfate, *S. cerevisiae* cells at 1 mL volume were stained with 5 uL of 1 mg/mL propidium iodide solution. To quantify total cells, 5 uL of 5 mM calcofluor white M2R, dissolved in water, was added to cells. Cell solutions were incubated with dye at room temperature for 10 mins protected from light. After staining, cells were washed twice in PBS (pH 7.2), re-suspended in glucose-HEPES (GH, pH 7.0) buffer with 4% formaldehyde (v/v) and fixed at room temperature for 10 mins. Fixed cells were centrifuged at 10,000xg for 5 mins and re-suspended in 30 uL of GH. The cells were stored at 4°C until imaging with a confocal microscope (Nikon Eclipse Ti, Nikon Instruments Inc.; Tokyo, Japan).

Cells in YP-gal media were exposed to CuO NPs or copper sulfate for 1 hour, 4 hour or 24 hours at 30^{o}C shaking with (250 rpm). After CuO NPs and copper sulfate treatments cells were then stained with propidium iodide (Biotium) and calcofluor white (MP Biomedicals) according to above procedure. The DAPI filter set was used for calcofluor white detection, with an excitation at 405 nm and emission range of 425-475 nm, the texas red filter set was used for propidium iodide detection, with an excitation at 561 nm and emission range of 570-620 nm. Images were analyzed using Image-J software.

6.3.2 Quantifying oxidative stress by reactive oxygen species staining

Intracellular ROS levels were determined using both Dihydroethidium (DHE) and Dihydrorhodamine 123 (DHR123) dyes (Sigma-Aldrich, St. Loius, MO). DHE is a cell permeable dye which can become oxygenated upon interaction with various ROS from

hydroethidium to ethidium, resulting in cells with fluorescent red observable at excitation/emission at 480 and 567 nm, respectively. DHR123 is a cell permeable dye which becomes reduced to rhodamine 123 (RH123) a red fluorescent chemical upon interaction with peroxynitrates and other ROS. The RH123 becomes localized to the mitochondria after reduction and is observable with excitation/emission wavelengths of 500 and 536 nm, respectively. Cells were exposed to Cu treatments, centrifuged, washed with YP media, and then resuspended in PBS (pH 7.2) for staining. Cells were stained with DHE and DHR123 at a final concentration of 1 ug mL^{-1} and 1.25 ug mL^{-1}, respectively, in PBS (pH 7.2) for 2 hour at room temperature post exposure. After staining cells were washed once with PBS and resuspended in 100 uL PBS and observed with fluorescent microscope immediately.

6.3.3 Quantifying metabolic activity via the alamar blue assay

The inhibitory effects of CuO NPs were determined by quantifying cellular metabolic activity using alamarBlue (aB, Invitrogen), a cell-permeable redox-sensitive dye that turns from a non-fluorescent blue color to a highly fluorescent pink color upon reduction by metabolically active cells. Fluorescence detection of the reduced aB signal was performed in a Spectra Max® M2e spectrophotometer (Molecular Devices Inc.).

The metabolic activity assay was performed according to the following protocol: copper treatments were generated by adding copper sulfate, or released Cu^{2+} fraction from NPs, or dispersed CuO NPs into YP-gal media to achieve 300 uL volume at desired concentration. Freshly inoculated cultures of *S. cerevisiae* in YP-Gal media were incubated at 30^{o}C for 3-4 hour until OD_{600} 0.3 was reached, centrifuged at 4,000 rpm for 2 min, supernatant removed, and cell pellets were then resuspended with YP-Gal media containing different copper treatment. Each experimental treatment was amended with 10% (v/v) alamarBlue dye to achieve a final volume of 330 µL, which was then aliquoted

to 3 separate wells to a final volume of 100 µL per well in a 96-well plate (Costar polystyrene flat bottom, non-treated, black sided, clear bottom). Cell free YP-Gal media was added to cell free control wells for background subtraction. Plates were covered with aluminum foil to prevent light exposure and incubated at 30^{o}C, with shaking at 250 rpm for 1.5 hour. Fluorescence was recorded at 550/585nm excitation/emission with a 570 nm cutoff every 5 min for 1.5 hour. Cellular metabolic rate was determined by employing SpectraMax software to calculate rate of fluorescence at the linear portion of each curve. Each respective treatment was performed in triplicate wells and the results were averaged per well. Data are mean of three independent experiments $\pm$ range of values.

6.4 Copper oxide nanoparticle protocols

6.4.1 Determining nanoparticle primary particle diameter and morphology using electron microscopy

Transmission electron microscopy (TEM) was employed to characterize both CuO NPs morphology and primary particle diameter. Diluted CuO NPs suspensions in water or YP-gal media were deposited onto formvar coated copper 200 mesh grids and allowed to settle for 10 min prior to removal of the excess liquid. TEM imaging was performed on a Hitachi H9000NAR Analytical High Resolution Transmission Electron Microscope, 300 KeV (dpr) and the primary particle diameters were assessed using ImageJ image processing and analysis software. Briefly, the measuring tool was employed, after altering the scale to nanometers, in order to assess dimensions of 100 individual NPs of both 28 nm and 64 nm CuO NPs in 15 or more images. Measurement of NPs diameter was performed only when well-defined individual nanoparticles could be observed. TEM micrographs of gold nanoparticles at established dimensions were

analyzed in identical fashion with ImageJ to confirm validity of measurements (data not shown).

6.4.2 Nanoparticle dispersion protocol

A stock solution of CuO NPs (8,000 mg L^{-1}) was prepared in sterile ddH_2O and dispersed by using a 450 W probe sonicator (Branson Digital Sonifer; Danbury, CT) for 5 minutes on ice at 20% amplitude, pulse on for 20 sec and off for 20 sec. The pulse was employed in order to limit ROS formation or overheating of NPs suspension. After dispersion different volumes of the CuO NPs stock solution was aseptically added to the yeast cultures to achieve predetermined concentrations of CuO NPs for cell exposure.

6.4.3 Nanoparticle hydrodynamic diameter from agglomeration and aggregation

To determine the average hydrodynamic diameters of CuO NPs agglomerates, NPs were diluted to 40 mg/L in sterile double distilled water (ddH_2O) or growth medium (YP-gal) and injected using a sterile syringe into the viewing chamber of NS500 platform (Nanosight Ltd) equipped with a 640-nm laser. All measurements were taken at room temperature. Average diameters and standard deviations were measured using the Nanoparticle Tracking Analysis (NTA) 2.0 Build 127 analytical software for real-time dynamic nanoparticle visualization and measurement. The samples were measured for 30 sec with manual shutter and gain adjustments and six measurements of the same sample were performed for all of the respective time points. Although Nanosight has a minimum limit of detection of 10 nm, the smaller CuO NPs employed in the present study have an average primary particle diameter, as measured by TEM, of 28 nm. However, it should be noted that any populations of CuO nanoparticles or agglomerations smaller than 10 nm would not be detected by NTA. To exclude artifacts

from organic components within media, analysis of YP growth media without addition of CuO NPs was performed and run in batch processing as 5 separate runs to avoid introducing additional artifacts from altering fluidic flow.

The data were combined and averaged to provide background intensity data which was then used to exclude organic matter from conflicting with the NPs/organic matter agglomeration measurements. This exclusion was accomplished through the use of the 'intensity comparison' tool in the NTA 2.0 Build software which allows the user to establish intensity values as a cutoff for the minimal intensity necessary to be incorporated in the sample analysis. To determine Zeta potentials of CuO NPs in YP-gal media, NPs in solution were pipetted into Folded Capillary Cells (Malvern Instruments) and Zeta potential was measured using a Zetasizer Nano-ZS (Malvern Instruments).

6.4.4 Nanoparticle aging and preparation for media-NPs interaction assay

To explore media component-NPs interactions, CuO NPs were dispersed into YP media as described above to 40, 80, or 240 mg L^{-1} concentration in 4 mL volume in 15 mL polypropylene disposable centrifuge tubes (VWR). The NPs solutions were covered to prevent light exposure and placed at 30^{o}C in a table top incubator at 250 rpm for 24 hour. A 2 mL aliquot of the 'aged' NPs were centrifuged at 14,000 rpm for 30 mins and supernatant was then removed and used as released fraction. The CuO NPs pellet was resuspended in sterile YP-gal media and used as aged NPs in fresh media. The remaining 2 mL of aged NPs in released fraction was used as an additional treatment. Fresh suspensions of CuO NPs were prepared by diluting stock to 40, 80, and 240 mg L^{-1} and immediately adding to cell suspensions.

6.4.5 Quantifying copper ions via the zincon colorimetric assay and ICP-MS

To define the amount of Cu^{2+} ions released from CuO NPs in the growth media, aliquots of each NPs suspension in YP-gal medium were collected immediately after dispersion in the media, after 1.5 hour, or 24 hour incubation at 30^{o}C with shaking (250 rpm) and ultracentrifuged (45,000 g for 30 mins) to remove cells and suspended CuO NPs. Aliquots were stored at 4^{o}C (up to one week) until Zincon analysis was performed. The Cu^{2+} ion concentration was measured using Zincon assay as described by Sabel *et al* [85] with modifications described herein. Prior to analysis, supernatants were examined for NPs presence using NTA and concluded that NPs were not detectable. Nanoparticles with a diameter less than 10 nm were not detected due to the limit of detection by NTA but may be present. However even if a small NP fraction of <10 nm is present, preliminary experiments indicate that Zincon dye does not interact directly with CuO NPs (data not shown). Measurement of Cu^{2+} within the supernatant was performed on a Spectra Max® M2e spectrophotometer (Molecular Devices) using Zincon reagent (MP Biochemicals). All samples were diluted in Tris-HCl buffer (20 µM, pH 7.2) containing Zincon (40 µM). A standard curve with Cu^{2+} (0 - 2.4 mg/L) was prepared from copper sulfate in the same buffer. Samples were incubated at room temperature for 10 min and absorbance was measured at 615 nm. The relationship between absorbance at 615 nm and the known concentration of Cu^{2+} standard served to determine Cu^{2+} ion concentration. To observe the influence of organic material and anions, identical experiments were performed in double distilled water. To remove the pH as a potential variable, distilled water was adjusted to pH 6.4, identical to the growth media. All measurements were performed in triplicate.

To define the amount of total Cu released from CuO NPs in the growth media, aliquots of previously ultracentrifuged supernatant were digested with equal volume 70% (w/v) HNO_3 at 65^{o}C for 2 hour and stored in acid-washed glass vials at 4^{o}C for no more

than 1 week. Samples were then further diluted to 2% HNO_3 with ddH_2O, containing 0.5% HCL, prior to sample analysis using an ICP-MS system (7700x ICP-MS with autosampler, Agilent Technologies). ICP-MS detects total copper regardless of copper ion species, copper in strong-association with organic material, or copper in the form of nano-solids.

6.4.6 Determining zeta potential of nanoparticles via Zeta sizer

To determine Zeta potentials of CuO NPs in YP media, NPs in solution were pipetted into Folded Capillary Cells (Malvern Instruments, Worcestershire, UK) and Zeta potential was measured using a Zetasizer Nano-ZS (Malvern Instruments).

6.4.7 NPs aging in the growth media

Note that *S. cerevisiae* has a high copper tolerance, up to 480 mg/L CuO NPs for 12 hours of exposure in YP media before lethal effects are observed (data not shown). In the current study, sub-lethal nanoparticle concentrations in the range of 40 – 240 mg/L were employed in 1.5 hour exposure scenario to study the NPs effect on *S. cerevisiae* cell metabolism. To explore media component-NPs interactions, CuO NPs were dispersed into YP-gal media as described above to 40, 80, or 240 mg/L initial mass in 4 mL volume in 15 mL polypropylene disposable centrifuge tubes. The NPs solutions were covered to prevent light exposure and placed at 30^{o}C in a table-top incubator at 250 rpm for 24 hour. A 2 mL aliquot of the 'aged' NPs were ultracentrifuged at 45,000 g for 30 min (Optima MAX-E Ultracentrifuge) and supernatant was then removed and used as released fraction. The CuO NPs pellet was resuspended in sterile YP-Gal media and used as aged NPs in fresh media. The remaining 2 mL of aged NPs in released fraction was used as an additional treatment. Fresh suspensions of CuO NPs were prepared by

diluting stock solution (8,000 mg/L) to 40, 80, and 240 mg/L and immediately added to cell suspensions for exposure.

In cases of NPs exposure with Cu^{2+} chelation, ethylenediaminetetraacetic acid (EDTA) in final concentration of 0.5 mM was added to CuO NPs or the released ionic copper fraction in YP-gal medium and incubated at 30^{o}C for 1 hour prior to the addition of *S. cerevisiae* cells. The *S. cerevisiae* cells used as the untreated control were pelleted and resuspended in growth media which was also supplemented with EDTA.

6.4.8 Preparing released fraction exposure scenario

When copper sulfate was used to mimic the released Cu^{2+} from CuO NPs, less metabolic inhibition was observed compared to exposure with the actual released fraction from NPs. This observation of soluble Cu salt treatments not being an adequate mimic of NPs-released Cu ion treatment has also been reported in other studies [17]. Only after incubation of copper sulfate in YP-gal (to simulate the Cu ions released from CuO NPs) was the metabolic inhibition more similar to the metabolic inhibition observed with released Cu treatments. Instead of aged copper sulfate, the released copper ion-containing supernatant from the CuO NPs was used in the subsequent experiments to better represent the nature of the soluble copper within the YP-gal media. To characterize the released copper from CuO in the growth media, total copper was measured with inductively coupled plasma mass spectrometry (ICP-MS). Cu^{2+} is a dominant fraction in the 'released copper only' exposure scenario as the concentration of total copper, as measured with ICP-MS, was not significantly different than Cu^{2+} ions concentrations, as measured with zincon assay.

In order to generate the released Cu ion treatment, CuO NPs at 800 mg/L were incubated for 24 hour, the suspended NPs were then centrifuged (14,000rpm 30 min) and the supernatant was then filtered (0.1 µM syringe filter, Supor® low protein binding,

Acrodisc® PALL Life Sciences). The supernatant was assayed using Zincon dye as per [18] and determined to contain 200 mg Cu^{2+}/L. This supernatant was considered the 'released Cu ion' treatment stock and was diluted to a working concentration as required.

6.5 Supplementary data for Caenorhabditis elegans

6.5.1 Statistics to compare copper treatment and untreated nematode strains for toxicological endpoints analyzed

Table S1. Statistical difference between untreated and copper exposed nematodes.

Effect vs Untreated	**Conc.** (mg Cu/L)	**Reproduction**		**Feeding Behavior**		**Population Body Length**	
		CuO NPs	Cu^+	CuO NPs	Cu^+	CuO NPs	Cu^+
N2	3.8	NSD	NSD	<0.001	NSD	0.014	NSD
	7.9	NSD	NSD	<0.001	NSD	<0.001	NSD
	15.9	NSD	0.031	<0.001	<0.001	<0.001	<0.001
CB4856	3.8	NSD	NSD	<0.001	NSD	NSD	NSD
	7.9	NSD	NSD	<0.001	NSD	<0.001	NSD
	15.9	0.0051	<0.001	<0.001	0.003	<0.001	<0.001
DL238	3.8	NSD	NSD	<0.001	NSD	NSD	NSD
	7.9	NSD	NSD	<0.001	NSD	<0.001	NSD
	15.9	0.0014	<0.001	<0.001	<0.001	<0.001	<0.001
JU258	3.8	NSD	NSD	<0.001	<0.001	NSD	NSD
	7.9	0.04	NSD	<0.001	<0.001	<0.001	NSD
	15.9	0.013	NSD	<0.001	<0.001	<0.001	<0.001

Statistical comparison, Tukey's honest significant difference (HSD) p values, of 24 hour copper exposed *Caenorhabditis elegans* and untreated nematode population body length, feeding behavior, and reproduction. *p*-values were determined by Tukey's HSD using Rstudio; $p<0.05$ was considered significant. NSD – no statistical difference.

6.5.2 Statistics to compare CuO NPs and copper sulfate for nematode toxicological endpoints analyzed

Table S2. Statistical differences between copper oxide nanoparticle inhibitory effects and the inhibitory effect from copper sulfate exposure.

CuO NPs vs Cu ions	**Conc.** (mg Cu/L)	**Reproduction**	**Feeding Behavior**	**Population Body Length**
N2	3.8	NSD	**<0.001**	**0.014**
	7.9	NSD	**<0.001**	**<0.001**
	15.9	NSD	**<0.001**	**<0.001**
CB4856	3.8	NSD	**<0.001**	NSD
	7.9	NSD	**<0.001**	**<0.001**
	15.9	**0.0051**	**<0.001**	**<0.001**
DL238	3.8	NSD	**<0.001**	NSD
	7.9	NSD	**<0.001**	**<0.001**
	15.9	**0.0014**	**<0.001**	**<0.001**
JU258	3.8	NSD	**<0.001**	NSD
	7.9	**0.04**	**<0.001**	**<0.001**
	15.9	**0.013**	**<0.001**	**<0.001**

Statistical comparison, Tukey's HSD p-values after exposure to 28 nm copper oxide nanoparticle and copper sulfate effects after 24 hour exposure on *Caenorhabditis elegans* population body length, feeding behavior, and reproduction. *p*-values were determined by Tukey's HSD using Rstudio; $p<0.05$ was considered significant. **Bold** values indicate more significant increase in effect from the CuO NPs exposure. NSD – no statistical difference.

6.5.3 Statistics to compare laboratory-adapted nematode N2 strain and wild strains for toxicological endpoints analyzed

Table S3. Statistical differences in response to copper exposure from the lab adapted N2 strain and the wild nematode strains.

N2 vs	**Copper oxide Nanoparticles**			**Soluble copper**		
Wild strain	**3.8 mg Cu/L**	**7.9 mg Cu/L**	**15.9 mg Cu/L**	**3.8 mg Cu/L**	**7.9 mg Cu/L**	**15.9 mg Cu/L**
JU258						
Population Body length	NSD	NSD	NSD	0.006	NSD	NSD
Feeding Behavior	NSD	NSD	NSD	<0.001	0.013	NSD
Reproduction	0.03	NSD	NSD	NSD	<0.001	NSD
DL238						
Population Body length	NSD	0.046	0.002	0.022	NSD	NSD
Feeding Behavior	NSD	0.004	0.025	0.023	NSD	NSD
Reproduction	NSD	NSD	NSD	NSD	NSD	NSD
CB4856						
Population Body length	0.002	NSD	0.047	NSD	0.013	NSD
Feeding Behavior	NSD	NSD	0.012	0.033	<0.001	0.027
Reproduction	0.027	NSD	NSD	NSD	0.002	NSD

Statistical comparison, Tukey's HSD p values, of the laboratory-adapted *Caenorhabditis elegans* N2 strain and the wild nematode strain population body length, feeding behavior, and reproduction after copper exposure. The laboratory-adapted N2 (Bristol) strain and three wild strains were exposed to 28 nm copper oxide nanoparticles or soluble copper ($CuSO_4$). *p*-values were determined by Tukey's HSD using Rstudio; $p<0.05$ was considered significant. NSD – No statistical difference.

6.5.4 Number of nematodes analyzed for neurodegeneration

Table S4. Total number of animals examined for neurodegeneration in each experiment after copper exposure.

	Conc. (mg Cu/L)	**Copper oxide nanoparticles**			**Copper Sulfate**		
		Expt. 1	Expt. 2	Expt. 3	Expt. 1	Expt. 2	Expt. 3
wild type	3.8	96	40	67	92	40	81
	7.9	101	40	40	87	113	66
	15.9	46	69	40	87	55	61
Δsmf-1	3.8	82	81	53	71	94	40
	7.9	113	77	56	77	90	40
	15.9	102	88	50	62	69	43
ΔSmf-2	3.8	52	68	56	73	84	73
	7.9	85	48	52	79	87	125
	15.9	76	66	40	58	65	70

6.5.5 Statistics and data regarding HSP-16.2 data

Table S5. Total animals examined and statistical differences in the induction of HSP-16.2 after exposure to copper.

Treatment	**Concentration** (mg Cu/L)	**Animals Imaged**	**p-value** (vs Unt.)
Untreated	0	25	-
Copper oxide	3.8	28	NSD
(28 nm)	7.9	34	<0.001
	15.9	32	<0.001
Copper sulfate	3.8	28	NSD
	7.9	25	<0.001
	15.9	31	<0.001

The total animals examined and statistical comparison, Tukey's HSD p-values, of exposed *Caenorhabditis elegans* to untreated nematodes for *hsp-16.2* induction after 24 hour exposure to copper. *p*- values were determined by Tukey's HSD using Rstudio; $p<0.05$ was considered significant. NSD – No statistical difference.

6.6 Supplementary data for Saccharomyces cerevisiae

6.6.1 Yeast sensitivity to hydrogen peroxide exposure

In contrast to copper exposure effects, we observed resistance to H_2O_2 in cells grown on YP-ethanol compared to cells on YP-dextrose media. The observed effect of H_2O_2 on metabolic activity on cells grown on different carbon source in our study is in conjunction with a previous report by Cabiscol *et al* [204]. They found that H_2O_2 and menadione treatments (5 mM H_2O_2 and menadione) resulted in lower cell survival and produced higher oxidative stress in *S. cerevisiae* cells grown on YP-dextrose than in cells grown on YP-gal, measured as amounts of protein carbonyl content [204]. The higher sensitivity of respiratory grown *S. cerevisiae* cells to copper exposures, in both CuO NPs and copper sulfate treatments, potentially indicates a different mode of action than the common ROS generating chemical.

6.6.2 Quantifying intracellular copper content of yeast cells

S. cerevisiae has a minimum copper quota of 8.3 x 10^5 to 1.3 +/- 0.2 x 10^6 atoms/cell when grown in nutrient rich media YP-dextrose containing 32-40 mg Cu/L (as analyzed by ICP-MS, [205]). We have measured 160-400 mg Cu/mL in our YP-gal medium and a minimum copper quota of 8.3 +/- 0.3 x10^7 atoms/cell when cultured in YP-gal (respiratory/fermentative metabolism).

In our study, short exposure (1.5 hour) to all 28 nm CuO treatments, fresh or aged, resulted in 1.8-8.5 x 10^8 Cu atoms/cell while 64 nm NPs exposure resulted in internalization of 3.0-9.5 x 10^8 Cu atoms/cell (Figure S1). CuO NPs treatments do notsignificantly increase Cu ion internalization after 1.5 hour. On initial inspection, these results appear surprising as 28 nm 24 hour aging results in 4-5 fold greater Cu^{2+} release

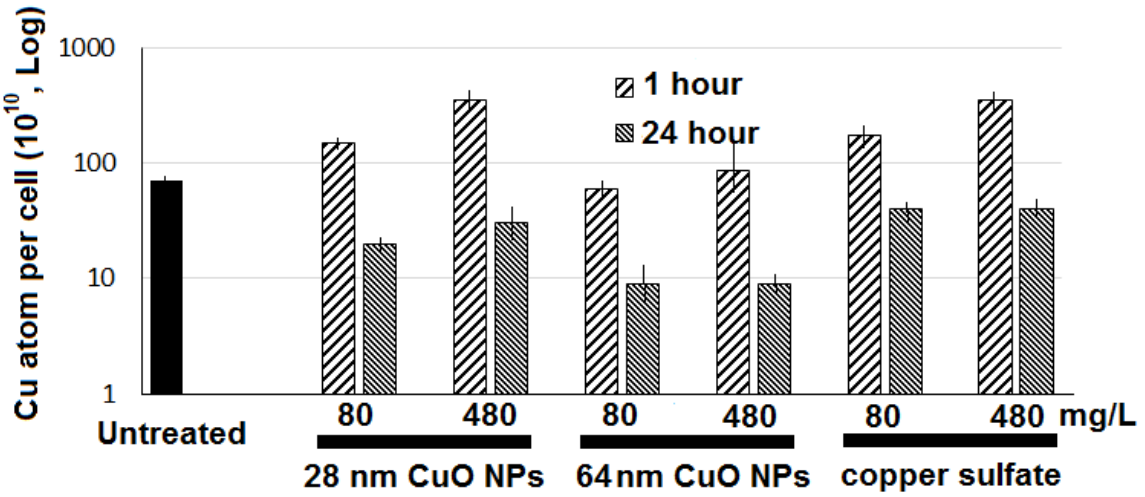

Figure S1. The internal copper atom concentration within yeast after exposure to copper oxide nanoparticles and copper sulfate.

compared to 64 nm NPs. However, *S. cerevisiae* has efficient and dynamic copper homeostasis mechanisms to stay at homeostatic copper levels via down regulation of Cu^{+} importers (*CTR1* and *CTR3*) or up regulation of Cu^{+} exporters (*CCC2*) in response to an increase in exogenous Cu^{+} ions [206]. This further supports the hypothesis that while Cu^{2+} release plays a role in CuO NPs toxicity, the nanoparticle component must also play a role in the effect on cellular metabolism.

6.6.3 Quantifying total released copper within YP media

In order to investigate whether the released Cu^{2+} ions account for the observed toxicity, *S. cerevisiae* cells were exposed also to the extracted "released fraction", i.e. the supernatants collected after 4 hour incubations of NPs dispersions at different concentrations (40, 80, and 240 mg Cu/L) in sterile growth medium followed by separation of the remaining CuO solids by filtration (0.2 µM). The previously-aged NPs (24 hour) resuspended in fresh media or released fraction released 6-10 times more Cu

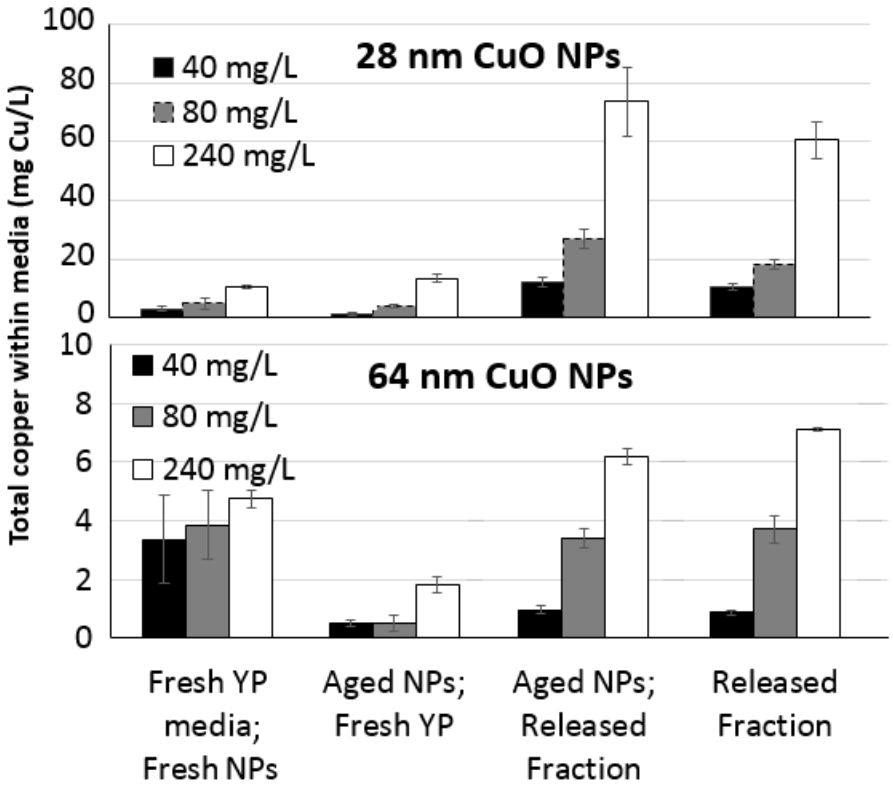

Figure S2. The total copper within YP media after incubation for 4 hour with the respective exposure scenario.

into media compared to the freshly suspended NPs (Figure S2) during the same time period (1.5 hour).

6.6.4 Nanoparticle impact on cellular respiration

To examine the impact that CuO NPs have on the mitochondrial respiratory capacity of cells, we measured changes in the cellular respiration rate based on measured O_2 consumption using a clark electrode. *S. cerevisiae* was cultured on YPE as ethanol is a carbon source supporting a respiratory metabolism and in addition these cells showed greatest sensitivity to copper treatments in the aB assay. The copper exposure scenarios are fresh suspensions of CuO NPs, 24 hour aged NPs in fresh media, 24 hour aged NPs in released fraction, and released fraction alone. The two

differently sized CuO NPs affected cellular respiration differently as both fresh suspensions of 28 nm CuO NPs and aged 28 nm CuO NPs in released fraction had the most dramatic effect on O_2 consumption while the released fraction from 64 nm CuO NPs inhibited O_2 consumption more so than any other 64 nm treatment. Aged 28 nm CuO NPs in released fraction significantly inhibited cellular respiration more than the released fraction without the presence of NPs (80 mg/L) after 30 min treatment.

The aged 28 nm CuO NPs in release fraction also had a greater impact compared to the aged NPs in fresh media (69.9+/-0.8% versus 88.5+/-2.2%, $p < 0.01$) (Figure S3). The increased effect with the released fraction compared to replacement with fresh YP-gal media is the influence of the released Cu^{2+} ions as a component of 28 nm CuO NPs toxicity. Nonetheless, aged 28 nm CuO NPs in released fraction inhibited metabolism more compared to the released fraction alone which suggests an effect from the nanoparticle component itself. These results in total suggest a combined effect from both the nanoparticle component and the released Cu ions within the first 30 mins of exposure. Experiments analyzing exposure for periods beyond 30 mins revealed similar effects from the various copper exposures (Figure S4).

6.6.5 Copper oxide nanoparticles reactive oxygen species generation

The production of intracellular superoxide and hydroxyl radical production was measured after exposure to CuO NPs using the cell-permeable fluorescent probe Dihydrorhodamine 123 (DHR123). Exposure to either 28 or 64 nm CuO NPs for 1.5 hours resulted in no significant ROS production in any of the treatments used in this study (Figure S5). For comparison, the redox-cycling chemical menadione was used which did result in a significantly greater staining compared to untreated cells. These

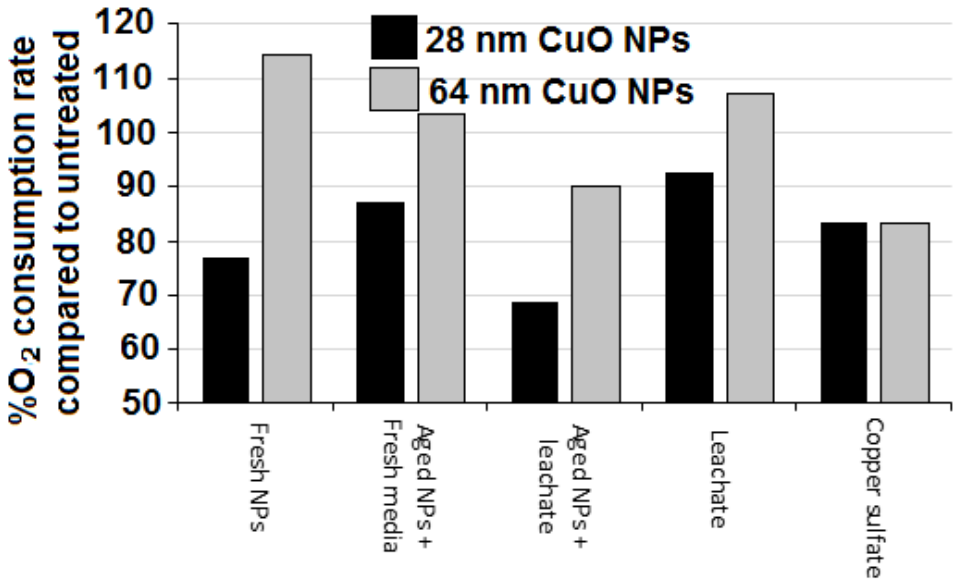

Figure S3. The influence of the effect of copper oxide nanoparticles, both fresh and aged, on yeast respiratory oxygen consumption.

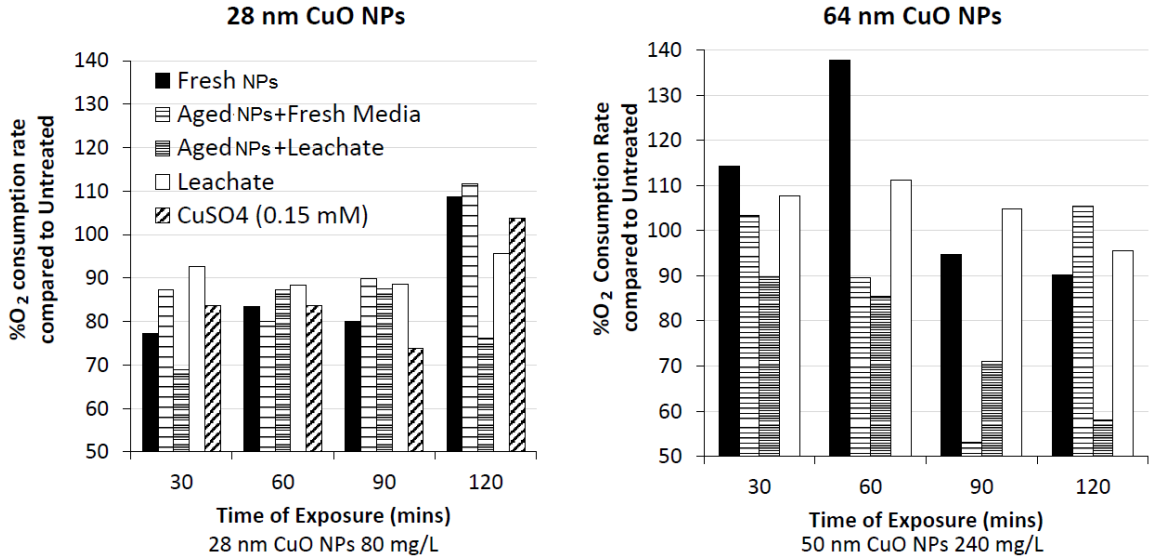

Figure S4. The influence of time on the effect of 28 nm copper oxide nanoparticles on yeast respiratory oxygen consumption.

data do not exclude ROS as the cause of toxicity, instead it suggests that CuO NPs treatments (for the short duration of exposure in this study) do not result in production of superoxide radicals to a sufficient degree to be detected and thus the cellular ROS defense system is not overloaded. Our study with mutant yeast strains indicates that *SOD1* and *PRX1* play an important role in the *S. cerevisiae* defense against ROS species generated during CuO NPs exposure. No observable increase in ROS occurred after exposure of only 1.5 hour, which may have been too short to observe a reduction in the antioxidant pool that each yeast cell retains to deal with exogenous stress. Farrugia *et al* suggest that a majority of ROS-related stress is associated with a depletion of the antioxidants within the cytoplasm of yeast [207] and this may not occur at the sublethal concentrations and short exposure time.

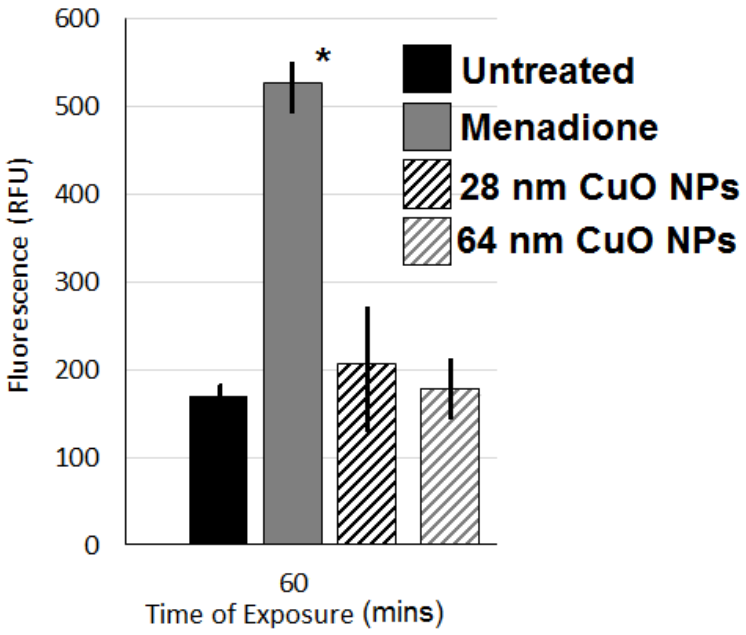

Figure S5. Reactive oxygen species produced by *S. cerevisiae* cells after copper exposure as detected by ROS-sensitive fluorescent probe DHR123.

6.6.6 The influence of copper exposures on reactive oxygen species sensitive yeast strains

Yeast strains containing deletions made in proteins involved in dealing with oxidative stress were exposed to both CuO NPs as well as $CuSO_4$ and hydrogen peroxide (H_2O_2). Differences in the reaction to treatment will assist in identifying the relationship of the deleted gene and the mechanism of inhibition. The yeast mutant strains examined include super oxide dismutase 1 (S*od1Δ*) and the cytoplasmic catalase 1 (C*tt1Δ*) genes in the *S. cerevisiae* BY4742 genetic background, as well as the peroxidase (*Prx1Δ*) gene in the *S. cerevisiae* W303-a genetic background, were exposed to the copper treatments.

Upon copper exposure, of the studied mutant strains the *Sod1Δ* and *Prx1Δ* show a phenotype with increased sensitivity compared to the wild type strain (Figure S6). The deletion of the gene *Sod1* showed increased sensitivity to both CuO NPs and to $CuSO_4$, but not to the H_2O_2 control, compared to the wild type. This similarity in sensitivity suggests a similar mechanism of toxicity of the CuO NPs and the Cu ions. Most likely, the *sod1Δ* mutants inability to generate hydrogen peroxide by dismutating the superoxide anion led to its accumulation in the cell and increased the toxicity of the copper treatments in the mutant. Unfortunately, menadione (a superoxide radical generator) was interfering with the aB dye and wasn't possible to be used as a control compound in the metabolic activity assay.

We expect that the removal of catalase will cause more generation of the hydroxyl radical through Fenton-like reactions with reduced metals including reduced Cu in the *Ctt1Δ* strain. Based on the metabolic activity assay, the C*tt1* single-gene deletion mutant for cytosolic catalase was not more sensitive to CuO NPs or H_2O_2 treatments in comparison to the wild type based on determined IC_{50} values.

PRX1 is a mitochondrial enzyme and has a thioredoxin peroxidase activity with a role in reduction of hydroperoxides, *e.g.* reducing H_2O_2 to water. Previously, it has been shown that peroxiredoxin-null yeast cells were more susceptible to oxidative and nitrosative stress (Wong, Siu et al. 2004) and *Prx1* is particularly required to protect against mitochondrial oxidation and heavy-metal induced oxidative stress (Greetham and Grant 2009). Interestingly, upon exposure to copper treatments, 28 nm and 64 nm CuO NPs, as well as $CuSO_4$, to the *prx1Δ* and *Sod1Δ* strains resulted in significantly increased sensitivity ($p<0.05$) in comparison to the wild type W-303a strain. These results suggest that CuO NPs may exert some toxicity to yeast cells via the mitochondrion induced oxidative stress resulting from the released Cu ions.

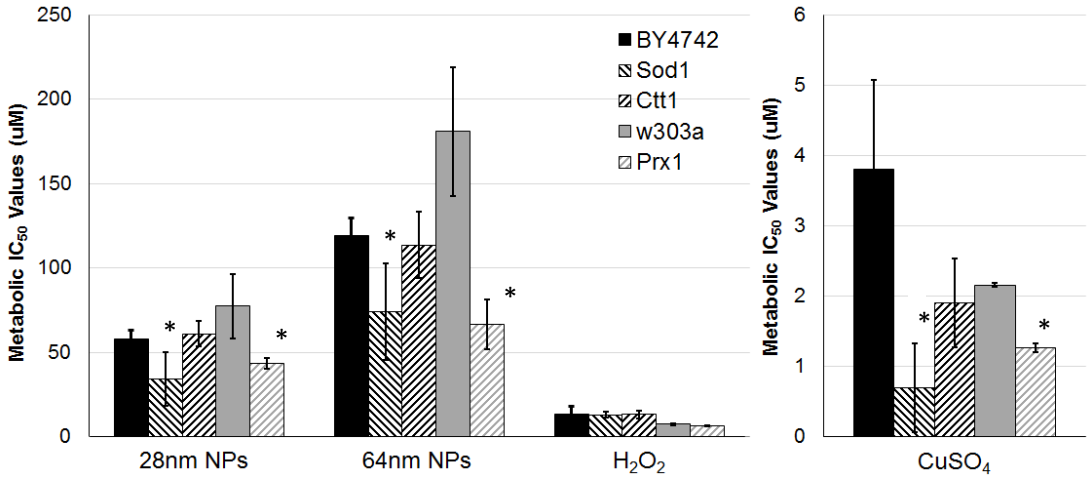

Figure S6. The inhibitive effect of copper treatments and hydrogen peroxide on the metabolism of yeast mutants containing gene deletions involved in dealing with oxidative stress.

REFERENCES:

[1] Nel A, Xia T, Madler L, Li N. 2006. Toxic potential of materials at the nanolevel. *Science* 311:622-627.

[2] Woyke A. 2007. "Nanotechnology" as new "key technology"? - Attempt at a historical and systematic comparison with other technologies. *J Gen Philos Sci* 38:329.

[3] Rubilar O, Rai M, Tortella G, Diez MC, Seabra AB, Duran N. 2013. Biogenic nanoparticles: copper, copper oxides, copper sulphides, complex copper nanostructures and their applications. *Biotechnol Lett* 35:1365-1375.

[4] Miyazaki J, Kuriyama Y, Miyamoto A, Tokumoto H, Konishi Y, Nomura T. 2014. Adhesion and internalization of functionalized polystyrene latex nanoparticles toward the yeast *Saccharomyces cerevisiae*. *Adv Powder Technol* 25:1394-1397.

[5] Oberdorster G, Maynard A, Donaldson K, Castranova V, Fitzpatrick J, Ausman K, Carter J, Karn B, Kreyling W, Lai D, Olin S, Monteiro-Riviere N, Warheit D, Yang H. 2005. Principles for characterizing the potential human health effects from exposure to nanomaterials: elements of a screening strategy. *Particle and fibre toxicology* 2:8.

[6] Luyts K, Dorota Napierska, Ben Nemery, Hoet PHM. 2013. How physico-chemical characteristics of nanoparticles cause their toxicity: complex and unresolved interrelations. *Environmental Science: Processes & Impacts* 15:23-38.

[7] Carlson C, Hussain SM, Schrand AM, Braydich-Stolle LK, Hess KL, Jones RL, Schlager JJ. 2008. Unique cellular interaction of silver nanoparticles: size-dependent generation of reactive oxygen species. *The journal of physical chemistry B* 112:13608-13619.

[8] Midander K, Cronholm P, Karlsson HL, Elihn K, Moller L, Leygraf C, Wallinder IO. 2009. Surface characteristics, copper release, and toxicity of nano- and micrometer-sized copper and copper(II) oxide particles: a cross-disciplinary study. *Small* 5:389-399.

[9] Bondarenko O, Juganson K, Ivask A, Kasemets K, Mortimer M, Kahru A. 2013. Toxicity of Ag, CuO and ZnO nanoparticles to selected environmentally relevant test organisms and mammalian cells in vitro: a critical review. *Archives of toxicology* 87:1181-1200.

[10] Unrine JM, Tsyusko OV, Hunyadi SE, Judy JD, Bertsch PM. 2010. Effects of Particle Size on Chemical Speciation and Bioavailability of Copper to Earthworms () Exposed to Copper Nanoparticles. *Journal of Environment Quality* 39:1942.

[11] Misra SK, Dybowska A, Berhanu D, Luoma SN, Valsami-Jones E. 2012. The complexity of nanoparticle dissolution and its importance in nanotoxicological studies. *The Science of the total environment* 438:225-232.

[12] Pokhrel LR, Dubey B, Scheuerman PR. 2013. Impacts of select organic ligands on the colloidal stability, dissolution dynamics, and toxicity of silver nanoparticles. *Environmental science & technology* 47:12877-12885.

[13] Hotze EM, Phenrat T, Lowry GV. 2010. Nanoparticle Aggregation: Challenges to Understanding Transport and Reactivity in the Environment. *Journal of Environment Quality* 39:1909.

[14] Bush AI. 2003. The metallobiology of Alzheimer's disease. *Trends Neurosci* 26:207-214.

[15] Beer C, Foldbjerg R, Hayashi Y, Sutherland DS, Autrup H. 2012. Toxicity of silver nanoparticles - nanoparticle or silver ion? *Toxicology letters* 208:286-292.

[16] Adam N, Vergauwen L, Blust R, Knapen D. 2015. Gene transcription patterns and energy reserves in *Daphnia magna* show no nanoparticle specific toxicity when exposed to ZnO and CuO nanoparticles. *Environmental research* 138:82-92.

[17] Gunawan C, Teoh WY, Marquis CP, Amal R. 2011. Cytotoxic origin of copper(II) oxide nanoparticles: comparative studies with micron-sized particles, leachate, and metal salts. *ACS nano* 5:7214-7225.

[18] Mashock MJ, Kappell AD, Hallaj N, Hristova KR. 2015. Copper oxide nanoparticles inhibit the metabolic activity of *Saccharomyces cerevisiae*. *Environmental Toxicology and Chemistry*:n/a-n/a.

[19] Kasemets K, Suppi S, Kunnis-Beres K, Kahru A. 2013. Toxicity of CuO nanoparticles to yeast *Saccharomyces cerevisiae* BY4741 wild-type and its nine isogenic single-gene deletion mutants. *Chemical research in toxicology* 26:356-367.

[20] Bertinato J, L'Abbe MR. 2004. Maintaining copper homeostasis: regulation of copper-trafficking proteins in response to copper deficiency or overload. *The Journal of nutritional biochemistry* 15:316-322.

[21] Regier N, Cosio C, von Moos N, Slaveykova VI. 2015. Effects of copper-oxide nanoparticles, dissolved copper and ultraviolet radiation on copper bioaccumulation, photosynthesis and oxidative stress in the aquatic macrophyte Elodea nuttallii. *Chemosphere* 128:56-61.

[22] Halliwell B, Gutteridge JM. 1990. Role of free radicals and catalytic metal ions in human disease: an overview. *Methods Enzymol* 186:1-85.

[23] Valko M, Morris H, Cronin MT. 2005. Metals, toxicity and oxidative stress. *Curr Med Chem* 12:1161-1208.

[24] Peña MMO, Lee J, Thiele DJ. 1999. A Delicate Balance: Homeostatic Control of Copper Uptake and Distribution. *The Journal of Nutrition* 129:1251-1260.

[25] Predki PF, Sarkar B. 1992. Effect of replacement of "zinc finger" zinc on estrogen receptor DNA interactions. *The Journal of biological chemistry* 267:5842-5846.

[26] Nevitt T, Ohrvik H, Thiele DJ. 2012. Charting the travels of copper in eukaryotes from yeast to mammals. *Biochimica et biophysica acta* 9:24.

[27] Gomes SI, Novais SC, Scott-Fordsmand JJ, De Coen W, Soares AM, Amorim MJ. 2012. Effect of Cu-nanoparticles versus Cu-salt in *Enchytraeus albidus* (*Oligochaeta*): differential gene expression through microarray analysis. *Comparative biochemistry and physiology Toxicology & pharmacology : CBP* 155:219-227.

[28] Gomes SI, Novais SC, Gravato C, Guilhermino L, Scott-Fordsmand JJ, Soares AM, Amorim MJ. 2012. Effect of Cu-nanoparticles versus one Cu-salt: analysis of stress biomarkers response in *Enchytraeus albidus* (*Oligochaet*a). *Nanotoxicology* 6:134-143.

[29] Aruoja V, Dubourguier HC, Kasemets K, Kahru A. 2009. Toxicity of nanoparticles of CuO, ZnO and TiO2 to microalgae *Pseudokirchneriella subcapitata*. *Sci Total Environ* 407:1461-1468.

[30] Wang Z, Li N, Zhao J, White JC, Qu P, Xing B. 2012. CuO nanoparticle interaction with human epithelial cells: cellular uptake, location, export, and genotoxicity. *Chemical research in toxicology* 25:1512-1521.

[31] Wang Z, Li J, Zhao J, Xing B. 2011. Toxicity and internalization of CuO nanoparticles to prokaryotic alga *Microcystis aeruginosa* as affected by dissolved organic matter. *Environmental science & technology* 45:6032-6040.

[32] Shi J, Abid AD, Kennedy IM, Hristova KR, Silk WK. 2011. To duckweeds (*Landoltia punctata*), nanoparticulate copper oxide is more inhibitory than the soluble copper in the bulk solution. *Environ Pollut* 159:1277-1282.

[33] Bhatt I, Tripathi BN. 2011. Interaction of engineered nanoparticles with various components of the environment and possible strategies for their risk assessment. *Chemosphere* 82:308-317.

[34] Scown TM, van Aerle R, Tyler CR. 2010. Review: Do engineered nanoparticles pose a significant threat to the aquatic environment? *Critical reviews in toxicology* 40:653-670.

[35] Nel AE, Madler L, Velegol D, Xia T, Hoek EM, Somasundaran P, Klaessig F, Castranova V, Thompson M. 2009. Understanding biophysicochemical interactions at the nano-bio interface. *Nature materials* 8:543-557.

[36] Drakulic T, Temple MD, Guido R, Jarolim S, Breitenbach M, Attfield PV, Dawes IW. 2005. Involvement of oxidative stress response genes in redox homeostasis, the level of reactive oxygen species, and ageing in *Saccharomyces cerevisiae*. *FEMS yeast research* 5:1215-1228.

[37] Moraitis C, Curran BP. 2004. Reactive oxygen species may influence the heat shock response and stress tolerance in the yeast *Saccharomyces cerevisiae*. *Yeast* 21:313-323.

[38] Xiao GG, Wang M, Li N, Loo JA, Nel AE. 2003. Use of proteomics to demonstrate a hierarchical oxidative stress response to diesel exhaust particle chemicals in a macrophage cell line. *The Journal of biological chemistry* 278:50781-50790.

[39] Fahmy B, Cormier SA. 2009. Copper oxide nanoparticles induce oxidative stress and cytotoxicity in airway epithelial cells. *Toxicol In Vitro* 23:1365-1371.

[40] Buffet PE, Tankoua OF, Pan JF, Berhanu D, Herrenknecht C, Poirier L, Amiard-Triquet C, Amiard JC, Berard JB, Risso C, Guibbolini M, Romeo M, Reip P, Valsami-Jones E, Mouneyrac C. 2011. Behavioural and biochemical responses of two marine invertebrates *Scrobicularia plana* and *Hediste diversicolor* to copper oxide nanoparticles. *Chemosphere* 84:166-174.

[41] Gomes T, Pereira CG, Cardoso C, Pinheiro JP, Cancio I, Bebianno MJ. 2012. Accumulation and toxicity of copper oxide nanoparticles in the digestive gland of *Mytilus galloprovincialis*. *Aquat Toxicol* 118-119:72-79.

[42] Ivask A, Bondarenko O, Jepihhina N, Kahru A. 2010. Profiling of the reactive oxygen species-related ecotoxicity of CuO, ZnO, TiO2, silver and fullerene nanoparticles using a set of recombinant luminescent *Escherichia coli* strains: differentiating the impact of particles and solubilised metals. *Anal Bioanal Chem* 398:701-716.

[43] George S, Pokhrel S, Xia T, Gilbert B, Ji Z, Schowalter M, Rosenauer A, Damoiseaux R, Bradley KA, Madler L, Nel AE. 2010. Use of a rapid cytotoxicity screening approach to engineer a safer zinc oxide nanoparticle through iron doping. *ACS nano* 4:15-29.

[44] Iversen TG, Skotland T, Sandvig K. 2011. Endocytosis and intracellular transport of nanoparticles: Present knowledge and need for future studies. *Nano Today* 6:176-185.

[45] dos Santos T, Varela J, Lynch I, Salvati A, Dawson KA. 2011. Effects of transport inhibitors on the cellular uptake of carboxylated polystyrene nanoparticles in different cell lines. *PloS one* 6:e24438.

[46] Schwegmann H, Feitz AJ, Frimmel FH. 2010. Influence of the zeta potential on the sorption and toxicity of iron oxide nanoparticles on *S. cerevisiae* and *E. coli*. *Journal of colloid and interface science* 347:43-48.

[47] Farias P.M.A., Santos B.S., Menezes F.D., Brasil J.R.A.G., Ferreira R., Motta M.A., Castro-Neto A.G., Vieira A.A.S., Fontes A., C.L. C. 2007. Highly fluorescent semiconductor core-shell CdTe-CdS nanocrystals for monitoring living yeast cell activity. *Appl Phys A* 89:957–961.

[48] Ivask A, Suarez E, Patel T, Boren D, Ji Z, Holden P, Telesca D, Damoiseaux R, Bradley KA, Godwin H. 2012. Genome-wide bacterial toxicity screening uncovers the mechanisms

of toxicity of a cationic polystyrene nanomaterial. *Environmental science & technology* 46:2398-2405.

[49] Fai PB, Grant A. 2009. A comparative study of *Saccharomyces cerevisiae* sensitivity against eight yeast species sensitivities to a range of toxicants. *Chemosphere* 75:289-296.

[50] Garcia-Saucedo C, Field JA, Otero-Gonzalez L, Sierra-Alvarez R. 2011. Low toxicity of HfO2, SiO2, Al2O3 and CeO2 nanoparticles to the yeast, *Saccharomyces cerevisiae*. *Journal of hazardous materials* 192:1572-1579.

[51] Kasemets K, Suppi S, Kunnis-Beres K, Kahru A. 2013. Toxicity of CuO nanoparticles to yeast *Saccharomyces cerevisiae* BY4741 wild-type and its nine isogenic single-gene deletion mutants. *Chem Res Toxicol*.

[52] Kasemets K, Ivask A, Dubourguier HC, Kahru A. 2009. Toxicity of nanoparticles of ZnO, CuO and TiO2 to yeast *Saccharomyces cerevisiae*. *Toxicol In Vitro* 23:1116-1122.

[53] Hadduck AN, Hindagolla V, Contreras AE, Li Q, Bakalinsky AT. 2010. Does aqueous fullerene inhibit the growth of *Saccharomyces cerevisiae* or *Escherichia coli*? *Applied and environmental microbiology* 76:8239-8242.

[54] Harada M, Sakisaka S, Terada K, Kimura R, Kawaguchi T, Koga H, Taniguchi E, Sasatomi K, Miura N, Suganuma T, Fujita H, Furuta K, Tanikawa K, Sugiyama T, Sata M. 2000. Role of ATP7B in biliary copper excretion in a human hepatoma cell line and normal rat hepatocytes. *Gastroenterology* 118:921-928.

[55] Diaz-Ruiz R, Rigoulet M, Devin A. 2011. The Warburg and Crabtree effects: On the origin of cancer cell energy metabolism and of yeast glucose repression. *Biochimica et biophysica acta* 1807:568-576.

[56] Askwith C, Kaplan J. 1998. Iron and copper transport in yeast and its relevance to human disease. *Trends in biochemical sciences* 23:135-138.

[57] Peña MMO, Koch KA, Thiele DJ. Dynamic Regulation of Copper Uptake and Detoxification Genes in *Saccharomyces cerevisiae*. Mol Cell Biol. 1998 May;18(5):2514-23.

[58] González M, Reyes-Jara A, Suazo M, Jo WJ, Vulpe C. 2008. Expression of copper-related genes in response to copper load. *The American Journal of Clinical Nutrition* 88:830S-834S.

[59] Martins LJ, Jensen LT, Simon JR, Keller GL, Winge DR. 1998. Metalloregulation of FRE1 and FRE2Homologs in Saccharomyces cerevisiae. *Journal of Biological Chemistry* 273:23716-23721.

[60] Georgatsou E, Mavrogiannis LA, Fragiadakis GS, Alexandraki D. 1997. The yeast Fre1p/Fre2p cupric reductases facilitate copper uptake and are regulated by the copper-modulated Mac1p activator. *Journal of Biological Chemistry* 272:13786-13792.

[61] Hassett R, Dix D, EIDE D, Kosman D. 2000. The Fe (II) permease Fet4p functions as a low affinity copper transporter and supports normal copper trafficking in *Saccharomyces cerevisiae*. *Biochem J* 351:477-484.

[62] Liu XF, Supek F, Nelson N, Culotta VC. 1997. Negative control of heavy metal uptake by the *Saccharomyces cerevisiae* BSD2 gene. *Journal of Biological Chemistry* 272:11763-11769.

[63] Liu XF, Culotta VC. 1999. Post-translation Control of Nramp Metal Transport in Yeast role of metal ions and the BSD2 gene. *Journal of Biological Chemistry* 274:4863-4868.

[64] Leary SC, Cobine PA, Kaufman BA, Guercin GH, Mattman A, Palaty J, Lockitch G, Winge DR, Rustin P, Horvath R, Shoubridge EA. 2007. The human cytochrome C oxidase assembly factors SCO1 and SCO2 have regulatory roles in the maintenance of cellular copper homeostasis. *Cell Metab* 5:9-20.

[65] Varabyova A, Topf U, Kwiatkowska P, Wrobel L, Kaus-Drobek M, Chacinska A. 2013. Mia40 and MINOS act in parallel with Ccs1 in the biogenesis of mitochondrial Sod1. *Febs J* 280:4943-4959.

[66] Felix MA, Braendle C. 2010. The natural history of *Caenorhabditis elegans*. *Current biology : CB* 20:R965-969.

[67] Harada H, Kurauchi M, Hayashi R, Eki T. 2007. Shortened lifespan of nematode *Caenorhabditis elegans* after prolonged exposure to heavy metals and detergents. *Ecotoxicology and environmental safety* 66:378-383.

[68] Boyd WA, Williams PL. 2003. Comparison of the sensitivity of three nematode species to copper and their utility in aquatic and soil toxicity tests. *Environmental Toxicology and Chemistry* 22:2768-2774.

[69] Song S-j, Guo Y-p, Yin K, Wu H-h, Zhang X-m, Yang M-l, MA E-b. 2008. Copper on Long-term role of Nematode physiological Characteristics. *Sichuan Journal of Zoology* 27:832-834.

[70] Alexander AG, Marfil V, Li C. 2014. Use of *Caenorhabditis elegans* as a model to study Alzheimer's disease and other neurodegenerative diseases. *Front Genet* 5.

[71] Gaggelli E, Kozlowski H, Valensin D, Valensin G. 2006. Copper Homeostasis and Neurodegenerative Disorders (Alzheimer's, Prion, and parkinson's diseases and amyotrophic lateral sclerosis). *Chemical Review* 106:1995-2004.

[72] Chen P, Martinez-Finley EJ, Bornhorst J, Chakraborty S, Aschner M. 2013. Metal-induced neurodegeneration in *C. elegans*. *Frontiers in aging neuroscience* 5:18.

[73] Aruoja V, Dubourguier HC, Kasemets K, Kahru A. 2009. Toxicity of nanoparticles of CuO, ZnO and TiO2 to microalgae *Pseudokirchneriella subcapitata*. *Science of the Total Environment* 407:1461-1468.

[74] Ivask A, Bondarenko O, Jepihhina N, Kahru A. 2010. Profiling of the reactive oxygen species-related ecotoxicity of CuO, ZnO, TiO2, silver and fullerene nanoparticles using a set of recombinant luminescent *Escherichia coli* strains: differentiating the impact of particles and solubilized metals. *Anal Bioanal Chem* 398:701-716.

[75] Kasemets K, Ivask A, Dubourguier HC, Kahru A. 2009. Toxicity of nanoparticles of ZnO, CuO and TiO2 to yeast *Saccharomyces cerevisiae*. *Toxicology In Vitro* 23:1116-1122.

[76] Kasemets K, Suppi S, Kunnis-Beres K, Kahru A. 2013. Toxicity of CuO nanoparticles to yeast *Saccharomyces cerevisiae* BY4741 wild-type and its nine isogenic single-gene deletion mutants. *Chemical research in toxicology*.

[77] Mortimer M, Kasemets K, Kahru A. 2010. Toxicity of ZnO and CuO nanoparticles to ciliated protozoa *Tetrahymena thermophila*. *Toxicology* 269:182-189.

[78] Heinlaan M, Kahru A, Kasemets K, Arbeille B, Prensier G, Dubourguier HC. 2011. Changes in the *Daphnia magna* midgut upon ingestion of copper oxide nanoparticles: a transmission electron microscopy study. *Water research* 45:179-190.

[79] Zhao J, Wang ZY, Liu XY, Xie XY, Zhang K, Xing BS. 2011. Distribution of CuO nanoparticles in juvenile carp (*Cyprinus carpio*) and their potential toxicity. *Journal of hazardous materials* 197:304-310.

[80] Gaggelli E, Kozlowski H, Valensin D, Valensin G. 2006. Copper Homeostasis and Neurodegenerative Disorders (Alzheimer's, Prion, and Parkinson's Diseases and Amyotrophic Lateral Sclerosis). *Chemical Reviews* 106:1995-2044.

[81] Sumner ER, Avery AM, Houghton JE, Robins RA, Avery SV. 2003. Cell cycle- and age-dependent activation of Sod1p drives the formation of stress resistant cell subpopulations within clonal yeast cultures. *Molecular Microbiology* 50:857-870.

[82] Sousa VS, Teixeira MR. 2013. Aggregation kinetics and surface charge of CuO nanoparticles: the influence of pH, ionic strength and humic acids. *Environ Chem* 10:313-322.

[83] Manusadzianas L, Caillet C, Fachetti L, Gylyte B, Grigutyte R, Jurkoniene S, Karitonas R, Sadauskas K, Thomas F, Vitkus R, Ferard JF. 2012. Toxicity of copper oxide nanoparticle suspensions to aquatic biota. *Environmental Toxicology and Chemistry* 31:108-114.

[84] Sun M, Yu Q, Hu M, Hao Z, Zhang C, Li M. 2014. Lead sulfide nanoparticles increase cell wall chitin content and induce apoptosis in *Saccharomyces cerevisiae*. *Journal of hazardous materials* 273:7-16.

[85] Sabel CE, Neureuther JM, Siemann S. 2010. A spectrophotometric method for the determination of zinc, copper, and cobalt ions in metalloproteins using Zincon. *Analytical biochemistry* 397:218-226.

[86] Arzul G, Quiniou F, Carrie C. 2006. *In vitro* test-based comparison of pesticide-induced sensitivity in marine and freshwater phytoplankton. *Toxicol Mech Method* 16:431-437.

[87] Conway JR, Adeleye AS, Gardea-Torresdey J, Keller AA. 2015. Aggregation, dissolution, and transformation of copper nanoparticles in natural waters. *Environmental Science and Technology* 49:2749-2756.

[88] Studer AM, Limbach LK, Van Duc L, Krumeich F, Athanassiou EK, Gerber LC, Moch H, Stark WJ. 2010. Nanoparticle cytotoxicity depends on intracellular solubility: comparison of stabilized copper metal and degradable copper oxide nanoparticles. *Toxicology letters* 197:169-174.

[89] Karlsson HL, Cronholm P, Hedberg Y, Tornberg M, De Battice L, Svedhem S, Wallinder IO. 2013. Cell membrane damage and protein interaction induced by copper containing nanoparticles--importance of the metal release process. *Toxicology* 313:59-69.

[90] Karlsson HL, Gustafsson J, Cronholm P, Moller L. 2009. Size-dependent toxicity of metal oxide particles--a comparison between nano- and micrometer size. *Toxicology letters* 188:112-118.

[91] Shannahan JH, Lai X, Ke PC, Podila R, Brown JM, Witzmann FA. 2013. Silver nanoparticle protein corona composition in cell culture media. *PloS one* 8:e74001.

[92] Li M, Lin D, Zhu L. 2013. Effects of water chemistry on the dissolution of ZnO nanoparticles and their toxicity to *Escherichia coli*. *Environmental pollution* 173:97-102.

[93] Ansari AA, Naziruddin Khan M, Alhoshan M, Aldwayyan AS, Alsalhi MS. 2010. Nanostructured materials: Classification, properties, fabrication, characterization and their applications in biomedical sciences. In Kestell AE, DeLorey GT, eds, *Nanoparticles: Properties, classification, characterization, and fabrication*. Nova Science Publishers, Hauppauge, NY, pp 1-78.

[94] Adam N, Vakurov A, Knapen D, Blust R. 2015. The chronic toxicity of CuO nanoparticles and copper salt to *Daphnia magna*. *Journal of hazardous materials* 283:416-422.

[95] Mahmoudi M, Serpooshan V. 2011. Large Protein Absorptions from Small Changes on the Surface of Nanoparticles. *J Phys Chem C* 115:18275-18283.

[96] Ohno T, Sarukawa K, Matsumura M. 2002. Crystal faces of rutile and anatase TiO 2 particles and their roles in photocatalytic reactions. *New journal of chemistry* 26:1167-1170.

[97] Auffan M, Rose J, Wiesner MR, Bottero JY. 2009. Chemical stability of metallic nanoparticles: A parameter controlling their potential cellular toxicity *in vitro*. *Environmental Pollution* 157:1127-1133.

[98] Oberdorster G, Kane AB, Klaper RD, Hurt RH. 2013. Nanotoxicity. In Klaassen CD, ed, Casarett and Doull's toxicology: The basic science of poisons. Mc Graw-Hill, New York, pp 1189-1229.

[99] Wright M. 2012. Nanoparticle Tracking Analysis for the multiparameter characterization and counting of nanoparticle suspensions. In Soloviev M, ed, *Nanoparticles in Biology and Medicine*. Vol 906-Methods in Molecular Biology. Humana Press, pp 511-524.

[100] Franklin NM, Rogers NJ, Apte SC, Batley GE, Gadd GE, Casey PS. 2007. Comparative toxicity of nanoparticulate ZnO, bulk ZnO, and $ZnCl_2$ to a freshwater microalga (*Pseudokirchneriella subcapitata*): the importance of particle solubility. *Environmental Science and Technology* 41:8484-8490.

[101] Brunner TJ, Wick P, Manser P, Spohn P, Grass RN, Limbach LK, Bruinink A, Stark WJ. 2006. *In vitro* cytotoxicity of oxide nanoparticles: comparison to asbestos, silica, and the effect of particle solubility. *Environmental Science and Technology* 40:4374-4381.

[102] Baek Y-W, An Y-J. 2011. Microbial toxicity of metal oxide nanoparticles (CuO, NiO, ZnO, and Sb 2 O 3) to *Escherichia coli*, *Bacillus subtilis*, and *Streptococcus aureus*. *Science of the total environment* 409:1603-1608.

[103] Li L, Fernández-Cruz ML, Connolly M, Schuster M, Navas JM. 2015. Dissolution and aggregation of Cu nanoparticles in culture media: effects of incubation temperature and particles size. *Journal of Nanoparticle Research* 17:1-11.

[104] Borm P, Klaessig FC, Landry TD, Moudgil B, Pauluhn J, Thomas K, Trottier R, Wood S. 2006. Research strategies for safety evaluation of nanomaterials, part V: role of dissolution in biological fate and effects of nanoscale particles. *Toxicological Sciences* 90:23-32.

[105] Oberdorster G, Oberdorster E, Oberdorster J. 2005. Nanotoxicology: an emerging discipline evolving from studies of ultrafine particles. *Environmental health perspectives* 113:823-839.

[106] Smith MR, Boenzli MG, Hindagolla V, Ding J, Miller JM, Hutchison JE, Greenwood JA, Abeliovich H, Bakalinsky AT. 2013. Identification of gold nanoparticle-resistant mutants of *Saccharomyces cerevisiae* suggests a role for respiratory metabolism in mediating toxicity. *Applied and environmental microbiology* 79:728-733.

[107] Heinlaan M, Ivask A, Blinova I, Dubourguier HC, Kahru A. 2008. Toxicity of nanosized and bulk ZnO, CuO and TiO2 to bacteria *Vibrio fischeri* and crustaceans *Daphnia magna* and *Thamnocephalus platyurus*. *Chemosphere* 71:1308-1316.

[108] Carlson C, Hussain SM, Schrand AM, Braydich-Stolle LK, Hess KL, Jones RL, Schlager JJ. 2008. Unique Cellular Interaction of Silver Nanoparticles: Size-Dependent Generation of Reactive Oxygen Species. *J Phys Chem B* 112:13608-13619.

[109] Xu M, Fujita D, Sagisaka K, Watanabe E, Hanagata N. 2011. Production of Extended Single-Layer graphene. *ACS nano* 5:1522-1528.

[110] Stern ST, McNeil SE. 2008. Nanotechnology safety concerns revisited. *Toxicological sciences : an official journal of the Society of Toxicology* 101:4-21.

[111] Studer AM, Limbach LK, Van Duc L, Krumeich F, Athanassiou EK, Gerber LC, Moch H, Stark WJ. 2010. Nanoparticle cytotoxicity depends on intracellular solubility: comparison of stabilized copper metal and degradable copper oxide nanoparticles. *Toxicology letters* 197:169-174.

[112] Semisch A, Ohle J, Witt B, Hartwig A. 2014. Cytotoxicity and genotoxicity of nano - and microparticulate copper oxide: role of solubility and intracellular bioavailability. *Particle and fibre toxicology* 11:10.

[113] Jo WJ, Loguinov A, Chang M, Wintz H, Nislow C, Arkin AP, Giaever G, Vulpe CD. 2008. Identification of genes involved in the toxic response of *Saccharomyces cerevisiae* against iron and copper overload by parallel analysis of deletion mutants. *Toxicological sciences : an official journal of the Society of Toxicology* 101:140-151.

[114] Labbe S, Zhu Z, Thiele DJ. 1997. Copper-specific transcriptional repression of yeast genes encoding critical components in the copper transport pathway. *The Journal of biological chemistry* 272:15951-15958.

[115] Hodgins-Davis A, Adomas AB, Warringer J, Townsend JP. 2012. Abundant gene-by-environment interactions in gene expression reaction norms to copper within *Saccharomyces cerevisiae*. *Genome biology and evolution* 4:1061-1079.

[116] Pope CR, De Feo CJ, Unger VM. 2013. Cellular distribution of copper to superoxide dismutase involves scaffolding by membranes. *Proceedings of the National Academy of Sciences of the United States of America* 110:20491-20496.

[117] Liu L, Qi J, Yang Z, Peng L, Li C. 2012. Low-affinity copper transporter CTR2 is regulated by copper-sensing transcription factor Mac1p in *Saccharomyces cerevisiae*. *Biochemical and biophysical research communications* 420:600-604.

[118] Jin YH, Dunlap PE, McBride SJ, Al-Refai H, Bushel PR, Freedman JH. Global Transcriptome and Deletome Profiles of Yeast Exposed to Transition Metals. PLoS Genet. 2008 Apr;4(4):e1000053. Epub 2008 Apr 25 doi:10.1371/journal.pgen.1000053.

[119] Yasokawa D, Murata S, Kitagawa E, Iwahashi Y, Nakagawa R, Hashido T, Iwahashi H. 2008. Mechanisms of copper toxicity in *Saccharomyces cerevisiae* determined by microarray analysis. *Environ Toxicol* 23:599-606.

[120] Rustici G, van Bakel H, Lackner DH, Holstege FC, Wijmenga C, Bahler J, Brazma A. 2007. Global transcriptional responses of fission and budding yeast to changes in copper and iron levels: a comparative study. *Genome Biol* 8:R73.

[121] Teste MA, Duquenne M, Francois JM, Parrou JL. 2009. Validation of reference genes for quantitative expression analysis by real-time RT-PCR in *Saccharomyces cerevisiae*. *BMC Mol Biol* 10:1471-2199.

[122] Vandesompele J, De Preter K, Pattyn F, Poppe B, Van Roy N, De Paepe A, Speleman F. 2002. Accurate normalization of real-time quantitative RT-PCR data by geometric averaging of multiple internal control genes. *Genome Biol* 3:18.

[123] Talloen W, Verbeke T. 2011. a4: Affymetrix Array Analysis umbrella package, R package version 1.16.0.

[124] Smyth GK. 2005. limma: Linear Models for Microarray Data. In Gentleman R, Carey V, Huber W, Irizarry R, Dudoit S, eds, Bioinformatics and Computational Biology Solutions Using R and Bioconductor. -Statistics for Biology and Health. Springer New York, pp 397-420.

[125] Boyle EI, Weng S, Gollub J, Jin H, Botstein D, Cherry JM, Sherlock G. 2004. GO::TermFinder--open source software for accessing Gene Ontology information and finding significantly enriched Gene Ontology terms associated with a list of genes. *Bioinformatics* 20:3710-3715.

[126] Huang da W, Sherman BT, Lempicki RA. 2009. Systematic and integrative analysis of large gene lists using DAVID bioinformatics resources. *Nat Protoc* 4:44-57.

[127] Huang da W, Sherman BT, Lempicki RA. 2009. Bioinformatics enrichment tools: paths toward the comprehensive functional analysis of large gene lists. *Nucleic acids research* 37:1-13.

[128] Kanehisa M, Goto S. 2000. KEGG: kyoto encyclopedia of genes and genomes. *Nucleic acids research* 28:27-30.

[129] Paalman JWG, Verwaal R, Slofstra SH, Verkleij AJ, Boonstra J, Verrips CT. 2003. Trehalose and glycogen accumulation is related to the duration of the G1 phase of *Saccharomyces cerevisiae*. *FEMS yeast research* 3:261-268.

[130] Gross C, Kelleher M, Iyer VR, Brown PO, Winge DR. 2000. Identification of the copper regulon in *Saccharomyces cerevisiae* by DNA microarrays. *The Journal of biological chemistry* 275:32310-32316.

[131] Piper PW, Ortiz-Calderon C, Holyoak C, Coote P, Cole M. Hsp30, the integral plasma membrane heat shock protein of *Saccharmyces cerevisiae*, is a stress-inducible regulator of plasma membrane H(+)-ATPase. Cell Stress Chaperones. 1997 Mar;2(1):12-24.

[132] Dudev T, Lim C. 2014. Competition among Metal Ions for Protein Binding Sites: Determinants of Metal Ion Selectivity in Proteins. *Chemical Reviews* 114:538-556.

[133] Jomova K, Valko M. 2011. Advances in metal-induced oxidative stress and human disease. *Toxicology* 283:65-87.

[134] Gomez-Escoda B, Ivanova T, Calvo IA, Alves-Rodrigues I, Hidalgo E, Ayte J. 2011. Yox1 links MBF-dependent transcription to completion of DNA synthesis. *EMBO Rep* 12:84-89.

[135] Parrou JL, Teste M-A, François J. 1997. Effects of various types of stress on the metabolism of reserve carbohydrates in *Saccharomyces cerevisiae*: genetic evidence for a stress-induced recycling of glycogen and trehalose. *Microbiology* 143:1891-1900.

[136] Pultz D, Bennetzen MV, Rodkaer SV, Zimmermann C, Enserink JM, Andersen JS, Faergeman NJ. 2012. Global mapping of protein phosphorylation events identifies Ste20, Sch9 and the cell-cycle regulatory kinases Cdc28/Pho85 as mediators of fatty acid starvation responses in *Saccharomyces cerevisiae*. *Molecular BioSystems* 8:796-803.

[137] Huang D, Moffat J, Wilson WA, Moore L, C.Cheng, Roach PJ, Andrews B. 1998. Cyclin partners determien Pho85 protein kinase substrate specificity in vitro and in vivo: control of glycogen biosynthesis by Pcl8 and Pcl10. *Molecular and cellular biology*.

[138] Measday V, Moore L, Retnakaran R, Lee J, Donoviel M, Neiman AM, Andrews B. 1997. A family of cyclin-like proteins that interact with the Pho85 cyclin-dependent kinase. *Molecular and cellular biology* 17:1212-1223.

[139] Niu W, Li Z, Zhan W, Iyer VR, Marcotte EM. 2008. Mechanisms of Cell Cycle Control Revealed by a Systematic and Quantitative Overexpression Screen in *S. cerevisiae. PLoS genetics* 4:e1000120.

[140] Tkach JM, Yimit A, Lee AY, Riffle M, Costanzo M, Jaschob D, Hendry JA, Ou J, Moffat J, Boone C, Davis TN, Nislow C, Brown GW. 2012. Dissecting DNA damage response pathways by analysing protein localization and abundance changes during DNA replication stress. *Nat Cell Biol* 14:966-976.

[141] Guacci V, Koshland D, Strunnikov A. A Direct Link between Sister Chromatid Cohesion and Chromosome Condensation Revealed through the Analysis of MCD1 in *S. cerevisiae*. *Cell* 91:47-57.

[142] Gasch AP, Werner-Washburne M. 2002. The genomics of yeast responses to environmental stress and starvation. *Functional & integrative genomics* 2:181-192.

[143] Swinnen E, Ghillebert R, Wilms T, Winderickx J. 2014. Molecular mechanisms linking the evolutionary conserved TORC1-Sch9 nutrient signalling branch to lifespan regulation in *Saccharomyces cerevisiae*. *FEMS yeast research* 14:17-32.

[144] Fong CS, Temple MD, Alic N, Chiu J, Durchdewald M, Thorpe GW, Higgins VJ, Dawes IW. 2008. RESEARCH ARTICLE: Oxidant-induced cell-cycle delay in *Saccharomyces cerevisiae*: the involvement of the SWI6 transcription factor. *FEMS yeast research* 8:386-399.

[145] Paalman JWG, Verwall R, Slofstra SH, Verkleij AJ, Boonstra J, Verrips CT. 2003. Trehalose and glycogen accumulation is related to the duration of the G1 phase of *Saccharomyces cerevisiae*. *FEMS yeast research* 3.

[146] Hanagata N, Zhuang F, Connolly S, Li J, Ogawa N, Xu M. 2011. molecular responses of human lung epithelial cells to the toxicity of copper oxide nanoparticles inferred from whole genome expression analysis. *ACS nano* 5:9326-9338.

[147] Bayat N, Rajapakse K, Marinsek-Logar R, Drobne D, Cristobal S. 2014. The effects of engineered nanoparticles on the cellular structure and growth of *Saccharomyces cerevisiae*. *Nanotoxicology* 8:363-373.

[148] Ashburner M, Ball CA, Blake JA, Botstein D, Butler H, Cherry JM, Davis AP, Dolinski K, Dwight SS, Eppig JT, Harris MA, Hill DP, Issel-Tarver L, Kasarskis A, Lewis S, Matese JC, Richardson JE, Ringwald M, Rubin GM, Sherlock G. Gene Ontology: tool for the unification of biology. Nat Genet. 2000 May;25(1):25-9. doi:10.1038/75556.

[149] Warner JR. 1999. The economics of ribosome biosynthesis in yeast. *Trends in Biochemical Sciences* 24:437-440.

[150] Shulman RG, Rothman DL. 2015. Homeostasis and the glycogen shunt explains aerobic ethanol production in yeast. *Proceedings of the National Academy of Sciences of the United States of America* 112:10902-10907.

[151] Ni H, LaPorte DC. 1995. Response of a yeast glycogen synthase gene to stress. *Molecular Mechanism* 16:1197-1205.

[152] Hounsa C-G, Brandt EV, Thevelein J, Hohmann S, Prior BA. 1998. Role of trehalose in survival of *Saccharomyces cerevisiae* under osmotic stress. *Microbiology* 144:671-680.

[153] Singer MA, Lindquist S. 1998. Multiple Effects of Trehalose on Protein Folding *In Vitro* and *In Vivo*. *Molecular Cell* 1:639-648.

[154] Parrou JL, Enjalbert B, Plourde L, Bauche A, Gonzalez B, Francois J. 1999. Dynamic responses of reserve carbohydrate metabolism under carbon and nitrogen limitations in *Saccharomyces cerevisiae*. *Yeast* 15:191-203.

[155] Seto-Young D, Perlin DS. 1991. Effect of membrane voltage on the plasma membrane H(+)-ATPase of *Saccharomyces cerevisiae*. *The Journal of biological chemistry* 266:1383-1389.

[156] Fernandes AR, Sá-Correia I. 2001. The activity of plasma membrane H+-ATPase is strongly stimulated during *Saccharomyces cerevisiae* adaptation to growth under high copper stress, accompanying intracellular acidification. *Yeast* 18:511-521.

[157] Kim Y, Chattopadhyay S, Locke S, Pearce DA. 2005. Interaction among Btn1p, Btn2p, and Ist2p Reveals Potential Interplay among the Vacuole, Amino Acid Levels, and Ion Homeostasis in the Yeast *Saccharomyces cerevisiae*. *Eukaryotic cell* 4:281-288.

[158] Gomes SIL, Novais SC, Gravato C, Guilhermino L, Scott-Fordsmand JJ, Soares AMVM, Amorim MJB. 2011. Effect of Cu-nanoparticles versus one Cu-salt: Analysis of stress biomarkers response in *Enchytraeus albidus* (*Oligochaeta*). *Nanotoxicology* 6:134-143.

[159] Bundy J, Sidhu J, Rana F, Spurgeon D, Svendsen C, Wren J, Sturzenbaum S, Morgan AJ, Kille P. 2008. 'Systems toxicology' approach identifies coordinated metabolic responses to copper in a terrestrial non-model invertebrate, the earthworm *Lumbricus rubellus*. *BMC Biology* 6:25.

[160] Lenburg ME, O'Shea EK. 1996. Signaling phosphate starvation. *Trends in Biochemical Sciences* 21:383-387.

[161] Tkach JM, Yimit A, Lee AY, Riffle M, Costanzo M, Jaschob D, Hendry JA, Ou J, Moffat J, Boone C, Davis TN, Nislow C, Brown GW. Dissecting DNA damage response pathways by analyzing protein localization and abundance changes during DNA replication stress. Nat Cell Biol. 2012 Sep;14(9):966-76. Epub 2012 Jul 29 doi:10.1038/ncb2549.

[162] Mai B, Breeden L. 1997. Xbp1, a stress-induced transcriptional repressor of the *Saccharomyces cerevisiae* Swi4/Mbp1 family. *Molecular and cellular biology* 17:6491-6501.

[163] Baek YW, An YJ. 2011. Microbial toxicity of metal oxide nanoparticles (CuO, NiO, ZnO, and Sb2O3) to *Escherichia coli*, *Bacillus subtilis*, and *Streptococcus aureus*. *The Science of the total environment* 409:1603-1608.

[164] Shi J, Abid AD, Kennedy IM, Hristova KR, Silk WK. 2011. To duckweeds *(Landoltia punctata),* nanoparticulate copper oxide is more inhibitory than the soluble copper in the bulk solution. Environ Pollut. 2011 May;159(5):1277-82. Epub 2011 Feb 18 doi:10.1016/j.envpol.2011.01.028.

[165] Calafato S, Swain S, Hughes S, Kille P, Sturzenbaum SR. 2008. Knock down of *Caenorhabditis elegans* cutc-1 exacerbates the sensitivity toward high levels of copper. *Toxicological sciences : an official journal of the Society of Toxicology* 106:384-391.

[166] Ma H, Biertsch PM, Glenn TC, Kabengi NJ, Williams PL. 2009. Toxicity of manufactured zinc oxide nanoparticles in the nematode *Caenorhabditis elegans*. *Environmental Toxicology and Chemistry* 28:1324-1330.

[167] Madsen E, Gitlin JD. 2007. Copper and iron disorders of the brain. *Annu Rev Neurosci* 30:317-337.

[168] Du M, Wang D. 2009. The neurotoxic effects of heavy metal exposure on GABAergic nervous system in nematode *Caenorhabditis elegans*. *Environmental toxicology and pharmacology* 27:314-320.

[169] Frézal L, Félix M-A. 2015. *C. elegans* outside the Petri dish. *eLife* 4.

[170] Andersen EC, Bloom JS, Gerke JP, Kruglyak L. 2014. A variant in the neuropeptide receptor npr-1 is a major determinant of *Caenorhabditis elegans* growth and physiology. *PLoS genetics* 10:e1004156.

[171] Andersen EC, Shimko TC, Crissman JR, Ghosh R, Bloom JS, Seidel HS, Gerke JP, Kruglyak L. 2015. A Powerful New Quantitative Genetics Platform, Combining *Caenorhabditis elegans* High-Throughput Fitness Assays with a Large Collection of Recombinant Strains. *G3: Genes|Genomes|Genetics*.

[172] Sterken MG, Snoek LB, Kammenga JE, Andersen EC. The laboratory domestication of *Caenorhabditis elegans*. *Trends in Genetics* 31:224-231.

[173] Weston DP, Poynton HC, Wellborn GA, Lydy MJ, Blalock BJ, Sepulveda MS, Colbourne JK. 2013. Multiple origins of pyrethroid insecticide resistance across the species complex of a nontarget aquatic crustacean, *Hyalella azteca*. *Proceedings of the National Academy of Sciences* 110:16532-16537.

[174] Browne RA, Moller V, Forbes VE, Depledge MH. 2002. Estimating genetic and environmental components of variance using sexual and clonal *Artemia*. *Journal of Experimental Marine Biology and Ecology* 267:107-119.

[175] Warming TP, Mulderij G, Christoffersen KS. 2009. Clonal variation in physiological responses of *Daphnia magna* to the strobilurin fungicide azoxystrobin. *Environmental Toxicology and Chemistry* 28:374-380.

[176] Andersen EC, Gerke JP, Shapiro JA, Crissman JR, Ghosh R, Bloom JS, Felix MA, Kruglyak L. 2012. Chromosome-scale selective sweeps shape *Caenorhabditis elegans* genomic diversity. *Nature genetics* 44:285-290.

[177] Petrella LN. 2014. Natural variants of *C. elegans* demonstrate defects in both sperm function and oogenesis at elevated temperatures. *PloS one* 9:e112377.

[178] Brenner S. 1974. The genetics of *Caenorhabditis elegans*. *Genetics* 77:71-94.

[179] Maydan JS, Flibotte S, Edgley ML, Lau J, Selzer RR, Richmond TA, Pofahl NJ, Thomas JH, Moerman DG. 2007. Efficient high-resolution deletion discovery in *Caenorhabditis elegans* by array comparative genomic hybridization. *Genome Research* 17:337-347.

[180] Thompson OA, Snoek LB, Nijveen H, Sterken MG, Volkers RJM, Brenchley R, van't Hof A, Bevers RPJ, Cossins AR, Yanai I, Hajnal A, Schmid T, Perkins JD, Spencer D, Kruglyak L, Andersen EC, Moerman DG, Hillier LW, Kammenga JE, Waterston RH. 2015. Remarkably Divergent Regions Punctuate the Genome Assembly of the *Caenorhabditis elegans* Hawaiian Strain CB4856. *Genetics* 200:975-989.

[181] Settivari R, Levora J, Nass R. 2009. The divalent metal transporter homologues SMF-1/2 mediate dopamine neuron sensitivity in *Caenorhabditis elegans* models of manganism and parkinson disease. *The Journal of biological chemistry* 284:35758-35768.

[182] Chu KW, Chan SK, Chow KL. 2005. Improvement of heavy metal stress and toxicity assays by coupling a transgenic reporter in a mutant nematode strain. *Aquatic toxicology* 74:320-332.

[183] Shimko TC, Andersen EC. COPASutils: An R package for reading, processing, and visualizing data from COPAS large-particle flow cytometers.

[184] Stiernagle T. 2006. Maintenance of *C. elegans*. *WormBook : the online review of C elegans biology*:1-11.

[185] Dengg M, van Meel JC. 2004. *Caenorhabditis elegans* as model system for rapid toxicity assessment of pharmaceutical compounds. *Journal of pharmacological and toxicological methods* 50:209-214.

[186] Song S, Guo Y, Zhang X, Zhang X, Zhang J, Ma E. 2014. Changes to cuticle surface ultrastructure and some biological functions in the nematode *Caenorhabditis elegans* exposed to excessive copper. *Archives of environmental contamination and toxicology* 66:390-399.

[187] Au C, Benedetto A, Anderson J, Labrousse A, Erikson K, Ewbank JJ, Aschner M. 2009. SMF-1, SMF-2 and SMF-3 DMT1 orthologues regulate and are regulated differentially by manganese levels in *C. elegans*. *PloS one* 4:e7792.

[188] Gaertner BE, Phillips PC. 2010. *Caenorhabditis elegans* as a platform for molecular quantitative genetics and the systems biology of natural variation. *Genet Res* 92:331-348.

[189] Hodgkin J, Doniach T. 1997. Natural variation and copulatory plug formation in *Caenorhabditis elegans*. *Genetics* 146:149-164.

[190] Koch R, van Luenen HGAM, van der Horst M, Thijssen KL, Plasterk RHA. 2000. Single Nucleotide Polymorphisms in Wild Isolates of *Caenorhabditis elegans*. *Genome Research* 10:1690-1696.

[191] Wu Q, Nouara A, Li Y, Zhang M, Wang W, Tang M, Ye B, Ding J, Wang D. 2013. Comparison of toxicities from three metal oxide nanoparticles at environmental relevant concentrations in nematode *Caenorhabditis elegans*. *Chemosphere* 90:1123-1131.

[192] So S, Miyahara K, Ohshima Y. 2011. Control of body size in *C. elegans* dependent on food and insulin/IGF-1 signal. *Genes to cells : devoted to molecular & cellular mechanisms* 16:639-651.

[193] Raizen D, Song BM, Trojanowski N, You YJ. 2012. Methods for measuring pharyngeal behaviors. *WormBook : the online review of C elegans biology*:1-13.

[194] Peterson RT, Nass R, Boyd WA, Freedman JH, Dong K, Narahashi T. 2008. Use of non-mammalian alternative models for neurotoxicological study. *Neurotoxicology* 29:546-555.

[195] Yu ZY, Zhang J, Yin DQ. 2012. Toxic and recovery effects of copper on *Caenorhabditis elegans* by various food-borne and water-borne pathways. *Chemosphere* 87:1361-1367.

[196] Heinlaan M, Kahru A, Kasemets K, Arbeille B, Prensier G, Dubourguier H-C. 2011. Changes in the *Daphnia magna* midgut upon ingestion of copper oxide nanoparticles: A transmission electron microscopy study. *Water Research* 45:179-190.

[197] Bergin IL, Witzmann FA. 2013. Nanoparticle toxicity by the gastrointestinal route: evidence and knowledge gaps*. Int J Biomed Nanosci Nanotechnol*. 2013;3(1-2):10.1504/IJBNN.2013.054515. doi:10.1504/IJBNN.2013.054515.

[198] Yang X, Gondikas AP, Marinakos SM, Auffan M, Liu J, Hsu-Kim H, Meyer JN. 2012. Mechanism of silver nanoparticle toxicity is dependent on dissolved silver and surface coating in *Caenorhabditis elegans*. *Environmental science & technology* 46:1119-1127.

[199] Boyd WA, Smith MV, Kissling GE, Freedman JH. 2010. Medium- and high-throughput screening of neurotoxicants using *C. elegans*. *Neurotoxicology and teratology* 32:68-73.

[200] Cha YJ, Lee J, Choi SS. 2012. Apoptosis-mediated in vivo toxicity of hydroxylated fullerene nanoparticles in soil nematode *Caenorhabditis elegans*. *Chemosphere* 87:49-54.

[201] Lim D, Roh J-y, Eom H-j, Choi J-Y, Hyun J, Choi J. 2012. Oxidative stress-related PMK-1 P38 MAPK activation as a mechanism for toxicity of silver nanoparticles to reproduction in the nematode *Caenorhabditis elegans*. *Environmental Toxicology and Chemistry* 31:585-592.

[202] Meyer JN, Lord CA, Yang XY, Turner EA, Badireddy AR, Marinakos SM, Chilkoti A, Wiesner MR, Auffan M. 2010. Intracellular uptake and associated toxicity of silver nanoparticles in *Caenorhabditis elegans*. *Aquatic toxicology* 100:140-150.

[203] Barriere A. 2005. Natural variation and population genetics of Caenorhabditis elegans. *WormBook : the online review of C elegans biology*.

[204] Cabiscol E, Piulats E, Echave P, Herrero E, Ros J. 2000. Oxidative stress promotes specific protein damage in *Saccharomyces cerevisiae*. *The Journal of biological chemistry* 275:27393-27398.

[205] Raja MR, Waterman SR, Qiu J, Bleher R, Williamson PR, O'Halloran TV. A Copper Hyperaccumulation Phenotype Correlates with Pathogenesis in. *Metallomics*. 2013 Apr;5(4):363-71. doi:10.1039/c3mt20220h.

[206] Cobine PA, Ojeda LD, Rigby KM, Winge DR. 2004. Yeast contain a non-proteinaceous pool of copper in the mitochondrial matrix. *The Journal of biological chemistry* 279:14447-14455.

[207] Farrugia G, Balzan R. Oxidative Stress and Programmed Cell Death in Yeast. *Front Oncol*. 2012;2:64. doi:10.3389/fonc.2012.00064.

[208] Stefano Di Talia, Jan M. Skotheim, James M. Bean, Eric D. Siggia and Frederick R. Cross. The effects of molecular noise and size control on variability in the budding yeast cell cycle. *Nature.* 2007,448. doi:10.1038/nature06072947-951.